AFIT/GA/ENY/93D-2

AD-A275 362

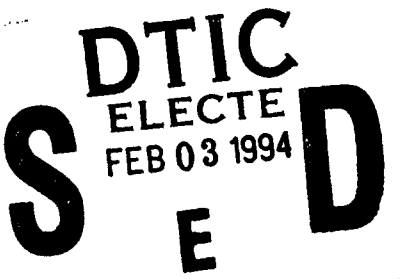

DESIGN AND CONSTRUCTION OF THE AEROBOT ROBOTIC MANIPULATOR (ARM)

THESIS

William L. Cochran, Captain, USAF

AFIT/GA/ENY/93D-2

93-30412

Approved for public release; Distribution Unlimited

93 12 15 092

AFIT/GA/ENY/93D-2

DESIGN AND CONSTRUCTION OF THE AEROBOT ROBOTIC MANIPULATOR (ARM)

THESIS

Presented to the Faculty of the Graduate School of Engineering

of the Air Force Institute of Technology

Air University

In Partial Fulfillment of the

Requirements for the Degree of

Master of Science in Astronautical Engineering

William L. Cochran, B.S.

Captain, USAF

December 1993

DTIC QUALITY INSPECTED 5

Accesion For
NTIS CRA&I [X]
DTIC TAB [ ]
Unannounced [ ]
Justification .....
By .....
Distribution /
Availability Codes
Dist | Avail and / or Special
A-1

Approved for public release; Distribution Unlimited

Preface

This thesis project brought with it, much new knowledge to this author. Because of the design nature of the project, many disciplines were used. Electrical engineering was used to design and build the joy stick circuit. Mechanical engineering was used to establish the specifications of the motors and the springs. Materials and structures were used to analysis and design the telescoping tubes. These are but a few examples of what it took to complete the project. Because it involved only one person instead of a group of people to draw this knowledge from, the project seemed overwhelming at times, but at the end it was all worthwhile.

To those who will follow my work , either on the ARM or the Aerobot, my intentions were to make this thesis report a complete as possible, thus leaving you with an "owner's manual", so to speak. Hopefully I succeeded in this attempt.

I would like to acknowledge those who helped in the completion of this thesis. First of all I would like to thank my advisor, Dr. Curtis Spenny, who initiated the idea of a manipulator for the Aerobot and provided me with invaluable assistance along the way. To my reading committee, Dr. Jones and Dr. Kramer, thank you for your patience and for your helpful insight. To Tim McIntyre and Timac Inc., who built the springs, I appreciate your added guidance. To John Brohaus and the AFIT fabrication shop, I extend my deep appreciation for your long hours of work building the ARM and lending me your knowledgeable support at crucial points. To Tom Bridgeman, who designed the joy stick circuitry, thank you for helping me through my "hour of need". To Mark Derriso, who constructed the joy stick circuit, I thank you, for the all the time you put into the making this project a success. And last but not least, I want to deeply thank my wife, Laura, for her undying support and patience through my time here at AFIT.

- William L. Cochran

Table of Contents

		Page
Acknowledgments		ii
List of Figures		v
List of Tables		vii
Abstract		viii
I.	Introduction	1
	A. The Aerial Robotics Competition	2
	B. The Moller Aerial Vehicle	5
	C. Thesis Objectives	7
II.	Conceptual Design	10
	A. Design Specifications	10
	B. Preliminary Designs	15
	1. Tripod	15
	2. Serial Arm	16
	3. Rail	18
	4. Lever Arm	19
	5. Landsberger Parallel Link Manipulator	20
	C. Final Design - The AFIT ARM	22
III.	Hardware Design	27
	A. Telescoping Arm	27
	1. Tubing	27
	2. Springs	36
	B. Magnet and Retractable Cord	38
	C. Motors	39
	D. Cable Spools	44
	E. Pulleys	45
	F. Diamond Plates	47
	G Revolute Joint	49
	H Mounting Hardware	49
	I. Joy Stick Control	51
IV.	Kinematic Analysis	56
	A. Geometry of the ARM	56
	B. Forward Kinematic Model	61
	C. Inverse Kinematic Model	65

Page

V. Performance 68

A. Qualitative Analysis 68
B. Quantitative Analysis 72

VI. Results, Conclusions and Recommendations 82

A. Lessons Learned and Their Solutions 82
B. Conclusions 86
C. Recommendations 87

Appendix A: Competition Rules 89

Appendix B: Dimensioned Drawings and Components Specifications 101

Bibliography 107

Vita 108

List of Figures

Figure		Page
1.	The Moller Aerial Vehicle	6
2.	Aerobot Cut-a-Way Diagram	7
3.	Tripod Design	16
4.	Serial Arm Design	17
5.	Rail Design	19
6.	Lever Arm Design	20
7.	Landsberger's Parallel Link Manipulator	21
8.	The AFIT ARM Design	23
9.	Top and Bottom Plate Movement Restrictions	26
10.	The Completed AFIT ARM	28
11.	The Expanded Diagram of the Telescoping Arm	29
12.	The Insides of the Tubes	30
13.	Tubing Tolerance Deflections	34
14.	The Springs	36
15.	The Electromagnet	39
16.	The Free Body Diagram of the ARM	40
17.	The Motor and Potentiometers	43
18.	The Motor Assembly (Top View)	43
19.	The Double Cable Spools	44
20.	The Swivel Pulley	46
21.	The Top and Bottom Plates	48

22. The Ball Joint 50
23. The Construction of the Ball Joint 50
24. The Tether Bracket 52
25. The Mounting Hardware 52
26. The Joy Stick 53
27. The Joy Stick Circuit 55
28. The Geometry of the ARM 58
29. D-H Reference Frames for the ARM 62
30. Problem of Two Pivot Points 70
31. Measured and Calculated Position Comparison 75
32. Measured and Calculated Motor Angle Comparison 77
33. Position Change for Motor Angle 1 79
34. Position Change for Motor Angle 2 80
35. Position Change for Motor Angle 3 81
36. The Universal Joint 84
37. The New Single Spool 85

List of Tables

Table		Page
1.	Final Tubing Measurements	32
2.	Mass Per Unit Length Values for PVC	35
3.	D-H Link Parameters for the ARM	63

Abstract

This thesis designed, constructed, and tested a robotic arm for the Aerobot (Aerial Robot). The main purpose of the ARM is to enable the Aerobot to retrieve objects for use in an annual robotics competition. Design of the ARM involved synthesizing the characteristics of simplicity, weight, strength, and size. The result was a three-degree-of-freedom manipulator that uses electric motors, cable linkages, and telescoping tubes to access a work space below the Aerobot. Forward and inverse kinematics were investigated to enable automation of the ARM. Data was collected from infrared sensors to validate the model. Manipulation of the ARM is presently under open loop control (joy stick) which demonstrates the use of tele-robotics and its capabilities.

DESIGN AND CONSTRUCTION OF THE AEROBOT ROBOTIC MANIPULATOR (ARM)

I. Introduction

In recent years, unmanned aerial vehicles (UAV's) have become increasingly important, especially in the military arena. They are typically used in areas such as airfield threat determination, damage assessment, and nuclear/biological/chemical detection. These areas all require the presence of sensors in hostile territory. By keeping humans in a safe environment and putting the aerial robot in the dangerous areas, information can be gathered in a safer way. In this way, information about airfield threats can be accomplished by UAV's without the danger of losing human life. Similarly, detection of nuclear/ biological/chemical weapon threats and conditions can be performed more safely by UAV's, rather than by humans. Information can also be obtained by UAV's without alerting the enemy, due to the small size of the vehicles and the low altitudes used (1:39-48).

Recently, the military has taken increasingly more interest in designing, developing and deploying aerial robots for various uses. By equipping UAV's with a robotic arm, existing vehicles should be of more value and have greater usefulness. Even though most of the uses of UAV's are military, the civilian sector should also benefit from this research. Civil government and commercial applications include: security surveillance; fire spotting; traffic surveillance; pipeline, transmission line, and rail inspection; video news gathering; and inspection of remote and hazardous areas. This research should further increase our technology by providing additional uses and capabilities of certain robots (1:21).

Most of the uses for UAV's presented so far have been for sensing. Typically, UAV's are not used to touch stationary objects, but are used to study objects at a distance. But, with the use of a robotic manipulator, new chores may be invented for the aerial vehicles. Jobs that actually require touching a grounded object include recovering hazardous or hard to reach material, defusing bombs, placing and delivering items with precision, stringing electrical or telephone wire, and manipulating objects (puncturing, tipping over, setting up, etc.). Touching grounded objects with aerial vehicles presents future research possibilities in vehicle flight stability.

Along with this increased interest in unmanned systems, the Association for Unmanned Vehicles (AUVS) sponsors an annual aerial robotics competition between academic, industrial and government teams. This competition is called the Aerial Robotics Competition. The concept of the competition is to design and build an autonomous aerial robot that will pick up and deliver objects without any human control. The Moller Aerial Vehicle is AFIT's potential entry into this competition. Modification of the vehicle with a robotic arm is crucial in accomplishing the specific task required for the competition. Producing this robotic arm is the real essence of this thesis.

A. The Aerial Robotics Competition

In 1991, the Association for Unmanned Vehicle Systems created the annual Aerial Robotics Competition to inspire engineering and science students to pursue careers in the field of unmanned system technology (in particular, the area of UAV's). The Association also established the competition to expand the technology in this area. By encouraging industry, academia and the government to participate hand in hand, the competition provides multiple benefits. Industry gains the exposure of potential employees to the company and product spin-offs to the general public. Students gain from the opportunity to use their own skills by solving practical problems. The

government gains from the demonstration of applied technology which might someday be used to meet national needs (2:1).

The objective of the competition is to design an unmanned and autonomous aerial vehicle to transfer six randomly placed metal disks, one at a time, from one 6-ft ring to another. The process must take 6 minutes or less. The rings are separated by a solid 3-ft vertical barrier, which does not allow the vehicle to view one ring from the other. The vertical barrier is placed in the center of the competition arena which is similar to a tennis court. The vehicles are restricted to flight inside the boundaries of this arena, although, external navigational aids (e.g., infrared or acoustic sensing devices) and computational power may be outside the boundaries. Information may be fed to the vehicles through data links by radio or other means, as long as no tethers are used to feed that information to the vehicle. The vehicle must be under autonomous operation (no human involvement) during the entire flight . During the flying portion of the competition, the aerial robots must remain airborne (capable of sustained flight outside of ground affect), although, they may land inside of the rings to retrieve the metal disks. Subvehicles are allowed to be used to search for, and/or acquire the metal disks inside of the rings. These subvehicles must be permanently attached to the main vehicle and be autonomous as well. The robotic arm of this thesis would be classified as a subvehicle. The details of the competition, diagrams of the arena boundaries, and a detailed drawing of metal disks are included in the competition rules contained in Appendix A (3:1-12).

To gain valuable information on the use of retrieval systems by competitors, the thesis author attended the 1993 Aerial Robotics Competition and recorded it onto video tape (4). Mainly, there were two types of retrieval systems used. One, a passive cable system with a magnet attached, was fairly primitive and had specific difficulties. The acquisition of the metal disks was achieved by the main vehicle which complicated the vehicle control by adding another task. Also, since the cable was not under control, the

magnet was allowed to roam on its own. This could create quite a problem for the controller.

The other type of retrieval system was an autonomous tethered robotic vehicle, looking much like the small remote control cars on the market today. In contrast, this system was very sophisticated, yet it had flaws also. Operation of the tethered robot started by lowering it into the ring from the main vehicle. Once it touched ground it used motorized wheels to propel it across the ring in search of the metal disks. Once the robot located a disk, it used an electromagnet to capture the disk. The robot was then retrieved back to the hovering main vehicle for flight to the drop-off ring. This is where the major flaw of this system was manifested. Because the mass of the tethered robot was significant, compared to the main vehicle, a pendulum effect was created which grossly affected the flight characteristics of the main vehicle. Under autonomous control, which is a requirement, this would have been very difficult to control. This may suggest that a more rigid device, like a robotic arm, may be more applicable for this task The process of picking up and delivering the metal disks was only demonstrated under human control of the main aerial vehicle. Autonomous flight was demonstrated very successfully, however, apart from the disk retrieval. To date no one in the competition has achieved the goal of autonomous flight and disks retrieval/delivery together in one flight.

There is one other observation of the 1993 Competition, which may provide follow on Aerobot projects with some valuable information. The only device used for altitude control, at the competition, was the very small and inexpensive range finders used on Polaroid cameras today. They process altitude information accurately and quickly on board the vehicle, without increasing weight. The horizontal positions of the vehicle were provided by external devices, outside the boundaries of the arena, which included TV cameras and infrared sensors.

B. The Moller Aerial Vehicle

AFIT presently possesses an unmanned aerial robot (Aerobot) developed by Moller International and built for the Wright Laboratory. Figure 1 shows a frontal view of the vehicle. Wright Laboratory used the Aerobot as part of a project involving friendly airfield threat detection and damage assessment. The Aerobot has the capability of vertical takeoff and landing, along with sustained hovering, making it an ideal vehicle to achieve the task required to compete in the Aerial Robotics Competition. Use of a ducted fan enables the vehicle to hover and fly vertically. For the Aerobot to actually compete, it would first need modifications to its design. Modifications that are required for the vehicle to compete include: a navigation system, a guidance and stability system, an autonomous controller and a robot manipulator. The guidance and stability system has already been designed in a prior thesis project (5). Designing and building a robotic manipulator arm, to retrieve metal disks, was the next major modification suggested. The design and construction of this manipulator arm is the focus of this thesis report. Further modifications include design of the autonomous control of the vehicle and of the ARM.

The Aerobot gets the lift needed for flight from a seven-blade ducted fan powered by a 48-horsepower rotary engine. Maximum lift produced by the ducted fan is 184 pounds, at sea level. The zero fuel weight of the vehicle is 146 pounds, yielding the available weight for fuel and payload at less than 40 pounds. An magneto provides on-board power which produces 400 watts at 24-28VDC. Maximum endurance is over 30 minutes and it is able to hover in maximum wind gusts of 10 mph.

For pitch and roll axis control, the vehicle uses eight air scoops which are located below the blades in the air flow. These butterfly shaped scoops move in and out of the slip stream and spoil the lift generated in that quadrant (acting like an aircraft's thrust reversers). Spoiling the lift in a quadrant produces an unbalanced moment on the vehicle, which tips it in that direction. Yaw control is provided by four systems of

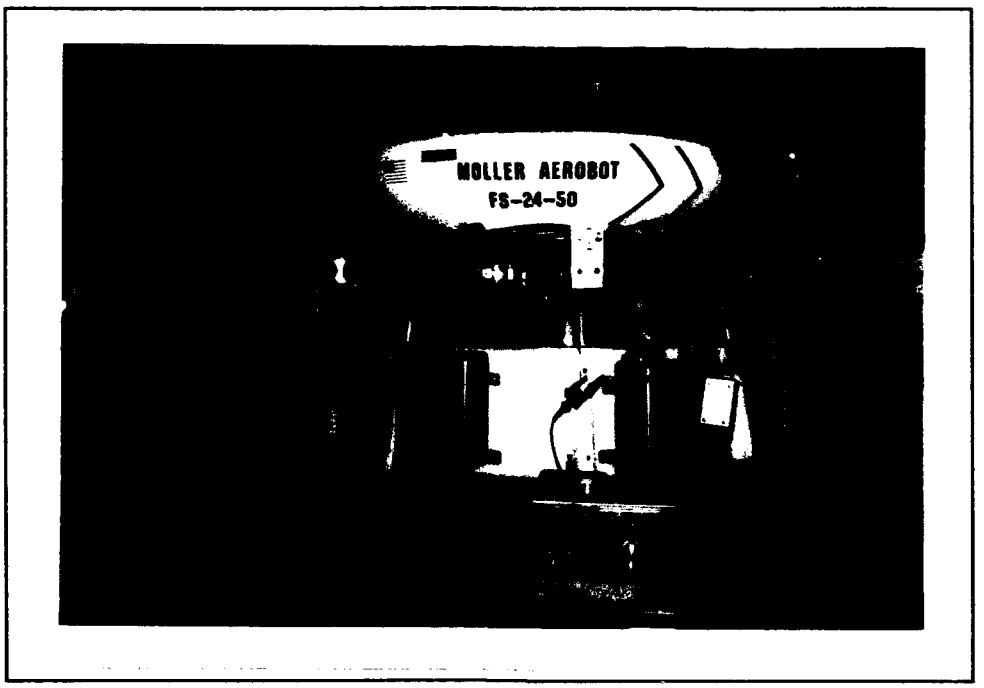

Figure 1. The Moller Aerial Vehicle

vanes (acting like an aircraft's rudder), which are also in the vehicle's slip steam. These vanes are mounted parallel to the fan's air flow and when deflected (in tandem), they deflect the thrust in a clockwise or counterclockwise direction. Figure 2 shows a cut-away diagram of the Aerobot.

The Aerobot uses a gyroscope to achieve stability in all axes. Manual control of the vanes, scoops and throttle is through a radio transmission link (similar to systems available to model aircraft enthusiasts). The radio transmitter sends a signal to the on-board receiver, which in turn sends a 5-volt pulse width command to the controller. The controller then deciphers the pulse width command (which is position control only) and sends 24-28VDC to the component (i.e., motors for the scoops or vanes). The controller continues to send the voltage to the motors until the commanded position is reached (identified by potentiometers) and maintains that position until another command is given. A more detailed description of the Aerobot systems is documented in the final contractor's report (1:4-23)

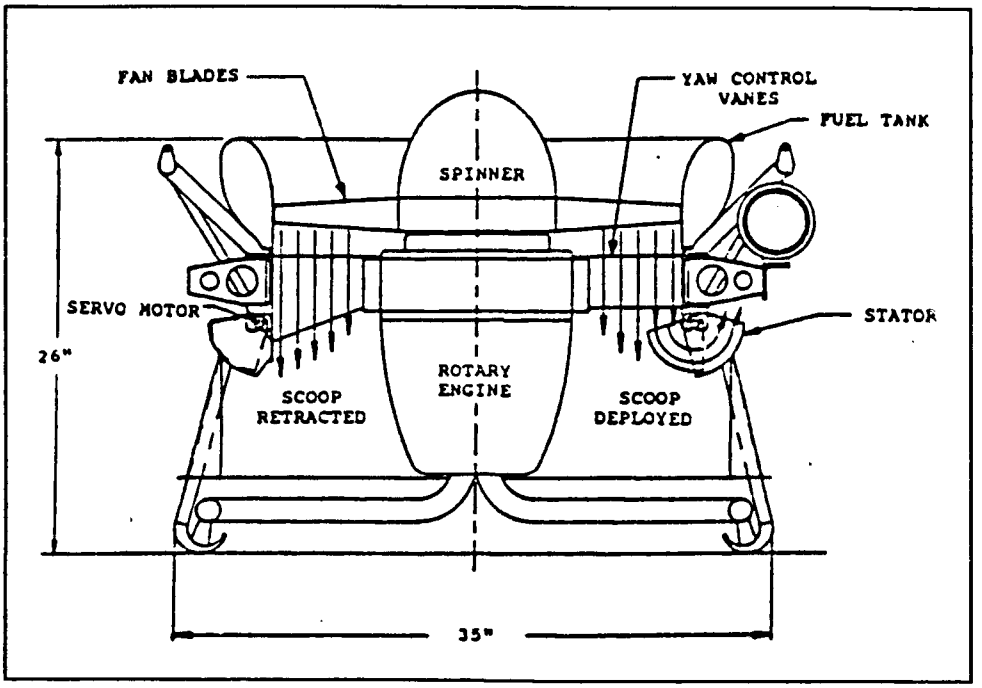

Figure 2. Aerobot Cut-Away Diagram (1:17)

C. Thesis Objectives

Because the Moller Aerobot was built as part of a government study and not specifically of use in the Aerial Robotics Competition, it must be modified with a retrieval system. Therefore, the objectives of this thesis are to design, build, mount, and bench test a robotic arm for the Aerobot. A product of this thesis will be the documentation of the robotic arm modification. Documentation of the work done on the robot arm will aid students who design other parts of the aerial robot and those who work specifically on the robotic arm. This thesis report in itself can act as the "owner's manual" for the ARM. This information will be of vital importance for achieving a fully capable UAV for competition.

The design of this particular arm will be specific to the task at hand. Picking up the ferrous metal disks, specified by the Aerial Robotic Competition, will be its sole

task. Also, the arm will be designed specifically for the Moller Aerial Vehicle, to enable the vehicle to possibly compete in the Aerial Robotics Competition at a later date. Although the design is going to be fairly specific, there will be other areas that this thesis will influence. By using the unique properties and characteristics of this arm, the abilities of other unmanned vehicles can be enhanced. Potential use of the arm could be as a boom (to mount sensors on). This would enable sensing away from the environment of the vehicle, insuring uncontaminated sampling. Another potential use of this arm concept could be as a mobile camera mount. A movable camera mount would enable virtually a 360° viewing area. A large viewing area would be of great use when obstacles or cover are present. Another potential use of the arm could be as a research vessel for aerial refueling booms on aircraft.

The order and organization of this thesis follows closely to the steps taken to design and construct the ARM. A discussion of these steps (i.e., chapters) follows:

(i). Design specifications were established for the project in order that a conceptual design could be finalized. Several designs were looked at closely before the final product was established. (Chapter II)

(ii). Individual parts of the ARM were then designed to match the overall specifications and to work in harmony with other parts. As each part was designed, the AFIT fabrication shop was tasked with making the parts. Dimensioned drawings of certain parts are included in Appendix B. (Chapter III)

(iii). A kinematic model was developed to facilitate automation of the robotic arm (for further research endeavors) and to simulate its operation. As a robotic standard, Denavit-Hartenberg convention was used to develop this kinematic model. (Chapter IV)

(iv). Performance of the ARM was evaluated first by observing its ease of operation and noting problems that might be a factor. To quantify how well the kinematic model actually simulated the operation, position data was collected from an

Optotrak noncontact, position sensing device. This data was compared to the model and analyzed. (Chapter V)

(v). Results of the project included the overall problems found and the possible solutions to those problems. Final conclusions were drawn and included in summary form. Recommendations by this thesis author were made to give further research topics for AFIT students to consider. Details of how some of the recommendations could change the operation of the ARM were also included. (Chapter VI)

II. Conceptual Design

Before a conceptual design of the ARM could be finalized, certain design specifications had to be established. Knowing these specifications, a particular design could be examined and evaluated on its merits as a possible manipulator for the Aerobot. Both the specific task of metal disk retrieval in the Robotics Competition and the individual characteristics of the Moller Aerial Vehicle played a part in establishing the specifications needed. Six different designs were proposed and eventually examined. Only two of those designs were considered in the final stages. This chapter will show the process which established these specifications. It will also describe the designs proposed along with their pros and cons. Finally it will present the resulting design along with the thought process that went along with its creation.

A. Design Specifications

During the first few months of this project, preliminary testing on the Aerobot for was conducted in connection with other research. Some of the initial findings showed potential problems in the areas of payload weight, center-of-gravity changes, vehicle vibrations, and excessive blast from the ducted fan. These areas were some of the first in which certain criteria was created for the finalized version of the robotic arm.

As presented earlier, the Aerobot's combined fuel load and payload weight (as stated by the builder) is less than 40 pounds, under the best of conditions. Given less than perfect conditions and a fuel load for at least a six minute flight, the resultant weight for any extra payload is reduced to a conservative figure of 20 pounds. It is reasonable to expect that additional equipment, other than the arm, will be mounted on the Aerobot to ready the vehicle for competition. In particular, the vehicle will need a navigation system which will probably include at least one TV camera. Both the vehicle and the ARM will need autonomous controllers along with radio data linking devices to

transfer information to computer banks on the ground. The robotic arm will need a camera or some other sensing device to acquire the metal disks. With all these added features to the Aerobot, the allowable weight goal for the ARM was set at 10 pounds or less.

Given this weight limit as a design specification, the ARM must be constructed with light, yet durable, material. Aluminum, graphite (or other composites), and plastic possess these traits. However, graphite is expensive and hard to obtain. Working within a tight budget dictated using material that were readily available. The AFIT fabrication shop had a good stock of aluminum and plastic with which the robotic arm could be built. Also, the experience level using these materials was high. Therefore, the actual construction time would be shorter using these two materials.

Obviously, since weight was such a factor, everything that could be done to keep the total weight of the ARM down, would be of importance. Use of small components, lightening holes, and thin materials would help to achieve this goal. Placement of the weight was also of significant concern. Placing 10 pounds on the side of the Aerobot could change the center-of-gravity (cg) considerably. How much the added weight of the ARM will change the center-of-gravity is unknown at this time. Also, another unanswered question was how well the present control system compensates for the robotic arm and stabilizes the vehicle (with the added weight and resulting moment). Obtaining flight test data to answer these questions was not a possibility because of vehicle maintenance problems, lack of flying experience, and another thesis project using the Aerobot extensively. The Aerobot thesis will provide the equations of motion, the simulation model and the actual flight testing of the control system. With this information in hand, questions of stability and control robustness can be addressed. Therefore, the best approach in establishing a conceptual design specification was to keep the weight as low as possible and to concentrate the weight as close as possible to the present center-of-gravity.

Vehicle vibration was another potential problem area. Robotic arms attached to the frame of the Aerobot will experience large vibrations caused by the ducted fan engine. To minimize the ill effects of vibrations, all tolerances in construction must be as small as possible and flexible building materials must be avoided. Herein lies the fundamental problem of design. When one changes an aspect of the design to better the performance in one area, there is a corresponding negative result in another area. In this example, using less flexible material usually means making the material thicker and more rigid, which in turn means more weight.

Preliminary operation of the Aerobot also presented a problem with using the area underneath the vehicle as a workspace for the ARM. Because of the size and weight of the vehicle, a large amount of lift (150-180 pounds) must be produced to allow it to become airborne. With this amount of lift, turbulence is present. Working in an area of great turbulence is not desirable. This complicates the process of retrieving the metal disks. The robotic arm would be buffeting around underneath the vehicle's slip stream making the task of collecting the disks nearly impossible Since the metal disks only weigh 4 ounces, they would also be blown around underneath the engine blast. Therefore the workspace for the robot to operate out of this turbulence was established well below and off to the side of the vehicle in flight. To quantify this area, the decision was to operate the vehicle at a height of 3 feet above the ground and retrieve disks just out of the vertical blast from that height. The target height of 3 feet was established because 2 feet was too low to operate the vehicle safely (because of the ducted fan blast and the possibility of operating in ground effect) and 4 feet was too far for a robotic arm to reach.

With the general area outside of the engine blast designated for the proper workspace, the next question to answer is about the size of that workspace. Typical accuracy requirements for robots are in fractions of inches, for the ARM the accuracy requirement will be set at one inch (given the diameter of the metal disks is 3 inches).

Using the results of Llewelyn's model of the guidance system designed for the Aerobot, errors in the plane parallel to the ground should be less than 6 inches. Errors expected for the vertical direction are even better (less than 1 inch) (5:6.6). This thesis project will assume that the Aerobot will provide an inertial platform with the stated error and the Arm will move to pick up disks. Since the ring that will hold the disks is 6 feet in diameter, making the workspace the size of the ring would be unwise because to accommodate the vertical and horizontal separation required for blast avoidance, the extended arm must be much longer than 6 feet. This would violate most of the previously determined design requirements. Therefore, the only possible recourse was to limit the size of the workspace below the 6 feet figure. Obviously the space must be large enough to allow the ARM to compensate for the error introduced by the vehicle's guidance system. Therefore the smallest possible workspace would have a 6 inch diameter. To accommodate any other errors that might be created, an 18 inch diameter workspace was therefore established as a design goal.

In order that this smaller workspace would accomplish the overall task of disk retrieval, a "plan of attack" must also be designated. Basically the navigation and guidance system would identify the coordinates of the ring. Then the vehicle would position itself over the ring. The ARM's disk acquiring device (probably a TV camera) would then identify the coordinates of the individual disks and have the vehicle center the ARM's workspace over the desired disk coordinate. Then the ARM would retrieve the metal disks.

Typically aerial vehicles are not given the task of touching objects or the ground while in flight. For this reason, very little documentation was available for vehicle designs that might achieve this task. Therefore, most of the designs examined here were new concepts specific to the task. Because the vehicle will work so close to the ground, a requirement for the final design must include the ability of the robotic arm to either fold up or retract out of the way in case of a crash landing or a sudden downward

movement of any kind. This is a safety concern for the vehicle. Working close to the ground and reaching out and touching the ground with a solidly mounted arm opens up the possibility of tipping the vehicle over during such an operation. If the arm has the ability to passively fold or retract, then damage to the vehicle in such a situation might be avoided. This is also an important feature for normal operation. Given the workspace described earlier, the arm must be able to reach this workspace and also be able to retract to a much smaller size for normal landings. Also, during flight, the weight of the arm should be concentrated near the center-of-gravity for stability reasons. Flying with a long extended arm could also increase drag considerably. Therefore retractability is an important specification for the final design.

Because of the short length of time allowed for this thesis project, several more criteria became important, namely, simplicity in analysis, controlled operation and construction. Therefore, it is a necessity for the ARM to stay as simple as possible yet meet the design specifications. This means that achieving decoupled operation with a linear mathematical model would be a goal that could achieve simplicity of both analysis and control. Decoupled operation means creating motion in one dimension at a time only. In other words, if an XYZ coordinate system is used, then motion of the ARM to achieve a point in the X direction will not yield any change to the Y or Z components. This is not necessarily an easy task. Because the ultimate goal is to pick up metal disks from the ground, which is in essence a plane, use of planar coordinates is necessary. Use of this coordinate system instead of polar coordinates introduces coupled operation. Therefore decoupled operation must be obtained through judicious design and not through the use of a convenient coordinate system. Linearity of the model can be obtained by linearizing the equations derived for the model of the robotic arm. It also can be achieved through the design process. Linearity yields a model that takes less calculation time in operation under automated control. Less computation time yields quicker response time and less lag time. It also yields less error as positions

change rapidly.

As stated earlier, a short construction time was an important constraint of the project. Keeping the design simple to build and using readily available material dictated much of the design process. A simple design meant using as many self contained components as possible. A self contained component can be viewed as one that can come "off the shelf" and do as many specific tasks as possible. A good example of this were the motors that were used (a more complete discussion of the components is found in chapter 3). They were electric motors and gear boxes mounted together as one unit and could be attached to optical encoders (again, as one unit). Therefore three tasks could be performed by one unit. The motor would provide motion to move the arm. The gear box would provide the necessary torque to compensate for any loading on the motor. And the optical encoder would provide motor angles which could be converted to position information for the robotic arm controller.

B. Preliminary Designs

As stated earlier, UAV's do not normally touch the ground during flight, therefore little research is available for ideas. Most of the preliminary designs were adaptations of other robotic devices. Basically they were modified to met the specifications that were established earlier. Each design was examined and evaluated on its own merit according to the specifications. The following five designs were examined and found to be lacking in important areas in which modification could not be performed reasonably.

1. *Tripod.* This design was a modification of a Stewart platform (6:371-386). The modification involved using only three legs instead of six. Thus the name *tripod* refers to the number of legs. Figure 3 shows the design. The *tripod* has a prismatic (linear) joint on each leg and a ball joint (three degrees of freedom, bend/roll/bend) at the spots where the legs attach to the bottom and top plates. This design would have

been mounted on the bottom of the Aerobot and would retract into space under the ducted fan engine. Advantages of this design included: it retracts into a small space within the vehicle, it is a very rigid design with the three legs attached at all ends, and its weight is centered below the center of gravity. One of its disadvantages is the lack of maneuverability and workspace. The disadvantage that could not be modified was the fact that it operated in the slip stream of the vehicle. This presented two problems. One which was stated earlier is the turbulence encountered within this region. The other problem is that the lifting ability of the ducted fan could be affected by putting objects into the slip stream. Consequently, this design was abandoned.

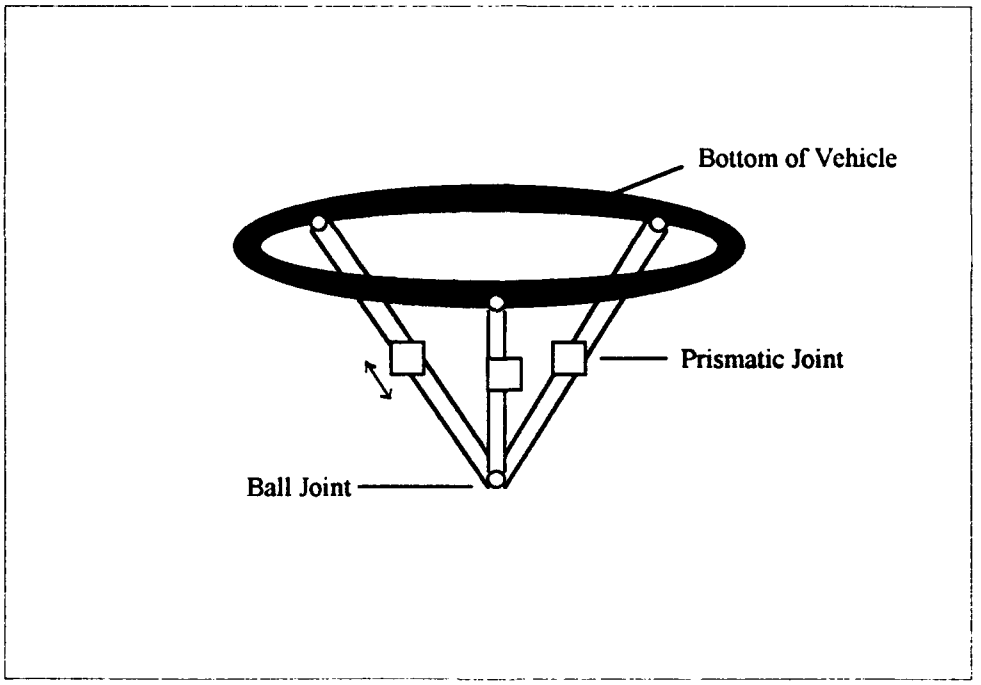

Figure 3. Tripod Design

2. *Serial Arm.* The majority of the robotic arms constructed today are patterned after the human arm. Basically they have successive arm segments connected in series. Figure 4 shows a representative sample of a *serial arm.* Each arm section has its own actuators and linkages which are usually mounted at the beginning of each segment.

Therefore, because much of the arm's weight is placed further from the base of the arm, a large moment is created and the base must carry most of this load. Because of the serial nature of this design, errors from each arm section add to create larger errors. Another disadvantage is the problem of achieving rigidity. With that much weight out on the end of a boom, vibrations will be a problem and so will the change in center-of-gravity. Typical design keeps the motor size small to control the weight but sacrifices strength in the process. On the plus side, the serial arm can be easily retractable and the maneuverability is quite impressive. Its maneuverability and the large work space it provides is a big selling point for this design. But the reason that it too was abandoned was its sophistication. With actuators and linkage in each successive arm segment, the construction was too complicated and expensive for this project. Finally, to carry the load on the extended portions, the base would require large amounts of strengthening, resulting in higher weight.

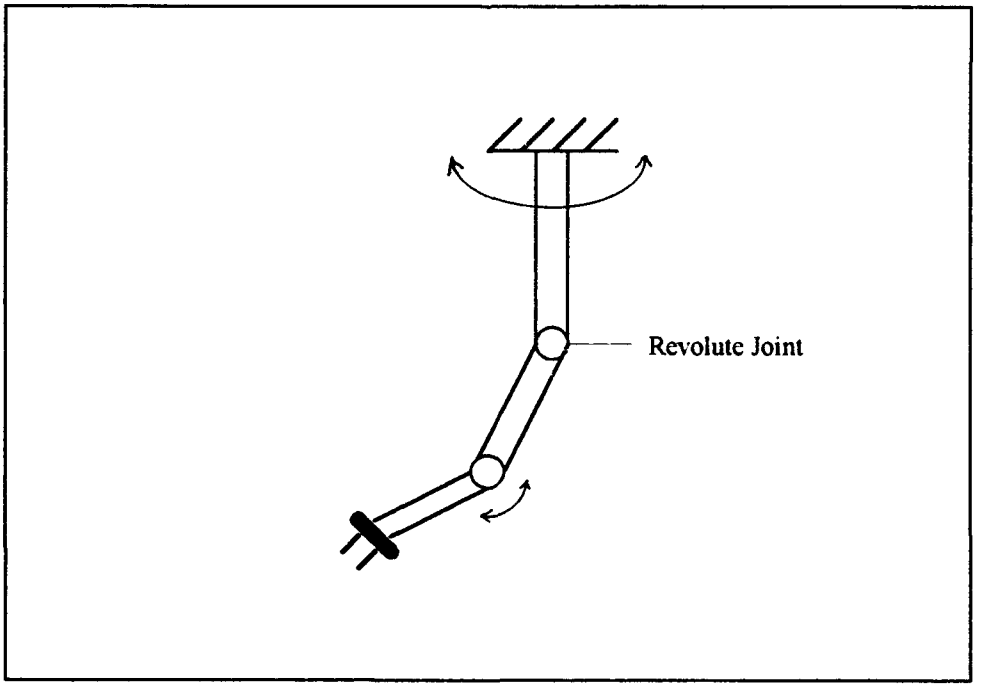

Figure 4. Serial Arm Design

3. *Rail.* This design was born from the necessity to find readily available components. Figure 5 shows a diagram of the *rail* design. The design of the *rail* manipulator came about from browsing through catalogs of linear drives. The parts were easily available through the companies and construction was only a matter of combining all of the various parts. At first, the thought was that a complete linear drive, manufactured by one of these companies, could be used. None of the pre-assembled drives were long enough to reach at least 3 feet, therefore the components were found that would reach that far. A discussion with the AFIT fabrication shop led to the determination that purchasing readily available parts was not necessary; the AFIT fabrication shop would be able to create most any part needed. Some of the high points of the design, besides the pre-assembled availability, were the rigidity and simplicity of design. This was the first design geared toward achieving decoupled operation. The negative aspects of the design included limited maneuverability and workspace, high weight, and slow speed. Because of the rails and the worm drive, this design was potentially very heavy. Speed was never considered before, but the worm drive rail could have been very slow (too slow to react to the vehicle movement or to satisfy the need for rapid retraction). This design did not fill all of the specifications so it was not considered a viable option.

Although the determination to discard this design came fairly quickly, major design features used on the final design began to materialize. Linear actuation of the arm, which indicates a prismatic joint, was seen as a solution to decoupling the motion. The planar motion actuators were mounted at right angles to each other and orthogonal to the worm drive. Motion from one actuator yielded displacement primarily in one dimension. Depending on the overall design, this does not necessarily achieve complete decoupled operation. But, for operation within a small region it can be approximated as being decoupled. Therefore key features to carry to the final design included: a prismatic arm, and three actuators (one for each degree of freedom)

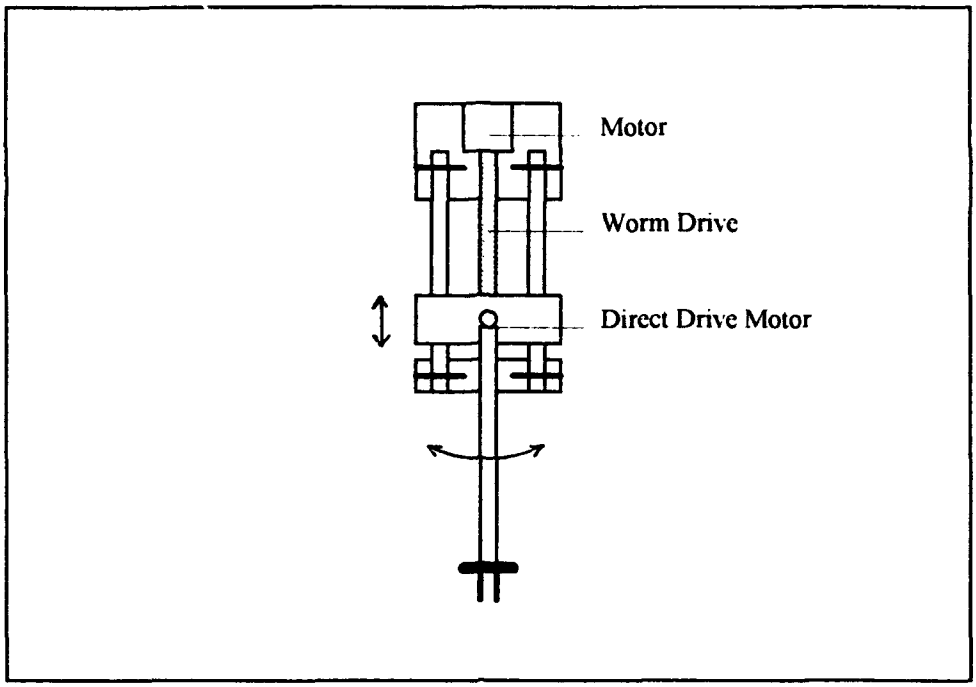

Figure 5. Rail Design

mounted orthogonally.

4. *Lever Arm.* The use of a prismatic joint for the arm was solidified in the last design. The basic concept of a prismatic joint is a telescoping joint. Figure 6 shows the *lever arm* design and its use of a telescoping arm instead of the worm drive. This design again used three actuators mounted orthogonally. The two actuators providing planar motion (parallel to the ground) were not used as direct drives as in the previous design. Some concern developed that the weight of the arm would be too much for the motors to handle if actuated at the pivot points. So, the motors were moved to locations further down the arm to provide more leverage. Moving the motors down and away from the pivot point created some problems, specifically the compactness of the design and the mounting of the motors to create leverage. Spreading out the motors took away the compact principle of the rail design. It also created a sprawling mass of booms, cables, springs and levers with which the planar motion would be achieved. This configuration would create complications in the construction phase and the control of

the device. Further investigation into available motors proved that direct drive could be achieved through the use of gearing. Increasing the gear ratio of the motors provided more torque for increased loading, but slowed the motors motion. This was not a problem because even the slowed motion was fast enough. This design was abandoned because it was not compact and because of the complicated configuration.

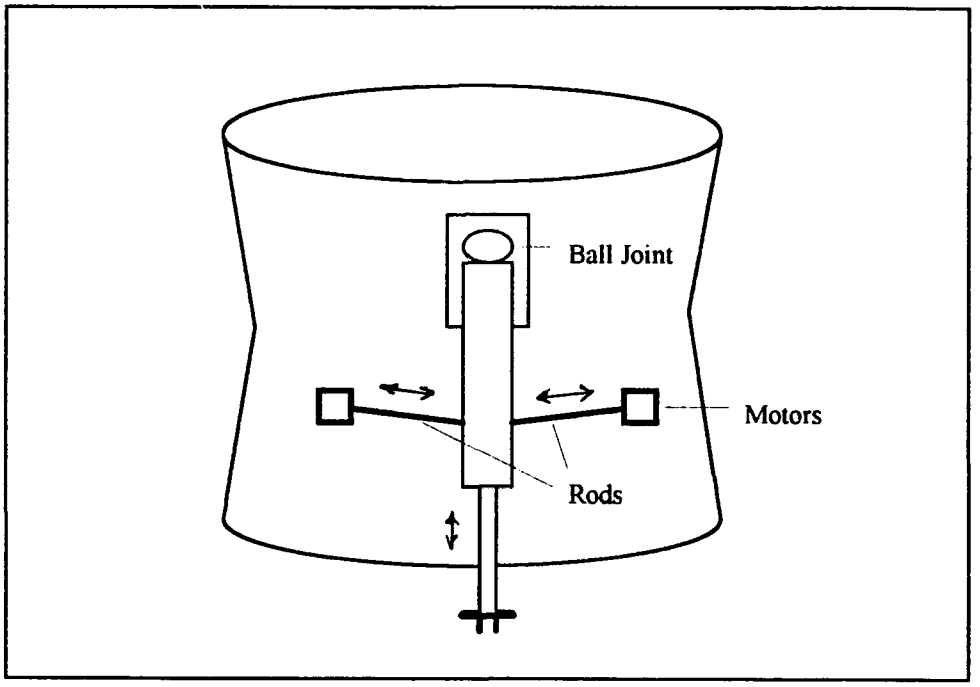

Figure 6. Lever Arm Design

5. *Landsberger Parallel Link Manipulator* During an earlier search for documentation of robotic designs, a robotic arm design by Samuel E. Landsberger was found to possess many of these needed traits. It showed great promise for application with the Aerobot. Landsberger (7) designed a three-motion parallel link arm as a masters thesis at MIT. Figure 7 shows a diagram of his design. The main components of the manipulator include: a telescoping arm, three active tension cables, three motors to operate the cables, a universal joint connecting the arm to the base, swivel pulleys and constant radius cable spools. Basic operation is achieved by coiling or uncoiling

cable on the spools. To retract the arm, all three motors coil cable onto the spools at the same rate. To extend the arm, all three motors uncoil cable at the same time. To move the end effector to a given position, one or two motors

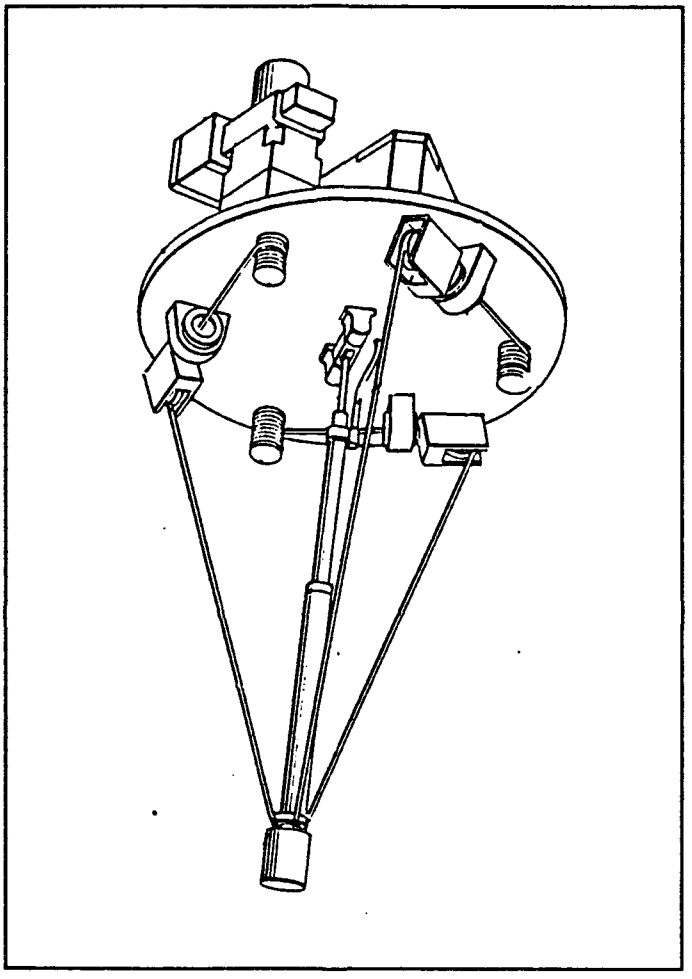

Figure 7. Landsberger's Parallel Link Manipulator Design (7:80)

coil cable while the other motor(s) uncoil. In essence, the three cables act as telescoping actuators, and each are independently position controlled. Because the actuators are not operating orthogonal to each other there is coupling. But Landsberger assures us that the kinematics are fairly simple (7:19-26).

This manipulator was of great interest for this thesis. It provided much rigidity with the use of the cable linkages. This would be of importance in preventing the

vehicles vibrations from negating the work of the arm. It also concentrated the weight of the actuators at the base. This would help keep the vehicle's center-of-gravity from changing drastically. The entire design came in one compact package, making it easy to mount. Retractability was achieved by the use of a telescoping arm. The arm keeps a constant tension on the cables by using passively controlled hydraulic pressure. This would be of great value on the vehicle. In case of a crash landing or touching the ground with the arm, it would retract as the load of the vehicle pressed down on the arm.

For many reasons the Landsberger arm seemed to be the right choice for the final design. Most all of the design specifications were met. The one real concern was the coupled operation. Coupling in itself is not bad. It just complicates the mathematics of deriving and using the model. With proper control, a robot with coupling can perform most any task. The problem lies in establishing the right controller. The underlying goal was to keep the control of the arm as simple as possible and if uncoupled motion could be established then that goal would be met. There were two reasons why this design was not used. The main reason was because of the coupled operation of the device. The other reason was because of the potential difficulty in achieving adequate speed in the lateral direction. Because the device must retract the arm to provide lateral movement, it has some difficulty with performance in this parameter. Therefore the decision was not to use the Landsberger design as it stood, but to use some of the features that made it such a good design and apply them to decoupled motion.

C. Final Design - The AFIT ARM

Specific features of some of the designs discussed earlier manifested themselves in the final design. The final design process basically meant taking the best parts of these designs and coordinating them together. Principle features that were taken from

the other designs included: a telescoping arm, compactness, and decoupled operation. The result was a hybrid of all the designs mentioned and was named the Aerobot Robotic Manipulator (ARM).

The ARM is the finalized design of this thesis project. It incorporates together all of the advantages seen in the prior designs. Figure 8 shows a conceptual diagram of the ARM. The design uses a telescoping arm which expands under passive control using springs and retracts under active control using a motor and cable assembly. The cable is attached to the last link and the arm retracts as the motor coils cable onto a spool. An electromagnet is attached at the very end of the arm to retrieve the metal disks.

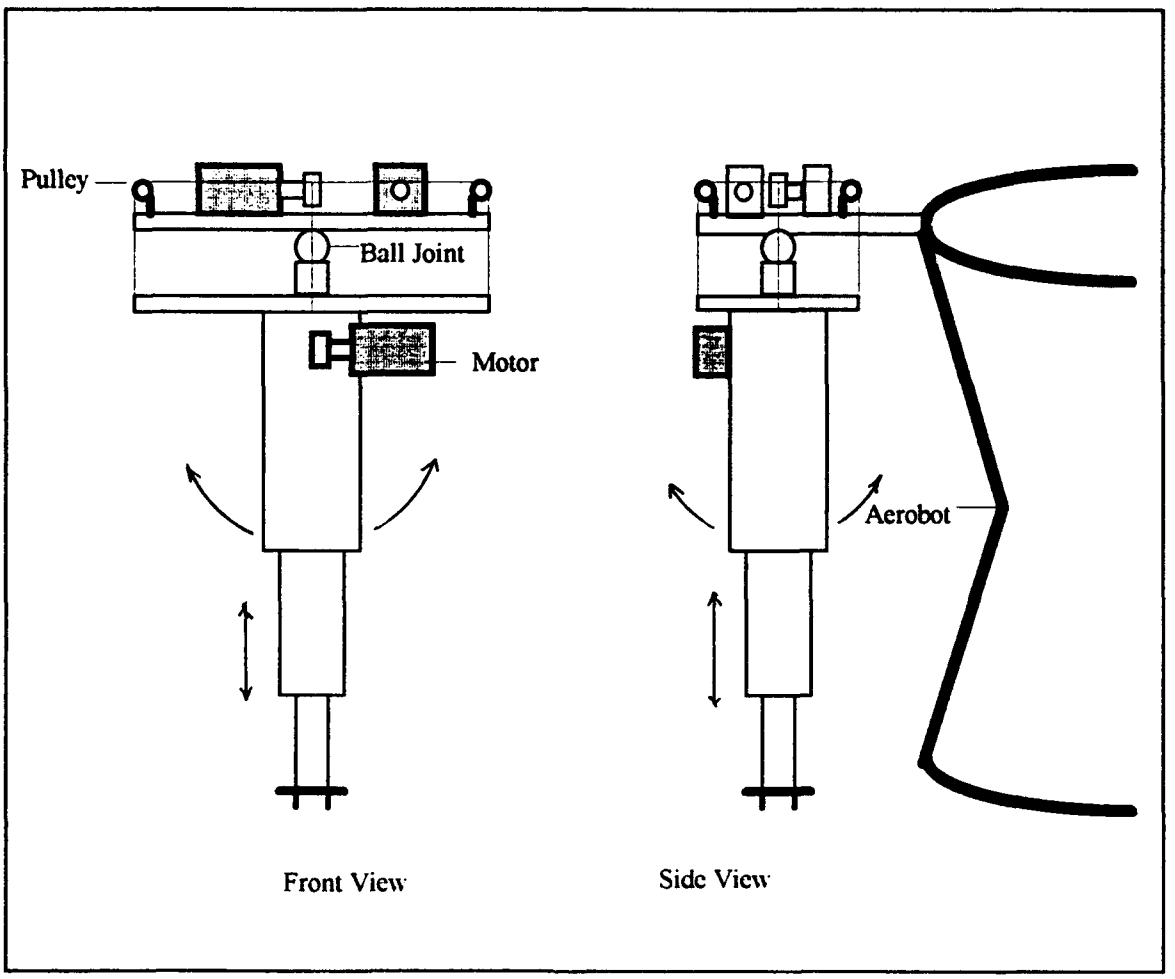

Figure 8. The AFIT ARM Design

The base of the entire assembly is the top metal plate, which can be mounted to the side of the Aerobot. The two motors used for planar motion are mounted on the top of the plate. The assumption is that the vehicle will hover in one spot and at a certain altitude, thereby creating an inertial platform. Because the top plate is firmly attached to the vehicle, the inertial reference frame of the robotic arm system will be conveniently located on the top plate, specifically at the center of the ball joint. The telescoping arm is attached to a bottom plate which acts as a lever arm. Cables from each motor are attached to the corners of the bottom plate. The bottom plate and telescoping arm assembly is attached to the top plate through the use of a ball joint. This ball joint provides the two degrees of freedom needed for planar motion of the end effector. The motor and cable assemblies are mounted at right angles to each other to achieve as much decoupled motion as possible. Movement of the bottom plate is provided by the motors, which coil cable onto a spool. Unlike the telescoping motion, the top motors have a double spool. To move the bottom plate in one direction, the motor coils cable on one spool (pulling on the corner of the bottom plate) and uncoils cable on the other spool (keeping constant tension on the cable system).

Examination of the final design shows that the ARM meets the specifications presented earlier in this chapter. Weight was minimized and concentrated as close to the original vehicle center-of-gravity, as possible. The design is compact and easy to mount or dismount from the vehicle. Components of the design are either easily obtainable or can be fabricated by the AFIT fabrication shop. Overall, the basic design is simple yet functional. Some uncoupled motion is obtained through the placement of the actuators at right angles to each other. Use of the cables should provide adequate rigidity to counter vehicle vibrations. Mounting to the side of the vehicle and providing enough length to the telescoping arm enables retrieval of the disks outside of the major engine blast area. And this design also allows for the arm to collapse on itself in an emergency setdown.

The question of workspace available is answered by looking at the dimensions of the design and identifying any restrictions of movement. Figure 9 shows basic restrictions of movement between the top and bottom plates in both degrees of freedom. The restriction of movement on the telescoping portion is the fact that it cannot extend more than the overall length shown in Figure 9 which is 62 inches. If the top of the ARM is mounted 26 inches above the bottom of the vehicle then, when the ARM is vertical, the vehicle will be 36 inches above the ground for maximum retrieval distance. Given the height between the plates and the length of the lever arm on the bottom plate (for the most restrictive angle), the angle that the bottom plate can move through is 20°. The height of the vehicle above the ground in this configuration is 32 inches. The maximum horizontal distance on the ground is 21 inches. Thus the workspace of approximately 3 feet below and 18 inches away from the bottom of the vehicle has been obtained.

With the conceptual design phase of the project finished, the actual construction of the ARM began. The next chapter discusses, in detail, how the specific components came into existence.

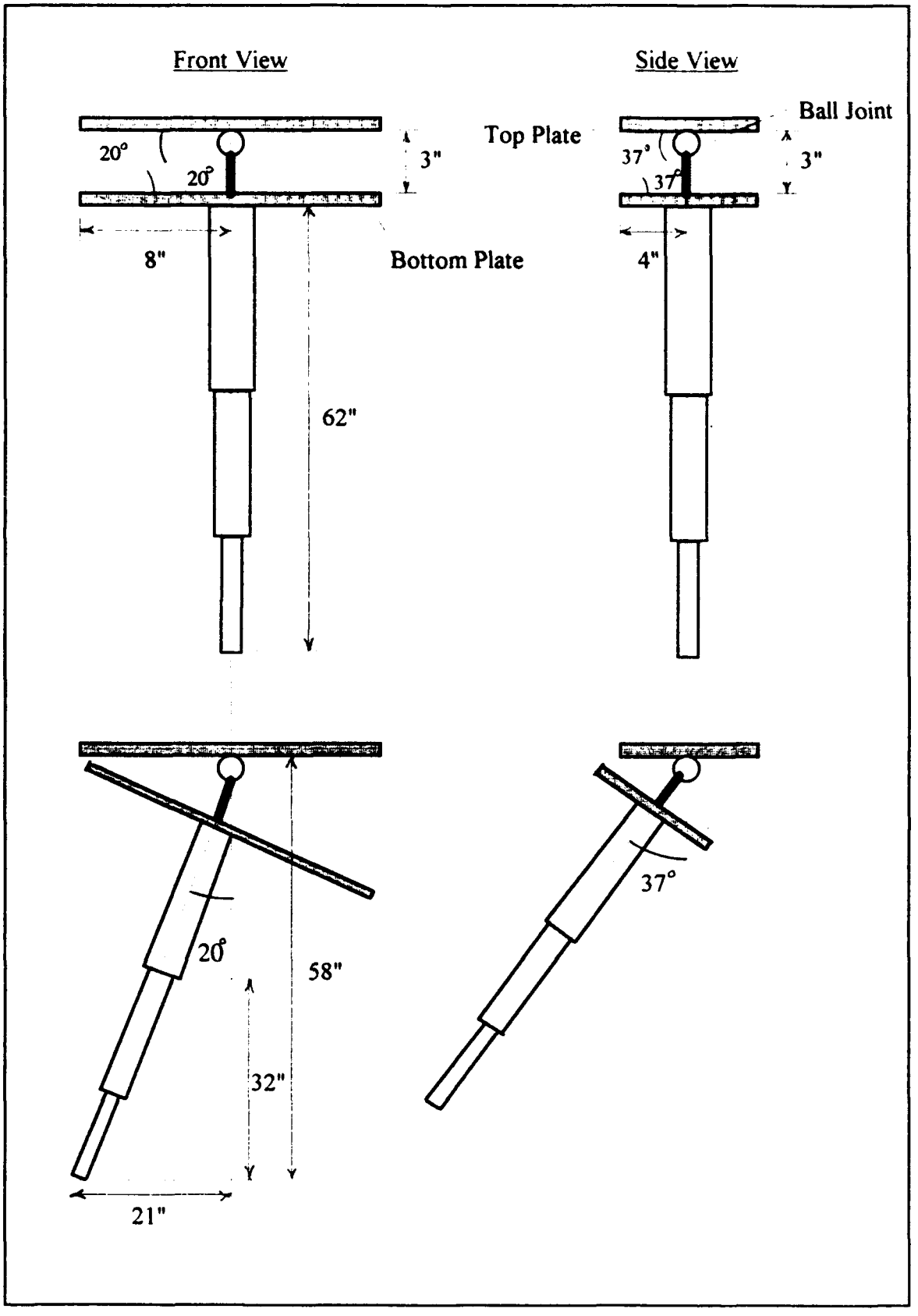

Figure 9. Top and Bottom Plate Movement Restrictions

III. Hardware Design

With the overall design finalized, the next step of the project was to design and fabricate individual components and parts to be integrated together into the final working manipulator . This chapter will describe each part in detail, including design problems and solutions. Applicable formulas used to derive final specifications will also be presented. Dimensioned drawings and component specifications are included in Appendix B. A full-scale version was constructed from the components described below. Figure 10 shows the completed ARM mounted to a prototype of the Moller Aerial Vehicle.

A. Telescoping Arm

The telescoping arm is designed to have passive control for extension and active control for retraction. Passive control is provided with springs. Because of the springs, there is an added safety feature. If for any reason the vehicle had to land immediately or if it lost altitude before the arm could be fully retracted, the arm would just collapse on itself with no damage. The active control comes from a motor. The motor turns, which winds cable on to a spool. The cable runs through all of the tubes and springs and is attached to the last telescoping tube. To achieve the telescoping feature, four progressively smaller diameter and shorter length tubes are placed inside of each other. Three springs are placed at the ends of the three smallest tubes. All of these parts are then locked together with set screws as blocks. Figure 11 shows how the telescoping portion breaks down into individual components.

1. Tubing. The first instinct was to use aluminum tubing because of its high strength and light weight. Because of its relatively high cost, however, it seemed appropriate to consider alternate materials. Polyvinyl chloride (PVC) tubing possesses many of the same qualities as aluminum, but costs much less and is readily available.

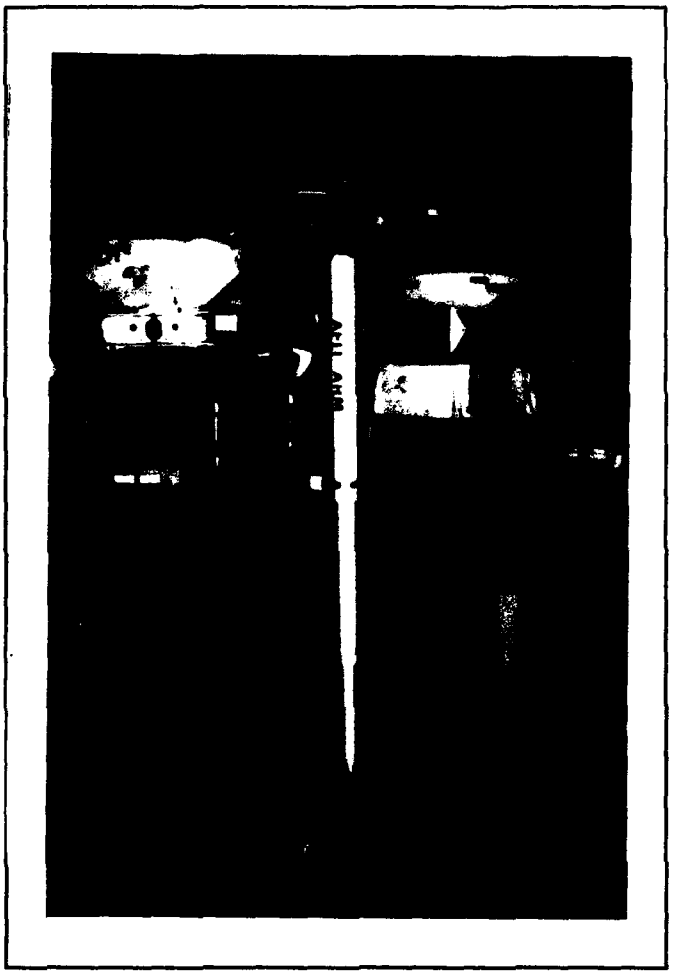

Figure 10. The Completed AFIT ARM

PVC is also easier to work with, resulting in shorter construction times. Other materials such as graphite epoxy or other composites could give higher strength and lighter weight, but the cost would be prohibitive. Because this thesis project was aimed at producing a bench model prototype only, the decision to use PVC was appropriate.

Because PVC comes in standard diameters that do not coincide with successive inside and outside diameters, Teflon sleeves are needed inside of the tubes to hold the next smaller size tube in place. Figure 12 shows the inside of the tubes, which contain the springs, collars and Teflon sleeves. The Teflon sleeves serve two other purposes. One purpose is that the Teflon provides a nearly frictionless surface to slide the tubing through. The other purpose is to provide a stop block for the smaller tubing inside of

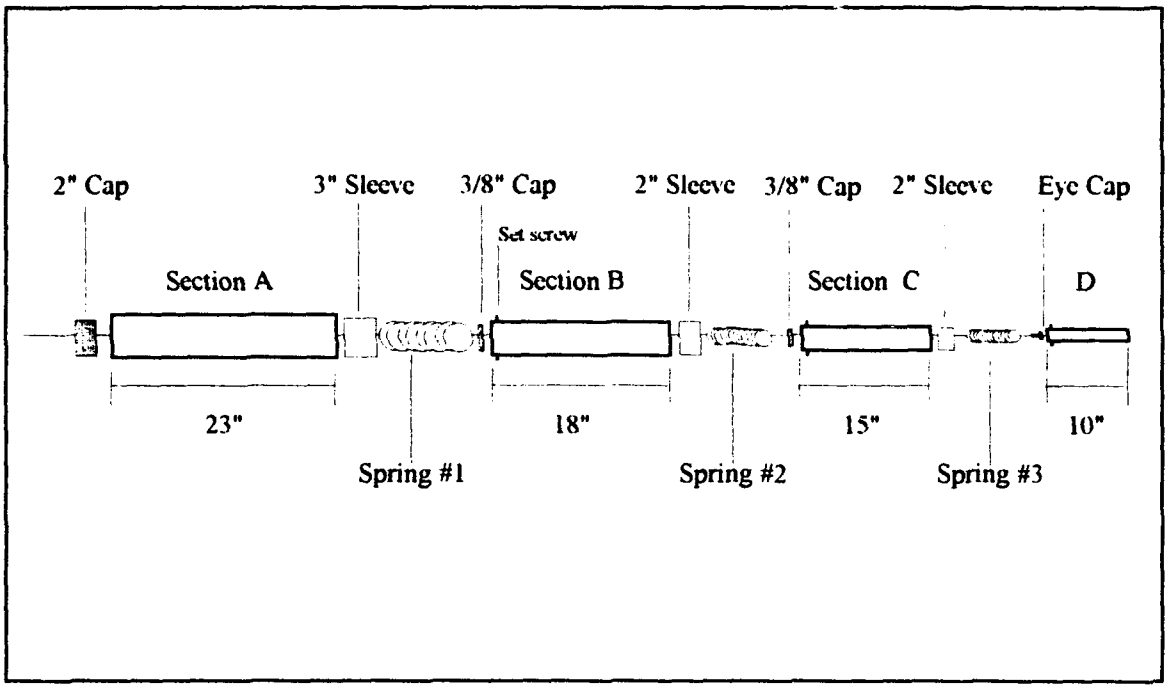

Figure 11. The Expanded Diagram of the Telescoping Arm

the larger tubes. Set screw are placed at the ends of the tubes in such a way that when the spring pushes against the tube, the tube stops as the set screws hit the back of the Teflon tubes (see Figure 11). Ample clearance must be made between the set screws and the inside of the outer tube for smooth operation to occur. Further details can be found in Appendix B.

When PVC tubing is manufactured, it is pulled from a form in a semi-liquid state. Disparities in the diameter are produced. Therefore all of the tubing was turned on a lathe to true them to round. Small deviations in the inside and outside diameters still were present after the initial truing. These deviations created friction that needed to be overcome by the forces of the springs and motors. A complete discussion of these problems are contained in the narrative on those parts. Turning the tubing down increased the tolerance of the fit between the tubing and the Teflon sleeve. This increased the amount of play in the extended arm which decreased the rigidity of the

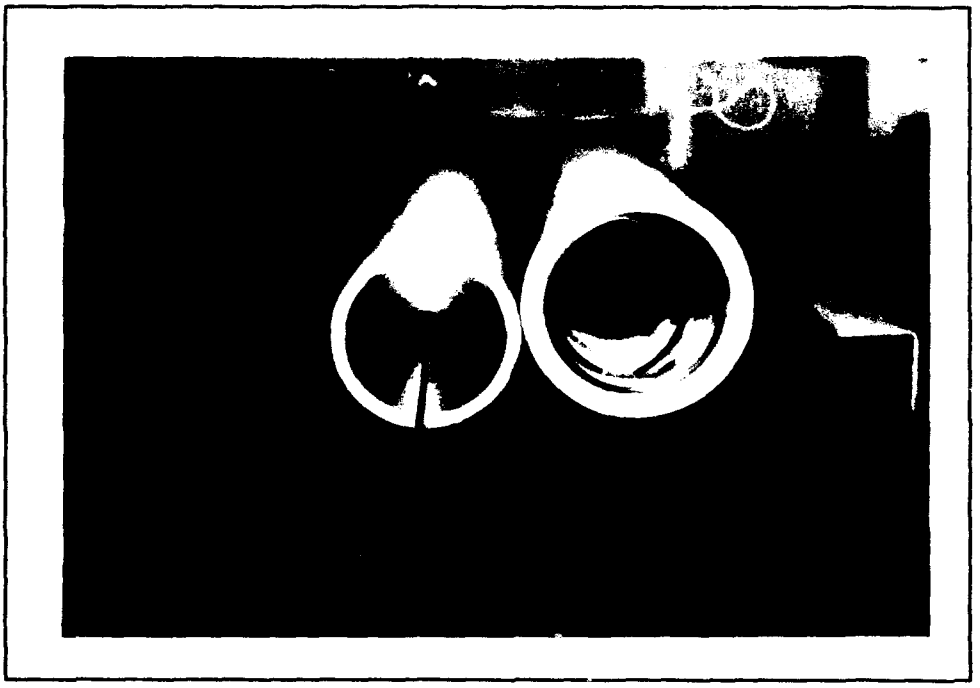

Figure 12. The Insides of the Tubes

entire structure. Therefore there was a tradeoff between eliminating friction and retaining rigidity. Quantifying the magnitude of the deflections, caused by the tolerances between the sleeves and the tubes, would yield valuable information on the rigidity of the arm. But, before the deflections could be derived, a final decision on the lengths of tubing was needed.

As is the case of any design work, there are always tradeoffs to consider. This was certainly the case in deciding the lengths of the tubes. The overall goal was to be able to reach to an area 3 feet below the vehicle and be able to retract the arm sufficiently for landing. Another consideration was to keep the arm mount near the vehicle periphery. There were also smaller details that played as much of a factor as the overall goals. For rigidity, a small portion of each telescoping section must be inside of the tube that it fits into. The Teflon sleeves also take space inside of the tubing that cannot be retracted. A small portion of space inside of the fully compacted arm must also be allocated for the fully compressed springs.

To show how the lengths of the tubes were obtained, some numbers must be presented. The basic constraints for the design of the telescoping arm were: total length, Teflon sleeve lengths (for support), compressed spring lengths, available reach of each section, and allowances for all components in the retracted position. Figure 2 shows the height of the vehicle as 26 inches. This was a target height for the fully retracted arm. Figure 9 shows the distance between the top and bottom plate as 3 inches. Figure 11 shows many of the dimensions that will be described below. Thus the largest tube (the tube that will contain all of the other tubes when it is retracted), labeled section A, must be no longer than 23 inches. Assuming at this point that the bottom of section A coincides with the bottom of the vehicle, the height requirement of 3 feet will be obtained by the other telescoping sections only. Due to the fact that all of the extended arm will be supported by this first section, it requires the longest Teflon sleeve to provide the highest rigidity possible. Inserting a sleeve inside each section subtracts from its available reach and from the overall total extended length of the arm. On the end of section A, an aluminum cap is used to mount the entire telescoping arm to the bottom plate. This cap (which smaller versions were used on all of the other sections) also is used to contain the spring within the section. Placing a cap inside of the tube subtracts from the length allowance for section B and subsequently the available reach. An allocated distance within section A is also reserved for the compressed spring. This allowance also produces a shorter section B and its available reach. Using the information from all of these constraints, the maximum total length of section B can be obtained and its available reach can be calculated. Each subsequent section can also be analyzed in the same way. Table 1 provides the final dimensions of all of the telescoping arm parts. Adding the available reaches of all of the sections yields the total telescoped length.

Table 1. Final Tubing Measurements

Section	Length	Sleeve	Spring	Cap	Reach
A	23"	3"	3"	2"	
B	18"	2"	3"	3/8"	15"
C	15"	2"	3"	3/8"	13"
D	10"			1/4"	8
Total					36"

Now that the lengths of the tubing are established, the deflection from the gaps between the tubing and Teflon sleeves can be calculated. Figure 13 shows the geometry involved in calculating the deflection. Basically, when a side load is placed on the tubing, the inside tube pivots at the point where it exits the previous tube. This forms two similar right triangles. It is possible to find the total deflection (E_{Total}) of the telescoping arm using the following formula:

$$E_{Total} = \sum_{i=1}^{3} T_i \tan\left[\sum_{k=1}^{i} \arcsin(e_k / t_k)\right] \qquad (1)$$

where t and T are the lengths of the tube inside and outside the previous tube, respectively, e is the gap between these tubes and subscripts 1, 2, and 3 correspond to sections B, C, and D, respectively. The average tolerance between tubes in the final product (after truing) is 0.005 inches. Therefore the total deflection due to the manufacturing tolerance of the tubes is less than 0.15 inches , which considered acceptable. This method of calculating deflections was used in an earlier iterative process to determine the smallest amount of tubing that must remain in the previous tube while still giving reasonable deflection values. This process was used to determine

the appropriate Teflon sleeve length found in the section earlier.

Because PVC tubing was being used instead of aluminum, there was some concern about the overall rigidity of the telescoping arm. This concern was addressed though a static deflection analysis on the entire arm. This analysis can be broken down into two parts. One part is the analysis for the deflection caused by an applied load at the end, such as the electromagnet. The other part is the analysis for the defection due to the distributed load of the arm itself. Both parts of the analysis will model the arm as a cantilevered beam with tapering sections.

For the applied load analysis, the second theorem of Castigliano was used. It may be written as:

$$q_r = \frac{\partial U}{\partial Q_r} \tag{2}$$

where the q is the displacement, r is any point on the structure, U is the total strain energy, and Q is the corresponding force. For a cantilevered beam, the strain energy expression is:

$$U = \frac{1}{2}\int_x \frac{M^2(x)}{EI}dx = \frac{1}{2}\int_0^{8}\frac{M_{12}^2}{EI_{12}}dx + \frac{1}{2}\int_0^{13}\frac{M_{23}^2}{EI_{23}}dx + \frac{1}{2}\int_0^{15}\frac{M_{34}^2}{EI_{34}}dx + \frac{1}{2}\int_0^{23}\frac{M_{45}^2}{EI_{45}}dx \tag{3}$$

where M is the moment applied at the point, E is $1450\ \text{lb in}^2$ the modulus of elasticity for PVC, and I is the moment of inertia for the given section. As labeled in Figure 13, section A corresponds to subscript 45, section B corresponds to subscript 34, section C corresponds to subscript 23, and section D corresponds to subscript 12. The moment is defined as $M = M_0 + F_y x$, where F_y is the load applied at the end of the beam and x is the length of the beam section and after the slope is found M_0 is set to zero which implies it was nonexistent at the start. Therefore, after substitution:

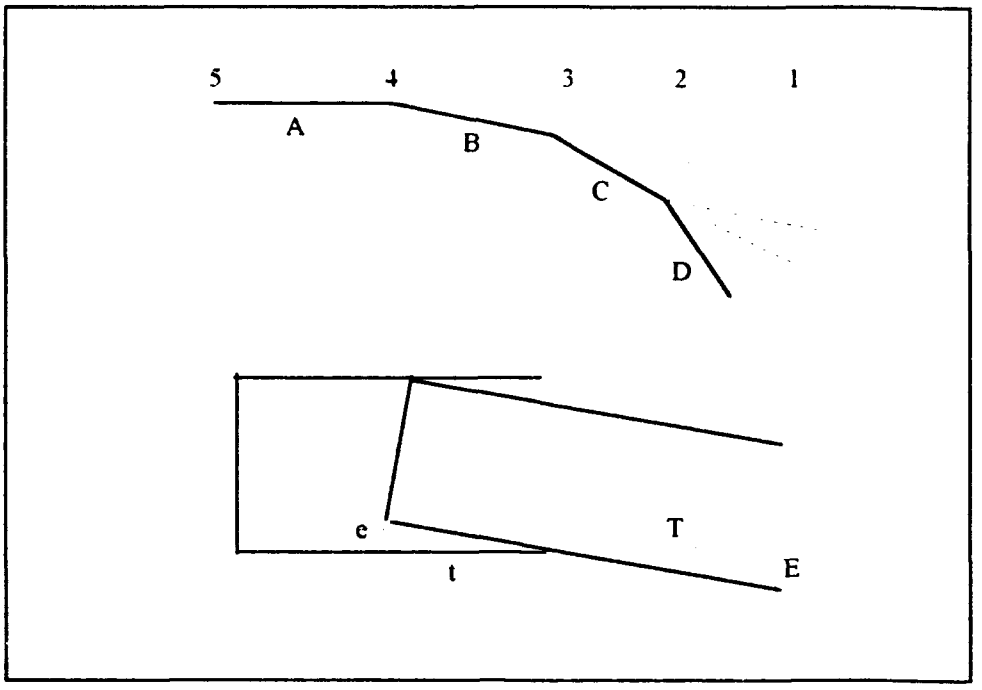

Figure 13. Tubing Tolerance Deflections

$$U = \frac{1}{2EI}\int_x \left(M_0 + F_y\right)^2 dx = \frac{1}{2EI}\left[x M_o^2 + x^2 M_0 F_y + \frac{1}{3}x^3 F_y^2\right] \tag{4}$$

And using Eqn. (1) yields:

$$\delta y = \frac{\partial U}{\partial F_y}_{M_0=0} = \frac{F_y}{3E}\left[\frac{8^3}{I_{12}} + \frac{13^3}{I_{23}} + \frac{15^3}{I_{34}} + \frac{23^3}{I_{45}}\right] \tag{5}$$

where δy is the displacement (8:150-153). The moments of inertia for each section is found with the formula:

$$I = \frac{1}{12}b^3 h \tag{6}$$

where b is the diameter and h is the length of each section. Thus

$$I_{12} = 0.446 in^4, I_{23} = 2.38 in^4, I_{34} = 12 in^4, \text{and } I_{45} = 36.45 in^4.$$

And finally the final displacement due to a 0.5 pound load at the end of arm (with the arm at 20° from vertical) is less than 0.1 inches

For the distributed load analysis, three equations are needed, they are as follow:

$$\delta y_i = \frac{m_i l_i^3}{8EI} = \frac{(q\, l_i) l_i^3}{8EI} = \frac{q\, l_i^4}{8EI} \tag{7}$$

$$\delta \psi_i = \frac{m_i l_i^3}{6EI} = \frac{(q\, l_i) l_i^3}{6EI} = \frac{q\, l_i^4}{6EI} \tag{8}$$

$$\delta Y = \left(\sum_{i=1}^{3} \delta y_i + \delta \psi_i l_i \right) + \delta y_4 l_4 \tag{9}$$

where δY is the total deflection of the arm due to the distributed load, δy is the deflection, $\delta \psi$ is the angle created by the deflection, m is the mass, l is the length, and q is the mass per length for each section (9:106). *Table 2 shows the values of q for* PVC. Therefore the total deflection for the distributed load is less than 0.1 inches. Adding the deflections from the tolerance error, the applied load, and the distributed load yields a total of less than 0.35 inches. Therefore deflection of the arm is not a problem and PVC was an adequate material.

Table 2. Mass Per Length Values for PVC (10:2336)

Diameter (inches)	q (pounds/inch)
2	0.0758
1.5	0.0548
1.25	0.0451
1	0.0327

2. *Springs.* Because there were three telescoping sections inside one large section, three springs were required for the passive extension. Figure 14 shows all three springs. Each of the springs had to be custom manufactured. Premade springs, that would match the tubing size, were not available. A spring had to fit into sections A, B, and C. So the maximum outside diameter of the springs were set at the inside diameter of the corresponding tube. Other dimensions of importance were maximum solid height (height of the spring fully compressed) and spring force at solid height. The solid height had to be less than 3 inches, as designated earlier. Also, free length (the length of the spring fully extended) was added into the design considerations. The free length controlled the force of the arm when it was fully extended.

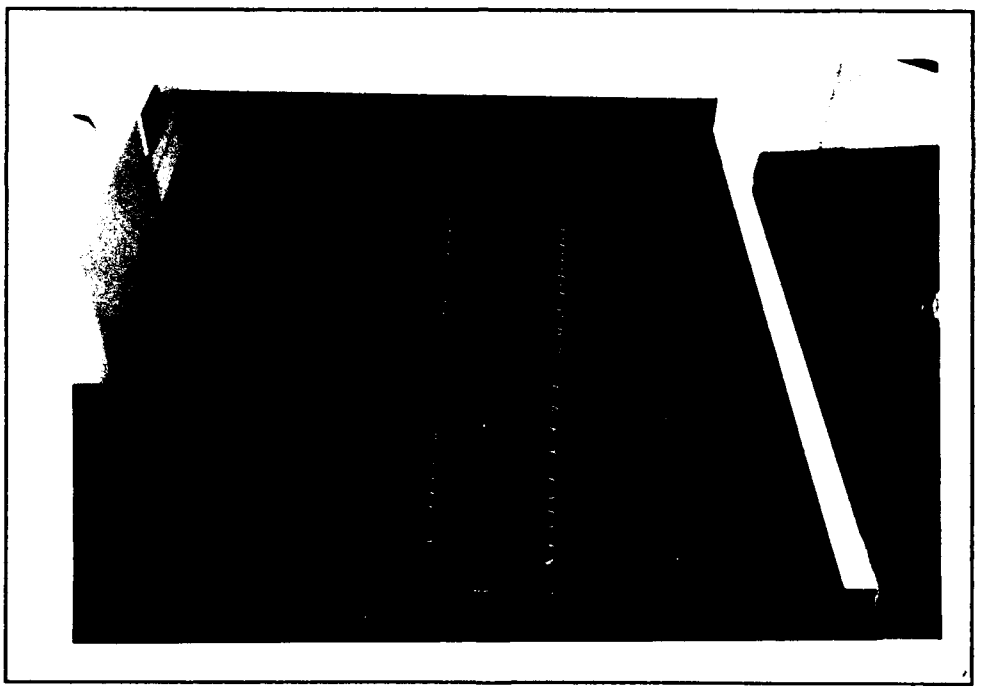

Figure 14. The Springs

The goal was to have the smallest spring force possible at solid height, because the motors had to work against this force at retraction . Another goal was to have the minimum force required to overcome the friction between the tubes and sleeves

throughout the travel of the arm. A rough estimate of the force needed was found by pushing the telescoping tubes down on a scale and reading the weight as the each portion slid into the larger section. The total mass was then subtracted from this force. Because springs increase the force provided when compressed, this force could be established as the freelength force. With a rough idea of spring specification described above, design of the springs was done on a computer program owned by the spring manufacturer. Basic equations that the program used to iteratively create the total specifications required to make the spring include:

$$w\,d = \frac{\sqrt[3]{2.55P(od)}}{s} \tag{10}$$

$$n = \frac{G\,L(w\,d)^4}{8P(od)^3} \tag{11}$$

$$p = \frac{FL - 2w\,d}{n} \tag{12}$$

$$TC = n+2 \tag{13}$$

$$SH = (TC+1)\,(wd) \tag{14}$$

where wd is the wire diameter, P is the spring forced required at solid height, od is the outside diameter of the spring, s is the torsional stress of the wire size used, n is the number of active coils, G is the modulus of elasticity in torsion, L is deflection of n coils, p is the pitch of the coils (length between coils at free length), FL is the free length, TC is the total number of coils, and SH is the solid height (10:510). Actual specifications of the springs are provided, along with other component specifications, in Appendix B.

One design feature that was not discussed yet was the addition of a tang on the ends of each spring. The tang can be seen on the end of the spring in Figure 12. The tang was added so that the spring would not roll over the edge of the telescoping tube and lodge self inside the space between the two tubes.

B. Magnet and Retractable Cord

To actually retrieve and deposit the ferrous metal disks, a specific end effector must be used. The device that is best suited is an electromagnet. Once the robot arm has touched the disk, the electromagnet would be energized and the magnet would attach to the disk. To release the disk, negative voltage (or a reversed current) must be applied to break the magnetic attraction. One of the major criteria for choosing a magnet was the weight. Because it will be mounted on the very end of the arm, a large moment arm will be developed. Therefore, the lighter the weight is, the less the moment will be. A very small (about 4 ounces) electromagnet with a 4 pound pull was acquired for the end effector. For an electromagnet to operate properly, the entire surface of the magnet must meet the surface of the disk. Therefore, to keep the magnet surface parallel to the ground at any point in the arm's work space, the magnet was mounted to the arm on a ball joint. This ball joint allowed gravity to freely move the magnet so that the surface was always parallel to the ground. Figure 15 shows the magnet attached with the ball joint and also shows how the ball joint allows the freedom of movement.

To power the magnet, a wire had to be connected to the magnet. Because the arm was telescoping the wire must also telescope. Putting the wire inside the length of the tubes was not considered because it would interfere with the springs and cable. Therefore, a simple retracting wire (like a phone cord) was used on the outside of the arm. A possible alternate to the wire on the outside might be to use insulated wire for

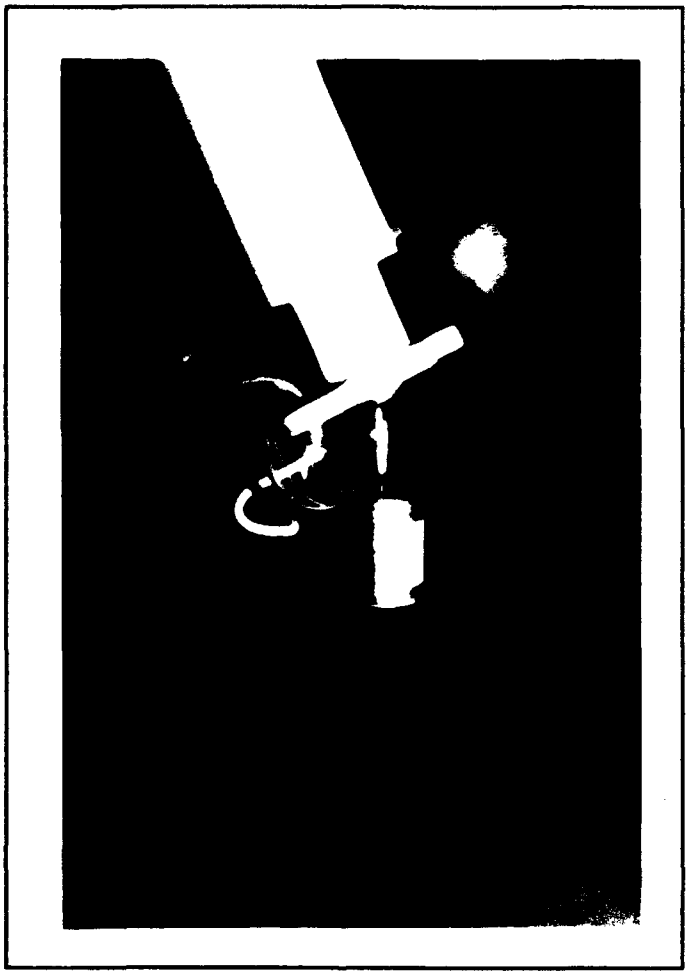

Figure 15. The Electromagnet

the telescoping cable to conduct current. It would eliminate some weight and make the design cleaner. This alternative was not used because of its complexity.

C. Motors

Availability of the motors used for the ARM was not a real problem because spare motors used on the Aerobot were available. Because spare Aerobot motors were available, the desire was to use them instead of purchasing new motors. The real question was if the motors at hand were able to do the job. Three motors were needed, two for the planar motion and one to retract the arm. To make that decision, the forces acting on the motors through the cables would need to be known. The ratings for the

motors were given in continuous torque. Torque is the product of the force, applied as tension in the cable, and the spool radius. The force applied through the cable is found by analyzing the moments created by the electromagnet and the arm itself, for the top two motors. The maximum force applied through the cable for the bottom motor was simply the force provided by the springs at retraction plus the weight of the arm.

Thus for the top two motors, the most tension required in the cables was at the arm's maximum lateral position, which is approximately 20° from vertical. Figure 16 shows a free body diagram of the forces. The moment that the cables must produce by pulling on the bottom plate is equal to the moment produced by the combined load of the arm, magnet, and metal disk. Approximating the weight of the arm at 2 pounds and applying that force at 22 inches below the bottom plate (the center-of-gravity of the telescoping arm) yields the moment due to the weight of the arm as 240 oz-in . The weight of the magnet and a metal disk is 8 oz and applying it at the full length of the arm yields the moment due to the magnet as 170 oz-in. The cable must produce a

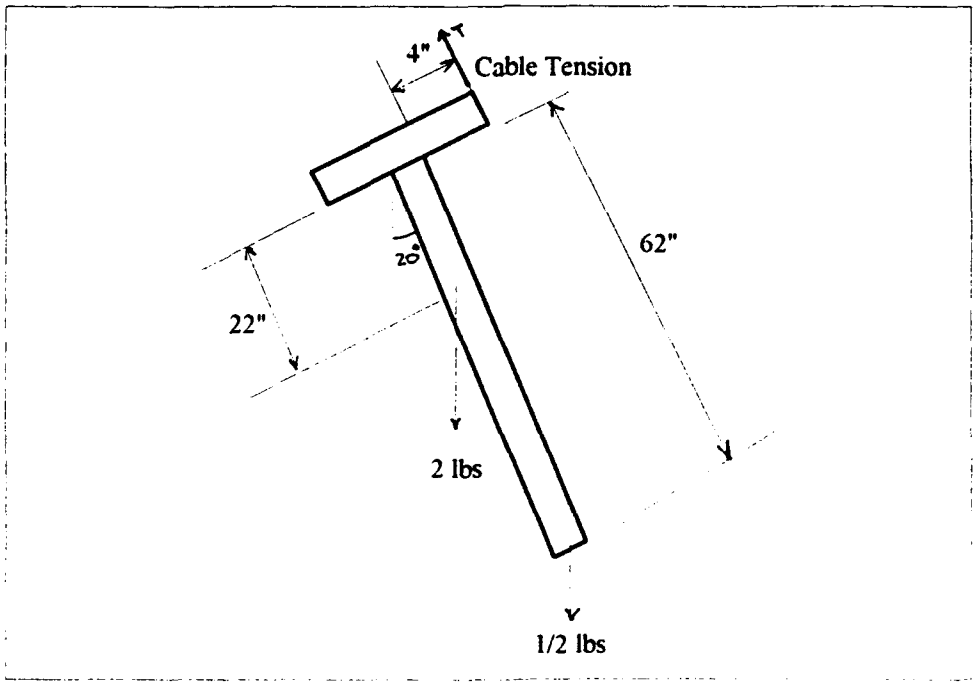

Figure 16. The Free Body Diagram of the ARM

tension multiplied by the 4 inch lever arm of the top plate that will equal the total of the moments described above. This tension is 103 oz. The motor must then produce a torque equal to the product of this tension and the spool radius. If we estimate the spool radius at 0.5 inches, then the torque required is 51 oz-in. The Aerobot motors are rated at 56 oz-in of continuous torque, therefore, considering only the torque required to lift the arm and payload, these motors should work in this application.

For the motor that retracts the arm, the torque analysis is slightly easier. The torque required by the motor is the product of the spool radius and the force at the point of retraction. The three springs produce a total 15 pounds of force when the arm is fully retracted. Adding this figure to the weight of the arm (because the motor is operating mostly in the vertical plane) yields a force to overcome of 17 pounds or 272 ounces. Finding the spool radius at this point is a little more difficult. After a certain number of windings, the cable begins to wrap on itself. Therefore , the effective radius of the spool increases. Because so much cable will be spooled up at retraction, a conservative estimate of the spool radius is 1 inch. This yields a torque of 272 oz-in, which is well above the rated continuous torque of the motors available. The motor would be still able to retract the arm half of its retractable distance. So, the decision was to mount one of the motors available while a replacement could be ordered. The motors are identical to each other, the only difference being in the gearing.

The motors used were made by Globe Motors, of Dayton, OH. They consist of a 24 VDC electric motor and a gear box that provides the necessary continuous torque . The motor that was ordered is fitted with an optical encoder to record motor angles. The electric motor provides 0.02 horsepower and draws a maximum of 1 amp of current at rated torque. The gearbox attached to the motors can be ordered in a wide range of ratios thus giving the maximum continuous torque. The optical encoder operates at a resolution of 512 cycles per revolution. Depending on the gearbox, the entire motor weighs 14 to 21 ounces.

In the analysis discussion to follow in the next chapter, the reason for the motor angle information will become more clear. For now, it is sufficient enough to say that the only position information readily available and easy to record are the motor angles. Because the motors readily available to this project did not have optical encoders, potentiometers (pots) were needed to record these angles. Optical encoders would do a better job of recording this information because they are not limited in the amount of turns they can make, unlike the potentiometers. Therefore, it is imperative that a complete set of gear motors with optical encoders be mounted on the ARM for future operation. For the data collections in this project, potentiometers were mounted to the shaft of each motor. The top two motors were equipped with five turn potentiometers because they only rotated about two times. The potentiometers were rated at 125k ohms which means that each turn produced 25k ohms. The lower motor was equipped with a ten turn potentiometer because it turns just under ten times in the region of interest for analysis. This potentiometers rated at 1k ohms which means each turn produced 100 ohms. Figures 17 and 18 show the layout of the motors and the potentiometers.

As detailed earlier, a large goal of this project was to create a manipulator that had largely uncoupled motion. To achieve this, it was felt that the actuators (i.e., the motors) had to be mounted orthogonal (at right angles) to each other. This is why the motors are mounted in this fashion. Direct drive from the motors was not quite possible in this configuration. That is why the cable linkage is present. Figure 18 shows a view of the motor and cable set up from the top. The motors pull and release cable that is attached to the bottom plate, pivoting the plate about a ball joint. The cable on each side of the motors is confined to operate in a plane, therefore the bottom plate acts as a lever arm, moving the telescoped arm to a position in this same plane.

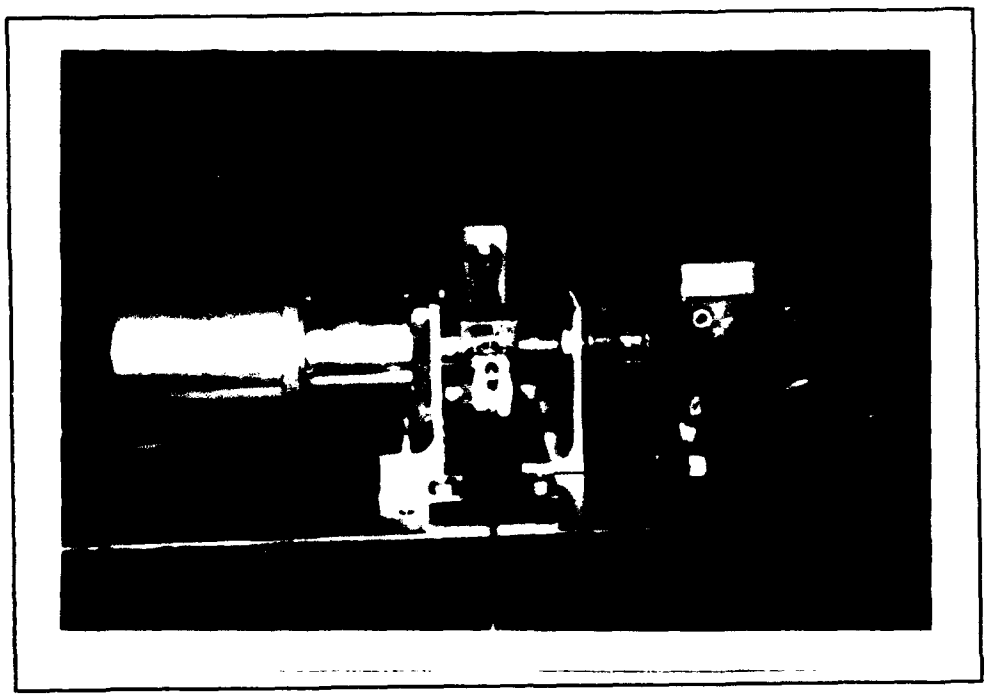

Figure17. The Motors and Potentiometers

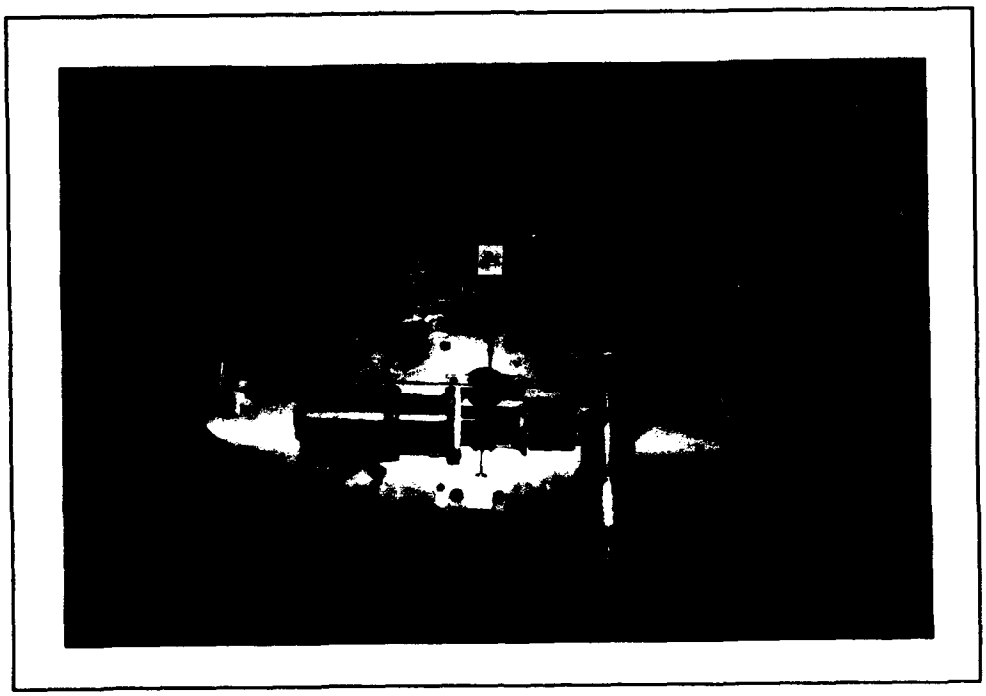

Figure18. The Motor Assembly (Top View)

D. Cable Spools

For the top motors to move the arm, a cable attached to the bottom plate must be pulled. This means that the other end of the cable must be attached to a spool on the motor shaft. As the motor turns, the cable winds onto the spool and the end of the bottom plate rotates about the ball joint toward the top plate, causing the arm to move. Because one end of the plate is pulled toward the top plate, and the other end rotates away from it, a double spool is used. Cable is wound in one direction on one side of the spool. The cable on the other side of the spool is wound in the other direction. When the motor turns in either direction, cable is coiled on one side and uncoiled on the other side, all at the same time. The result is that the motor pulls one end of the bottom plate while the other end is released, thus keeping constant tension on the cable linkage. Figure 19 shows these double cable spools.

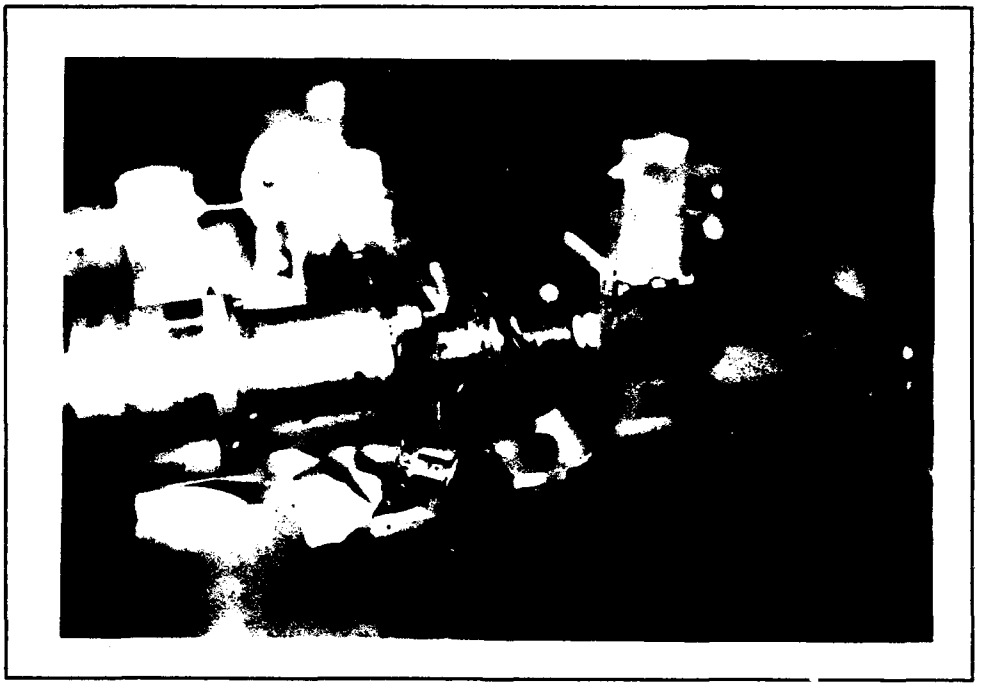

Figure19. The Double Cable Spools

The bottom motor only needs a single spool because the constant tension in the cable is provided by the springs. Therefore the motor coils the cable to retract and uncoils the cable for the springs to extend the arm. The actual spool must be deeper and wider than the top spools because more cable will wind on them to fully retract the arm. A rough estimate of the depth of the spool can be obtained by using the formula for the circumference of a circle to find how much cable will wrap on the spool in one turn. Knowing the desired width of the spool yields the number of turns that will be on one level of wrappings. With the fact that 26 inches of cable will be wound on the spool at retraction, the total number of levels of wrappings can be found. Given a spool width of 1/4 inch, a spool radius of .25 inches, and a cable diameter of 3/32 inches, the number of levels of wrappings is 10 and the depth of the spool must be greater than 1 inch One extra feature was added; the top of the spool was positioned just below the bottom plate so that coils of cable could not escape out of the spool and wind around the motor shaft.

The cable used to wind on the spools is 3/32", plastic coated, stainless steel wire rope. It has 7 spiral strains of wire in the bundle. This wire rope is actually used for aircraft control linkages. Therefore, it is very flexible and very strong. The flexibility was needed for the cable to wrap and unwrap around the spools and stay straight without kinking, snarling or keeping a coiled shape.

E. Pulleys

Two different kinds of pulleys were used with the cable linkages. A non-swivel pulley was used with the lower motor assembly. Because the motor was mounted onto the rotating bottom plate (so that the vertical motion was not affected by the other two motions) at a right angle to the arm, a pulley was needed to change the direction of the cable. The cable travels inside the entire length of the telescoping arm. When it reaches the end of the tubing that is mounted onto the bottom plate, it must change direction 90

degrees and exit the tubing through a slot provided. The actual pulley is housed in the 2" collar at the end of section A which is attached to the bottom plate. The cable travels over the pulley and out the tube to the single spool on the lower motor.

Four swivel pulleys are used on the top two motor assemblies. They change the direction of the cable from parallel to perpendicular to the top plate. The cable leaves the double spools traveling along the top plate until it reaches the edge where it changes direction 90 degrees. It then moves down to attach to the end of the bottom plate. The reason for the swivel capability is because the cables are attached to the bottom plate that rotates with respect to the stationary top plate. When the one motor drives the arm out of the vertical plane, the cables from the other motor must move out of the vertical plane also. Figure 20 shows the swivel pulleys and the reason for them. The whole swivel pulley system came in several parts. The mount was made to the right height for the cable. Then the actual pulley was constructed so that it rotated around the cable. The cable ran through a small tube that was attached to the pulley.

Figure 20. The Swivel Pulley

The tube, along with the pulley, was inserted into roller bearings which were then inserted into holes in the mount. Appendix B has detailed drawings of the swivel pulleys along with all the other parts as well.

F. Diamond Plates

The design of the top and bottom plates was derived through qualitative analysis of their function and the over all goals of the project. The function of the top plate was to provide a stable platform for the whole design. The function of the bottom plate was to act as a lever arm for the telescoping portion. The overall goals that are pertinent for this design are: light weight, rigidity, and center-of-gravity considerations. Early conceptual designs of the plates looked like "plus" signs. This design came from the concern of weight. For rigidity, the plates were then shaped like diamonds, adding more material to the lever arms. For lighter weight, much of the material in the plates could be strategically removed, as long as the basic shape remains the same. For this prototype, material was not removed because many changes, such as motor placement, were constantly being made.

The plates were originally made so that three corners of the bottom diamond plate would act as 8" lever arms. The fourth corner faced in towards the vehicle. Motion towards the vehicle, which results in working underneath the vehicle, was not recommended. Therefore, the lever arm in that direction was set at 4". This allowed the ARM to be mounted closer to the vehicle, which improved the overall center-of-gravity change. Unfortunately, this feature prevented the motor assembly from operating as expected. Because the lever arm was 4" on one side and 8" on the other, there was not a symmetry about the fulcrum or pivot point. This caused one side to need more cable than the other side could release, as the bottom plate rotated. The result was that as the arm rotated 5-10° from the vertical, the motor assembly locked, preventing the plate from rotating to its maximum position. This problem was solved by reduced the

opposing 8" lever arm to match the 4" lever arm. Because this direction has a shorter lever arm, the motor is required to produce more torque. This was not a problem, as shown in an earlier analysis. There is an advantage gained by shortening the lever arm. The angle restriction imposed by the 4" lever arm is 37° which is higher than the 21° given earlier for the 8" lever arm. In effect, this would almost double the horizontal distance obtainable normal to the vehicle.

For mounting purposes, the back of the top plate was fashioned with an extension section. This section was the same width as the tether bracket mount in order for easy mounting. The length was established at 5" so that the bottom plate could rotate to the top plate without restrictions and so that the arm would be clear of the bottom of the vehicle. A hole for the cable to run to the bottom plate had to be included on the extension section. Figure 21 shows the top and bottom plates.

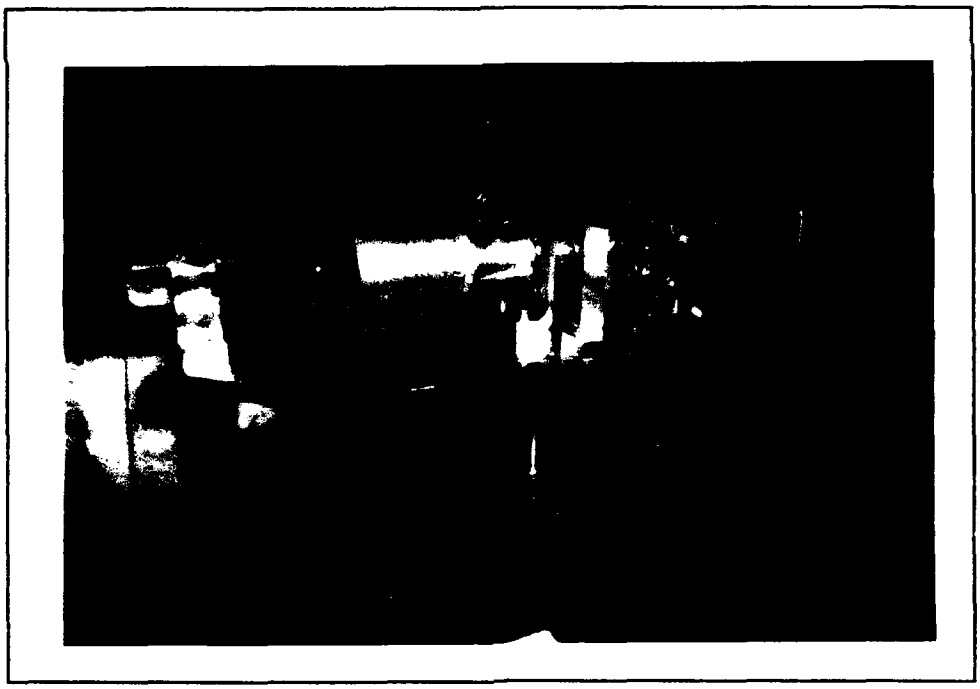

Figure 21. The Top and Bottom Plates

G. Revolute Joint

The requirement for the arm to pivot at one point in 2 directions is a challenge. Normal revolute joints used on robots usually only have one degree of freedom. This joint must have two. A ball joint was decided upon because of the ease in construction. Figure 22 shows the completed ball joint. To fabricate the ball joint, a 1" steel ball bearing was used. A three inch steel rod was then threaded into the ball bearing. The other end other end of the rod would be threaded into the bottom plate. To allow the ball bearing to rotate freely, it had to be nested in the top plate, without restrictions. To accomplish this, a hole was drilled into the top plate and then the hole was chamfered on both sides so the ball bearing could be nested and the rod would have room to move. A bracket was then placed on top of the ball bearing to provide the bearing surfaces for the ball joint. Figure 23 shows the process of constructing the ball joint.

H. Mounting Hardware

To mount the ARM to the Aerobot, a suitable place was needed. Most of the equipment on the vehicle was mounted on an aluminum rack about half way down the side of the vehicle. The rack runs all the way around the vehicle and also has mounts attached that protrude out from the vehicle. At first thought, this was an ideal spot to attach the ARM. There were several protruding mounts that were available and because the rack was firmly attached to the frame, the mount would be very rigid. The problem with this mount was the fact that it was only 16 inches above the bottom of the vehicle. Because the retracted length of the ARM is about 26 inches, long mounting brackets must be used. This increases weight and decreases rigidity. A better place to mount the ARM is the tether bracket. The vehicle has a tether system it uses for safety reasons. This bracket is also firmly attached to the frame and has mounting holes that are not being used. It also sits above the top of the vehicle which is 26" high. The tether bracket protrudes away from the vehicle to allow clearance for the ARM to operate.

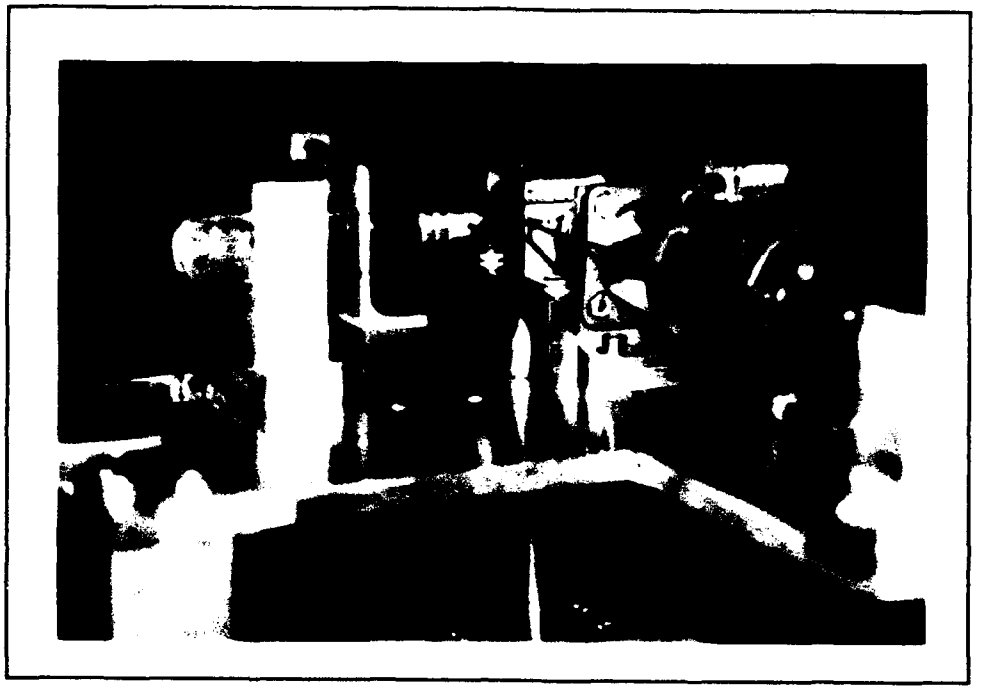

Figure 22. The Ball Joint

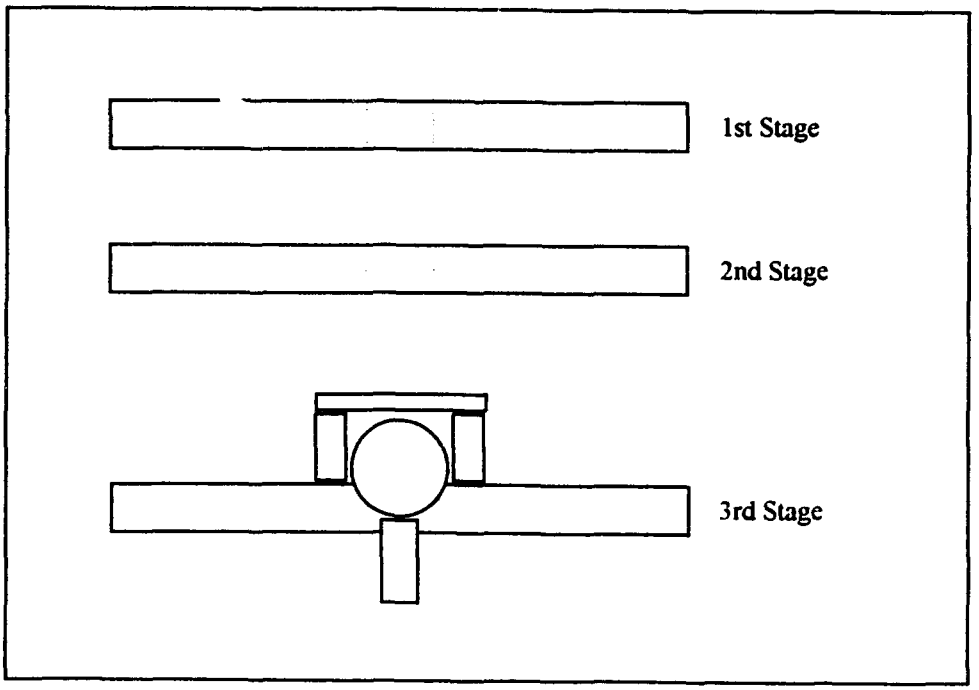

Figure 23. The Construction of the Ball Joint

Attaching the ARM to the tether mount was just a matter of securely attaching two "L" brackets underneath the extended mounting section of the top plate and bolting them both to the tether bracket. This provided the shear strength in the vertical plane. For the torsional strength, a retaining strap was attached from the top of the extended section to the tether bracket, thus preventing the whole device from rotating under its own weight. Figure 24 shows the tether bracket and Figure 25 shows the "L" brackets.

I. Joy Stick Control

For the arm to operate in a coordinated manner, the ARM needs some sort of control. To reach to a particular position, touch an object, and retrieve it means that several tasks must be accomplished together. Use of this controller coordinates these tasks into essentially one task. Various controllers are available. Since the ultimate goal is to place the Aerobot into competition, the obvious choice would be autonomous closed loop control administered by a computer. Closed loop control is highly desirable because updated information on position and velocities can be feed back through the controller, making the entire process more accurate. Control through a computer is desirable because software can be written to meet the specific needs of the ARM. Unfortunately, the autonomous control through the computer is far beyond the scope of this thesis project and will be left as a future research topic.

Since autonomous control was not an option at this point, closed loop radio control seemed to be the next most desirable controller. This scheme is what is used on the Aerobot, presently. It uses man-in-the-loop control along with feeding back information on position (with the use of potentiometers). This type of control, although not autonomous, allows the ARM to be operated while the vehicle is flying. There were several major obstacles that prevented radio control from being used for the ARM. The controller used for vehicle control was not able to accommodate the added task of operating the arm. Therefore another controller had to be used. Actually building a

Figure 24. The Tether Bracket

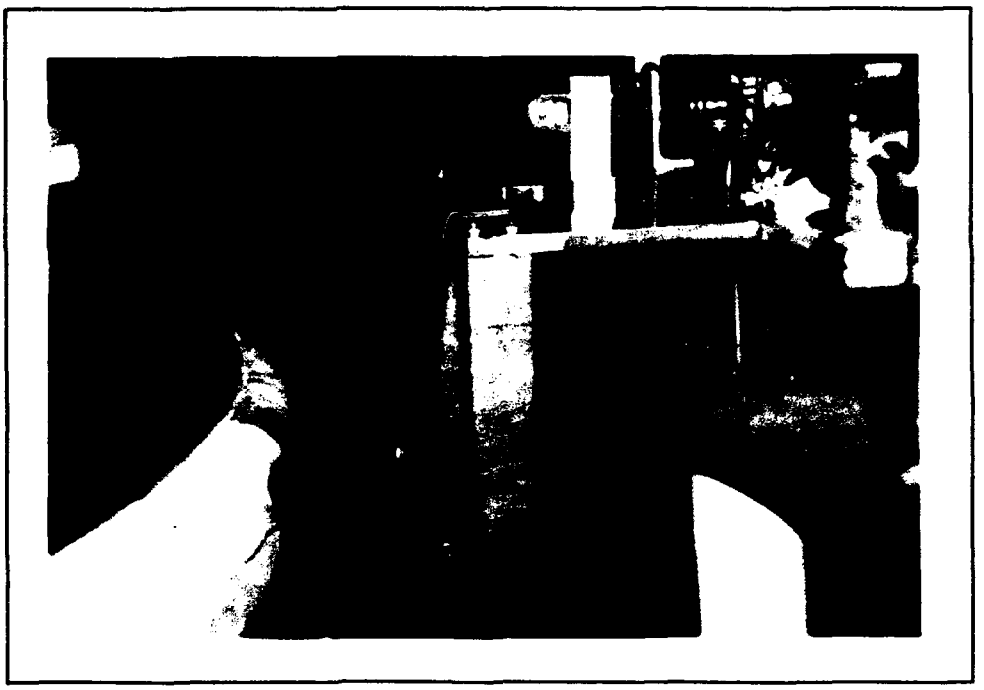

Figure 25. The Mounting Hardware

controller was beyond the scope of the project and a commercially available controller that would match the specifications needed was not found. Also, the extra radio transmitter and receiver available for use with the ARM was not in working order and timely repair was not possible. Along with all of this, the decision not to fly the ARM on the Aerobot at this time led to the present form of control.

An open loop joy stick controller (man-in-the-loop wire rather than radio control) was designed and built. Figure 26 shows the completed joy stick. This type of control is fairly simple because it is open loop, meaning that no information is being sent back to the controller; the human controller can recognize the position or rate and use that information for achieving the desired placement.

Basic requirements for the controller were: all of the functions of the ARM must be controlled by one hand held unit, rate control should be provided, and the voltage requirements should match the vehicle as much as possible. The functions of the ARM include lateral motion by the top two motors, vertical motion by the bottom motor, and

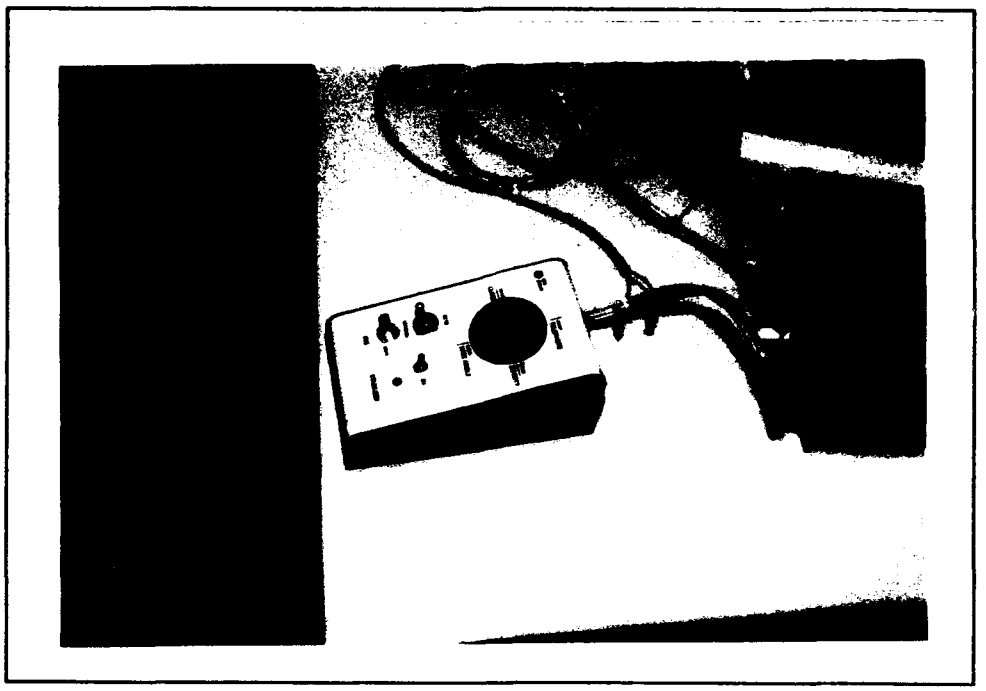

Figure 26. The Joy Stick

activation of the electromagnet. A three position switch and a potentiometer were used to control the bottom motor. The potentiometer controlled the rate of the motor by varying the voltage provide to the motor and the switch controlled the direction that the motor turned (and thus the vertical direction of movement of the arm). One position of the switch was attached to the leads of the motor. The other far position was attached to the swapped leads producing the opposite motion of the motor. The middle position of the switch is the off setting to allow the arm to stay in one vertical position. The magnet was connected to a on/off, two position switch. Both the electromagnet and the bottom motor were powered by 24 VDC, which is what the vehicle supplies.

To produce a coordinated planar motion, a two-axis joy stick was used to control the top two motors. To provide rate control also meant that the joy stick had to have potentiometers attached which would vary the voltages that powered the motors. Therefore, to increase the rate of motion, the voltage must be increased. Changing the resistance of the potentiometers (by turning them) changed the voltage produced, because they are proportional to each other. Therefore increasing the speed of the motors was achieved by rotating the joy stick. Another task of the joy stick was to provide opposite motion of the motors by reversing the direction of the joy stick. Both of these requirements meant designing and building a circuit to go along with the joy stick.

The major problem with the controller was matching a low current joy stick with high current motors. Because of the current rating difference, circuitry was needed in order to use the joy stick for motor control. Figure 27 shows the final circuit that was built. The following paragraph is a description of how the circuit operates.

A power supply with low current is connected to one of the potentiometers on the joy stick and to two resistors. This set is used to create a variable resistance differential between the potentiometer and the resistors. This differential is then fed through a differential amplifier to yield a small voltage with a range of positive and

negative values (about ±5 volts). The voltage is then passed to a operational amplifier to amplify the voltage to a peak of ±22 volts. At this point if the voltage is positive, it is fed to a by-pass transistor which will regulate the current and voltage from the main power supply (and not through the joy stick). This current is then fed through the normally closed leads of a relay to the leads of a motor, creating motion. If, however, the voltage is negative, diodes direct the negative voltage to an inverter amplifier to change the negative value to a positive value, and sent through another by-pass transistor. The relay is energized by the negative voltage circuit and the normally open leads of the relay are closed. The by-pass transistor draws the appropriate current and voltage from the main power source and delivers it to the normally open leads of the relay which are connected to the swapped leads of the motor, creating the opposite motion. This entire circuit is repeated for the other motor.

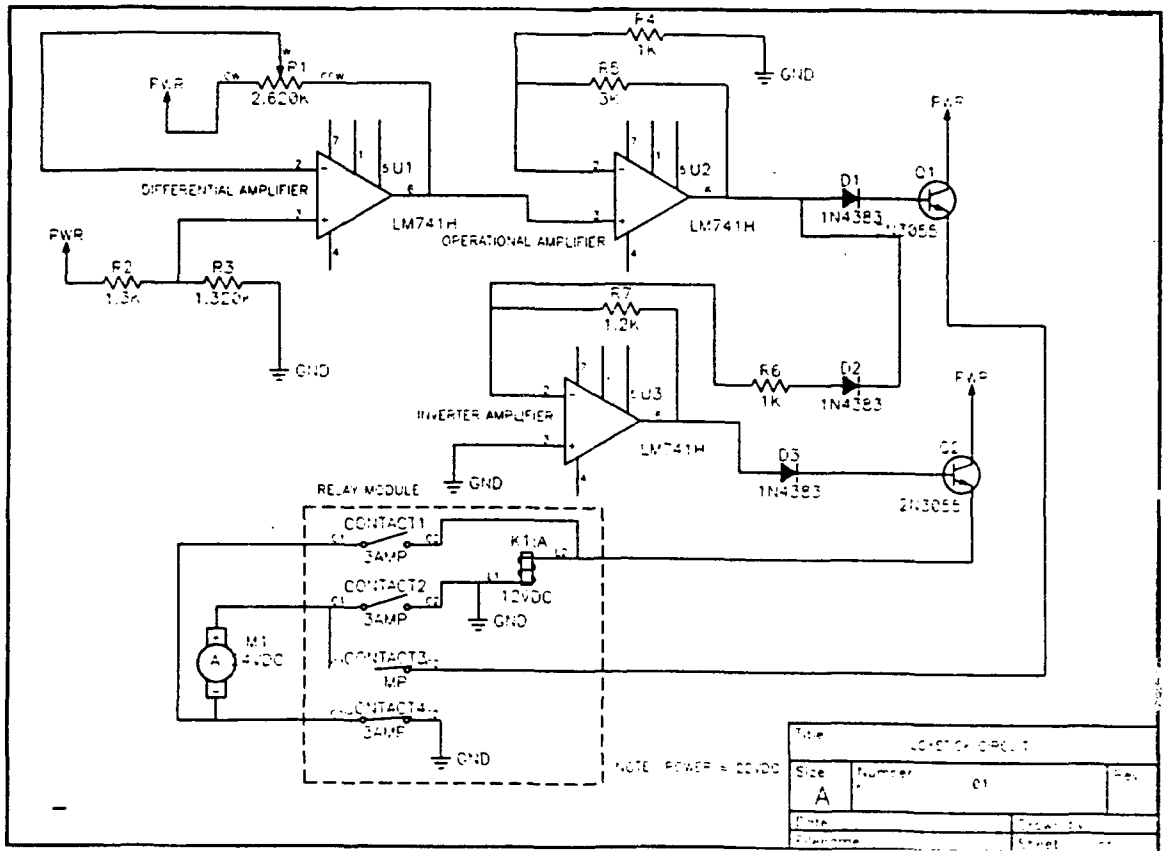

Figure 27. The Joy Stick Circuit

IV. Kinematic Analysis

During autonomous operation, a computer has the ability to drive a manipulator, but it must be given the kinematic equations that govern its movement. Another reason for the model is to evaluate the performance of the device. There are several ways to derive this model. In robotics, it is common to determine forward kinematics that yield the position and the orientation of the end-effector, when the joint variables of the robot are known and inverse kinematics that yield the joint variables necessary to place the end-effector at a certain position and orientation. In other words, with forward kinematics you know where you are by knowing the joint variables and with inverse kinematics you know how to move to get to where you want to go. The joint variables are the angles between the links of the robot in the case of revolute joints and the amount of extension for prismatic or linear joints. This chapter will derive the forward and inverse kinematics and relate them to the one measurable piece of information, the motor angles (11:62).

A. Geometry of the ARM

The motors actuate the arm through cable linkages, so motor angles must be related to joint variables. Because the top two motors actuate the ball joint, their angles are related to the joint angles. The bottom motor actuates a prismatic joint , so its angle is related to the link extension. Motor angles are used to map to position because, with the use of potentiometers or optical encoders, they can be recorded easily and accurately whereas the joint angles would be difficult to measure. Another reason to use motor angles is that voltages are required by the controller to move the motors (and ultimately the arm) and voltages are easily transformed to motor angles.

At this point each individual motor will be discussed separately so a numbering convention is in order. The top two motors are numbered 1 and 2. Motor 1 is the motor

that provides motion tangent to the side of the vehicle. Its motor angle is ϕ_1 . Motor 2 is the motor that provides motion normal to the side of the vehicle. Its motor angle is ϕ_2 . The joint angles that will be discussed in next section are numbered to correspond to the motors that move them. Therefore, the joint angle θ_1 is controlled by motor 1 and θ_2 is controlled by motor 2. The bottom motor is motor 3 and its motor angle is ϕ_3 . Because the joint that it controls is prismatic, the joint variable in this case is a link extension. This change in length of the of the arm is d_3 .

The reason for defining the geometry of the arm is to be able to map the motor angles to the joint variables. Mapping the joint variables to the position and orientation of the end effector is covered in the section to follow. Figure 28 shows the diagrams of the geometries of motors 1 and 2. Since both motors assemblies are similar (only constants are different) the discussion is generic. Starting at the motor, the motor angle is related to the length of cable pulled or released by,

$$\Delta l = r\phi \tag{15}$$

where Δl is the change in length of the cable, r is the radius of the spool and ϕ is the motor angle, in radians, measured from the initial starting point with the arm vertical. Figure 28 shows the geometry of motors 1 & 2 and their relationship to joint angles. As the bottom plate rotates, the angle α changes. This angle is the one created by drawing a line connecting the swivel pulley to the ball joint and then to the end of the bottom plate where the cable is connected. The distances between these points remain constant, only the angle between them changes. Using the Law of Cosines, the length of the cable (ℓ) from the swivel pulley to the bottom plate is related to angle α. This formula is,

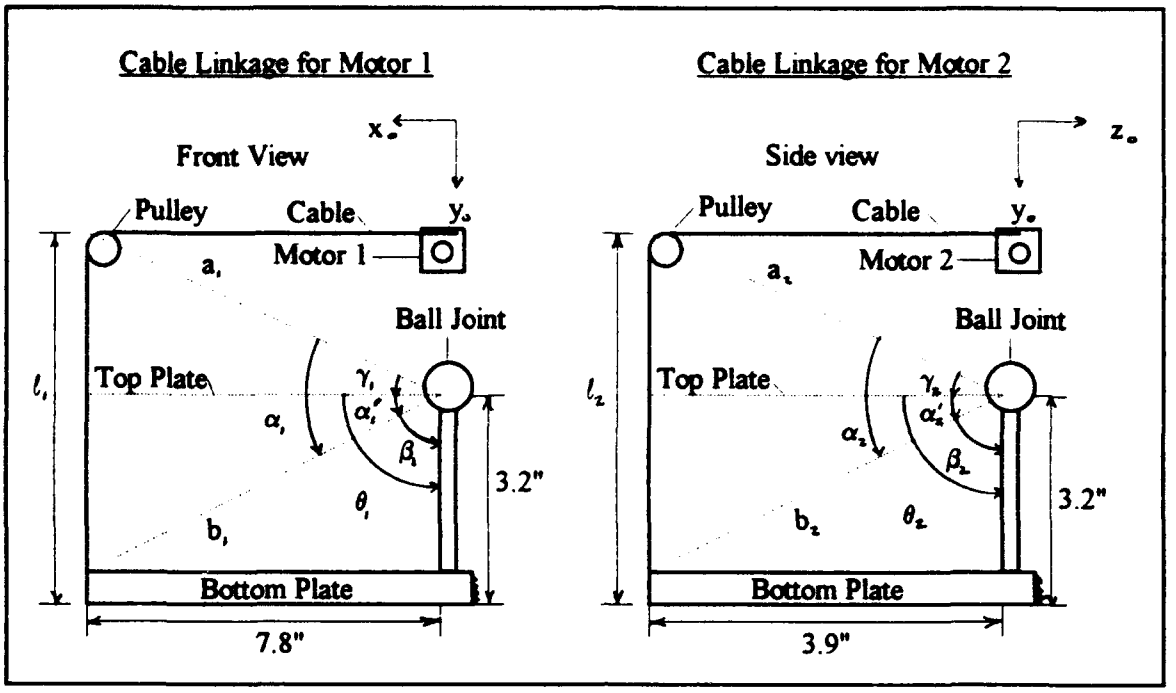

Figure 28. The Geometry of the ARM

$$l^2 = a^2 + b^2 - 2ab\cos\alpha \tag{16}$$

or

$$l = \sqrt{a^2 + b^2 - 2ab\cos\alpha} \tag{17}$$

where a is the distance from the swivel pulley to the ball joint and b is the distance from the ball joint to the end of the bottom plate. The relationship between l and Δl is in the form,

$$l = l_0 \pm \Delta l \Rightarrow \Delta l = \pm(l - l_0) \tag{18}$$

where l_0 is the initial length of l. The plus or minus sign exists because the angle α can be related to either an increasing or decreasing l. More about this peculiarity will be discussed later. Combining Equations (15), (17), and (18) yields,

$$\phi = \pm\frac{\sqrt{a^2 + b^2 - 2ab\cos\alpha} - l_0}{r} \tag{19}$$

Further examination of Figure 28 shows that,

$$\alpha = \alpha' + \gamma \tag{20}$$

and,

$$\theta = \beta + \alpha' \Rightarrow \alpha' = \theta - \beta \tag{21}$$

yielding,

$$\alpha = \theta + \gamma - \beta \tag{22}$$

where α, α', γ, and β are the angles established in Figure 28. Substituting Equation (22) into Equation (19) yields,

$$\phi = \pm\frac{\sqrt{a^2 + b^2 - 2ab\cos(\theta + \gamma - \beta)} - l_0}{r} \tag{23}$$

This equation will be used for the inverse kinematic mapping of position to motor angles. It must now be solved for θ so that it may be used for forward kinematic mapping,

$$\theta = \beta - \gamma + \arccos\left[\frac{(l_0 \pm r\phi)^2 - a^2 - b^2}{-2ab}\right] \tag{24}$$

To make Equations (23) and (24) specific to a particular motor, simply plug in the constants. The constants are as follows: $a_1 = 7.9$ in, $b_1 = 8.4$ in, $\gamma_1 = 10.2°$, $\beta_1 = 67.7°$, $a_2 = 4.2$ in, $b_2 = 5.0$ in, $\gamma_2 = 22.9°$, $\beta_2 = 39.4°$, and $r_1 = r_2 = 0.45$ inches, where

the subscripts 1 and 2 refer to the specific motors.

Because the relationship between ℓ and α is governed by the Law of Cosines, it is not a linear relationship. So, when the motor turns the double spool, on one side the angle α increases a certain amount. On the other side, α decreases the same amount. But, the change in the length of the cable is not the same for both sides, because of the non-linear equation. The difference in lengths becomes worse as the arm moves further from vertical. This peculiarity suggests that there is a right and left kinematic mapping. Determining which mapping to use (basically to use the plus or minus sign), depends on which action (the pulling or releasing on the double spool) dominates the process. The problems that it caused will be discussed in a later chapter and suggestions for a remedy will be presented.

The mapping of motor angle 3 is simpler than the other two. The change in length of the arm is d_3 . Because the amount of cable that is wound or unwound from the spool equals the change in length of the arm, the motor angle (ϕ_3) is directly related to d_3 . This relationship is,

$$d_3 = r_3\phi_3 \tag{25}$$

for forward kinematics, and

$$\phi_3 = \frac{d_3}{r_3} \tag{26}$$

for inverse kinematics. Unfortunately, finding a value for r_3 is much more of a problem. Because so much cable is wrapped onto the spool as it nears the full retraction stage, the effective radius increases. For this project most of the work that was done with the arm was while it was extended. Therefore an average effective radius of 0.38 inches was used. For the real model to be accurate, the increasing radius must be matched with a function that will match this phenomenon mathematically. The other

choice may be to find certain average radii that are good for a particular region. A suggestion for the remedy of this problem will be presented in the last chapter.

B. Forward Kinematic Model

The ARM has four links numbered from 0 to 3 and three joints numbered from 1 to 3. The ball joint used by the ARM is actually one joint with two degree-of-freedom. It will be modeled as two, single degrees-of-freedom joints with a link of zero length in between. Modeling begins with attachment of a coordinate frame to each link. Frames were chosen using the Denavit-Hartenberg (D-H) convention. The inertial frame is attached to the base and is labeled frame 0. Successive frames are attached to links 1-3 and labeled accordingly. Frames should be attached so that motion of the robot does not change the position of any part of a link with respect to its frame (11:62-63). Figure 29 shows the frames chosen for the arm. The figure also shows the symbolic representation of the ARM. For a detailed algorithm for establishing reference frames and deriving the forward kinematics of a manipulator, see Spong (11:71-72).

D-H convention uses a homogeneous matrix $\mathbf{A}_i$ to transform the coordinates of a point from frame i to frame i-1 (where i represents the link). This matrix is a function of the joint variable corresponding to the same link, only. A homogeneous matrix that transforms the coordinates of a point in the last frame of the robot (where the end-effector is located) to the inertial frame is referred to as a transformation matrix $\mathbf{T}_0^n$. Specifically for the ARM, where $n = 3$, this transformation matrix is the product of all of the individual link homogeneous matrices, or in equation form,

$$\mathbf{T}_0^3 = \mathbf{A}_1(\theta_1)\,\mathbf{A}_2(\theta_2)\,\mathbf{A}_3(d_3) \tag{27}$$

This matrix can be partitioned off to yield a position vector and an orientation matrix,

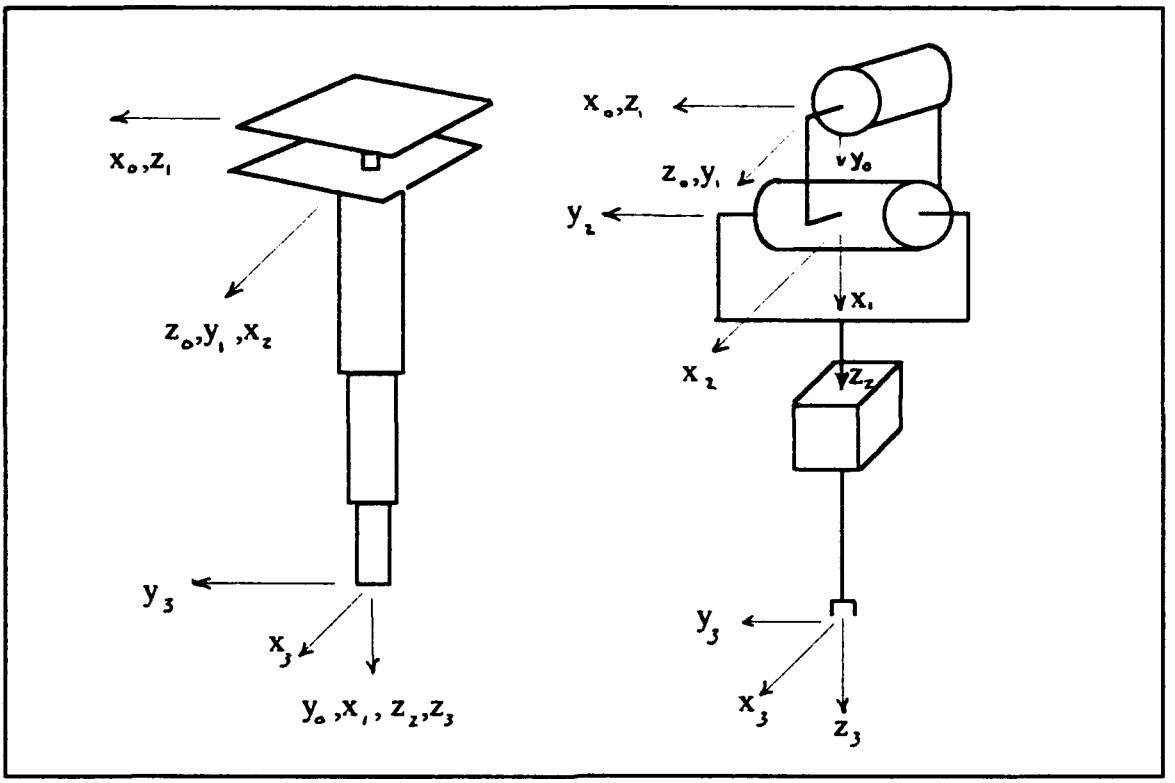

Figure 29. D-H Reference Frames for the ARM

$$\mathbf{T}_0^3 = \begin{bmatrix} \mathbf{R}_0^3 & \mathbf{d}_0^3 \\ 0 & 1 \end{bmatrix} \tag{28}$$

where $\mathbf{R}_0^3$ is a 3×3 rotation matrix that describes the orientation of the end-effector with respect to the base frame, and $\mathbf{d}_0^3$ is a 3×1 vector that defines its position also with respect to the base frame. For this design and the task is was built for, the orientation of the end effector is unimportant. Therefore, the main emphasis will be on the position vector (11:64).

By D-H convention, the homogeneous transformation $\mathbf{A}_i$ is defined as,

$$\mathbf{A}_i = \begin{bmatrix} \cos\theta_i & -\sin\theta_i\cos\sigma_i & \sin\theta_i\sin\sigma_i & f_i\cos\theta_i \\ \sin\theta_i & \cos\theta_i\cos\sigma_i & -\cos\theta_i\sin\sigma_i & f_i\sin\theta_i \\ 0 & \sin\sigma_i & \cos\sigma_i & D_i \\ 0 & 0 & 0 & 1 \end{bmatrix} \tag{29}$$

where the quantities $\theta_i, \sigma_i, f_i, D_i$ are parameters of link i with respect to link i-1. These parameters receive the following names: θ_i is the angle, σ_i is the twist, f_i is the length, and D_i is the offset. For a given link, the matrix $\mathbf{A}_i$ will only have one variable, the other three quantities will be constant. The variable will either be θ_i for a revolute joint or D_i for a prismatic joint (10:66)

With the background presented, the transformation matrix for the ARM can now be derived. Table 3 shows the four quantities $\theta_i, \sigma_i, f_i, D_i$ for each link. They were found using D-H conventions. Substituting these quantities into Equation (29)

Table 3. D-H Link Parameters for the ARM

Link	f_i	σ_i	D_i	θ_i
1	0	90°	0	θ_1
2	0	90°	0	θ_2
3	0	0	D_3	0

yields,

$$\mathbf{A}_1 = \begin{bmatrix} c\theta_1 & 0 & s\theta_1 & 0 \\ s\theta_1 & 0 & -c\theta_1 & 0 \\ 0 & 1 & 0 & 0 \\ 0 & 0 & 0 & 1 \end{bmatrix} \tag{30}$$

$$\mathbf{A}_2 = \begin{bmatrix} c\theta_2 & 0 & s\theta_2 & 0 \\ s\theta_2 & 0 & -c\theta_2 & 0 \\ 0 & 1 & 0 & 0 \\ 0 & 0 & 0 & 1 \end{bmatrix} \tag{31}$$

$$\mathbf{A}_3 = \begin{bmatrix} 1 & 0 & 0 & 0 \\ 0 & 1 & 0 & 0 \\ 0 & 0 & 1 & D_3 \\ 0 & 0 & 0 & 1 \end{bmatrix} \tag{32}$$

where,

$$D_3 = 26 + d_3 \text{ (inches)} \tag{33}$$

Equations (30), (31), and (32) can now be substituted into Equation (27) to yield,

$$\mathbf{T}_0^3 = \begin{bmatrix} c\theta_1 c\theta_2 & s\theta_1 & c\theta_1 s\theta_2 & D_3 c\theta_1 s\theta_2 \\ s\theta_1 s\theta_2 & -c\theta_1 & s\theta_1 s\theta_2 & D_3 s\theta_1 s\theta_2 \\ s\theta_2 & 0 & -c\theta_2 & -D_3 c\theta_2 \\ 0 & 0 & 0 & 1 \end{bmatrix} \tag{34}$$

Using Equation (28) to partition this matrix, the position vector becomes,

$$\mathbf{d}_0^3 = \begin{bmatrix} D_3 c\theta_1 s\theta_2 \\ D_3 s\theta_1 s\theta_2 \\ -D_3 c\theta_2 \end{bmatrix} \tag{35}$$

or in scalar notation,

$$x = D_3 \cos\theta_1 \sin\theta_2 \tag{36}$$

$$y = D_3 \sin\theta_1 \sin\theta_2 \tag{37}$$

$$z = -D_3 \cos\theta_2 \tag{38}$$

These three equations are the forward kinematic mapping from the joint variables to the

position variables with respect to the inertial frame. To achieve the full mapping from the motor angles to the position variables, substitute Equations (24), (25), and (33) into Equations (36), (37), and (38) (make sure that the right constants in Equation (24) are being used for the joints specified in Equations (36) - (38))

$$x = (26 + r_3\phi_3)\cos\left\{\beta_1 - \gamma_1 + \arccos\left[\frac{(l_{1_0} \pm r_1\phi_1)^2 - a_1^2 - b_1^2}{-2a_1b_1}\right]\right\}\sin\left\{\beta_2 - \gamma_2 + \arccos\left[\frac{(l_{2_0} \pm r_2\phi_2)^2 - a_2^2 - b_2^2}{-2a_2b_2}\right]\right\} \tag{39}$$

$$y = (26 + r_3\phi_3)\sin\left\{\beta_1 - \gamma_1 + \arccos\left[\frac{(l_{1_0} \pm r_1\phi_1)^2 - a_1^2 - b_1^2}{-2a_1b_1}\right]\right\}\sin\left\{\beta_2 - \gamma_2 + \arccos\left[\frac{(l_{2_0} \pm r_2\phi_2)^2 - a_2^2 - b_2^2}{-2a_2b_2}\right]\right\} \tag{40}$$

$$z = (26 + r_3\phi_3)\cos\left\{\beta_2 - \gamma_2 + \arccos\left[\frac{(l_{2_0} \pm r_2\phi_2)^2 - a_2^2 - b_2^2}{-2a_2b_2}\right]\right\} \tag{41}$$

C. Inverse Kinematic Model

In contrast to the model above, the inverse kinematic model will present the joint variables in terms of the end-effector position. As stated earlier, because of the nature of the design (it contains no duplicate orientations to achieve the same point in space), the orientation is unimportant. The equations for inverse kinematics are very important because they will be the equations used to automate the ARM. The location of the metal disks will be determined by the vehicle's navigation/acquisition device, then used, through these equations, to move the ARM to the designated location. The actual command to move the ARM will be in the form of voltages to achieve specific motor angles.

The formation of the inverse kinematic model starts at the point where the equations for forward kinematics are derived. There are three independent equations and three unknown variables θ_1, θ_2, D_3 that need to be presented in terms of the known variables x, y, z . Therefore, the three final equations of the inverse kinematic model can be found through substitution. Solving for θ_2 in the Equation (38) yields,

$$\theta_2 = \arccos\left(-\frac{z}{D_3}\right) \tag{42}$$

Substituting (39) into (36) and gives,

$$x = D_3 \cos\theta_1 \sin\left[\arccos\left(-\frac{z}{D_3}\right)\right] \tag{43}$$

and solving for θ_1 yields,

$$\theta_1 = \arccos\left\{\frac{x}{D_3 \sin\left[\arccos\left(-\frac{z}{D_3}\right)\right]}\right\} \tag{44}$$

Using the identity,

$$\sin(\arccos X) = \sqrt{1 - X^2} \tag{45}$$

and realizing that D_3 is the magnitude of the vectors $\underline{x}, \underline{y}, \underline{z}$,

$$D_3 = \sqrt{x^2 + y^2 + z^2} \tag{46}$$

yields the expression for θ_1 as,

$$\theta_1 = \arccos\left(\frac{x}{\sqrt{x^2 + y^2}}\right) \tag{47}$$

and the expression for θ_2 as,

$$\theta_2 = \arccos\left(\frac{-z}{\sqrt{x^2+y^2+z^2}}\right) \tag{48}$$

The use of the arccosine function for this equation is ideal because it is uniquely defined between the angles 0 to π ,which is the range of the joint angles. These three Equations, (46), (47), and (48) are the inverse kinematic mapping from the end effector position to the joint variables. For the full mapping from the position to the motor angles, Equations (23), (26), and (33) must be substituted into these three equations

$$\phi_1 = \pm\frac{\sqrt{a_1^2+b_1^2-2a_1b_1\cos\left[\arccos\left(\frac{x}{\sqrt{x^2+y^2}}\right)+\gamma_1-\beta_1\right]}-l_{1_0}}{r_1} \tag{49}$$

$$\phi_2 = \pm\frac{\sqrt{a_2^2+b_2^2-2a_2b_2\cos\left[\arccos\left(\frac{-z}{\sqrt{x^2+y^2+z^2}}\right)+\gamma_2-\beta_2\right]}-l_{2_0}}{r_2} \tag{50}$$

$$\phi_3 = \frac{\sqrt{x^2+y^2+z^2}-26}{r_3} \tag{51}$$

The next chapter will qualitatively and quantitatively evaluate the performance of the ARM. The models will be compared to real time data to verify their validity.

V. Performance

When this thesis was at its earliest stages of development, there were hopes that the ARM might actually be flight tested on the vehicle. As time went by, it was clear that flight testing the ARM was not within the bounds of this thesis project, mainly because flight time on the Aerobot was so limited. Also, analyzing the effect of the ARM on the flight characteristics of the Aerobot should be done first with the mathematical model which is underway at this writing. Therefore bench testing was the best alternative for this prototype.

A. Qualitative Analysis

Without the aid of flight testing, a rather qualitative approach was taken to examine the performance of the ARM. One of the first items, was to measure the final weight. The total weight of the device was 13 pounds (the target had been 10 pounds). Because this prototype was to be bench tested only, no attempt was made to lighten the prototype by eliminating unneeded structure. Lightening holes could be used on the top and bottom plates and on the mounting bracket. If even more weight needed to be trimmed, it would be reasonable to even take some material from the PVC tubing.

Analysis of the performance was a continuing process through the design and construction phase. Even before all of the parts were combined, individual components were tested to verify their uniform operation. The PVC tubing was combined with the springs and tested for smooth, continuous motion. The top and bottom plate assembly was preassembled with the motor and cable assemblies so that any obstructions that might exist could be detected. Several revelations came about from this pretesting of parts. The irregularies that existed in the PVC tubing created considerable friction. The thought was that the springs would solve this problem. They did overcome most of the friction between the tubes, but the motion in some regions was slower than in others.

Basically, friction was dictating the rate of expansion and not the motors. This problem was solved by sanding the tubing, although that increased the deflection slightly (the deflection calculations in Chapter III include this design change).

Movement of the top and bottom plate assembly showed several more potential problems. As stated earlier in the geometry section of the last chapter, there was a problem because of a difference between the change in cable lengths on both sides of the double spools. This created slack in the cable, decreasing the rigidity of the device and potentially causing control problems for the future. This problem did not manifest itself in the longer lever arm assembly which controls motion tangent to the side of the vehicle (the x direction from D-H convention). Because the distance of the lever arm is longer than the height between the plates, the non-linear equation that governs the motion does not create a perceivable difference in the lengths. Because of the length difference, the angle in the equation remained small. On the other hand, the assembly that controls motion normal to the vehicle (the z direction) has a lever arm that is nearly the same as the distance between the plates. The angle dictating the length of the cable could become quite large. This is a problem inherent with the basic design and requires a more complicated solution which will be discussed in the last chapter. For now, the solution to the problem was to limit the travel to 20 degrees from vertical. At that angle there is only a small difference in lengths. Overall this problem did not hinder the operation of the ARM. It did cause some extra motion when the ARM was moving at a higher speed, but moving at a high speed is not the normal operating mode.

An added problem found in pretesting was the existence of another source of cable slack. Because the swivel pulleys are not placed in the center line of the ball joint, the cables on one assembly are loosened when the other assembly moves the arm out of the vertical. This problem is a coupling effect because it introduces error in the opposing dimension. Again the larger the angle, the worse the problem gets. Figure 30

shows a diagram of the two pivot points. In this figure it is evident that the cable length from the swivel pulley to the bottom plate is longer than the length from the ball joint to the bottom plate. There are two different radii of motion. The radius from the ball joint is smaller than the radius of the circle that the swivel pulley makes. Because the radius from the ball joint is actually a steel rod, the end of the cable is confined to travel in the smaller arc. Therefore when the plate rotates, the opposing cable assembly loosens because the distance from the swivel pulley to the bottom plate is less than it was at the vertical position. This in effect creates some coupling because it produces movement out of the intended plane. This problem can be fixed by moving the pivot point down to the bottom plate where the cable attaches to the plate. This solution will be discussed in more detail in the next chapter. Like the other problem with the cable system mentioned earlier, the ill effect of the loose cable was hardly perceivable as long as the angle remained small and speeds remained slow.

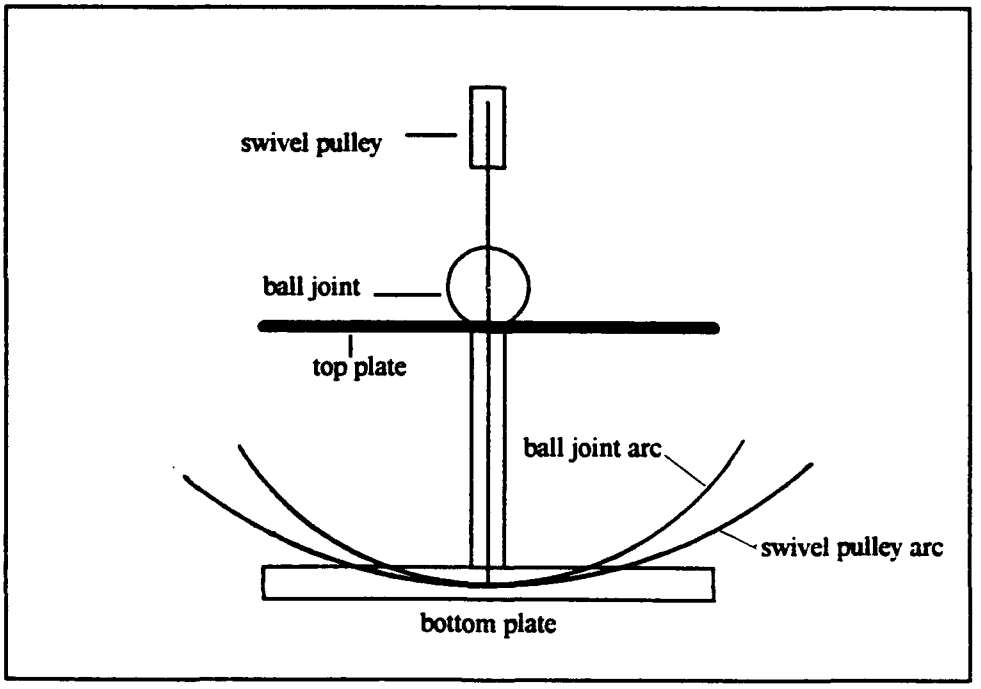

Figure 30. Problem of Two Pivot Points

One more problem with the plate assembly was detected in the pretesting phase. The problem was with the ball joint itself. A ball joint is a three degree-of-freedom device. It has two desirable rotational freedoms, which create lateral motion of the end-effector, and one undesirable rotation, which permits the telescopic arm to rotate about its axis of revolution. A careful examination of the plate assembly shows that the only restraint on this extra motion is the tension of the cable. A tighter cable means less rotation. Therefore when the arm is vertical, little rotation is evident. As the angles increase, the tension in the cable decreases allowing more rotation. Therefore it is compounded by the other problems . However, because this rotation is about the centerline of the telescoping arm, there is no effect on the positioning of the magnet. As before, the overall effect of this problem on the performance of the arm was quite small.

After completely assembling the ARM, the joy stick control was connected. The ARM was evaluated as a whole unit at this point. Movement was smooth, with little restriction. The motors had a bit of a problem reaching the very edge of the work space. This problem was due to the lack of available current from the power sources, not due to the motors. Other than the power source problem, no significant revelations occurred. The ARM was able to extend and contract while moving in the planar motion. It achieved the target workspace. Most of all of, it was able to move to a metal disk and pick the disk up, thus achieving the ultimate goal.

Another small problem that appeared in the total design testing was with the cable assembly for motor 3. Because the telescoping arm was under passive control on extension, there was nothing to stop the motor from continuing to turn when the arm touched the ground. This allowed the coils to unwind off of the spool and either tangle or jump out of the spool altogether. Also because the motor continued to turn, the potentiometers gave erroneous readings for the position of the end-effector. Fabrication of a larger spool cured the problem with the cable. Solving the problem of erroneous motor angle recordings can only be done by using some sort of limiting device, such as

a touch sensor on the end-effector (this is a requirement anyway, because the ARM needs to know when it has touched a metal disks).

With the ARM in operational order and the qualitative analysis fairly well exhausted, it was time for some quantitative analysis. The next section discusses how data was collected and compared.

B. Quantitative Analysis

For the quantitative analysis of the prototype, three areas were examined. First position data was collected and then compared to the values derived from the kinematic models. This comparison validated the models. The second area examined was decoupled operation. Each motor angle was moved while holding the other angles constant. Graphical analysis proved that, within a region about the vertical position, there was only a small amount of coupled operation. These same graphs were then used to look at the last area of concern. This area was to the determine the linearity of the operation. As the graphs will show, the relationships were quite linear even though the equations were not.

To begin the quantitative analysis, position data on the end-effector had to be collected. Moving the ARM and taking a measurement would have been a laborious task indeed. Instead, a device known as the Optotrak was used. The Optotrak is a unit consisting of three infrared detecting lens, aligned so that triangulation is used to measure the position of infrared emitting diodes (called markers). The lens unit is attached to a central control unit that also can receive analog signals from a data acquisition unit. The control unit is connected to a computer which runs a software package, created by the manufacturer, to control the whole process and collect the data.

Under normal operation the unit measures the position of the markers relative to a internal reference frame. When using this frame no calibrations are needed because they were all done by the manufacturer. Using this frame would have required

converting this data to the desired D-H frame by hand. The unit did have a method by which a new reference frame could be created. To make calculations simple, the D-H reference frame was established as the frame with respect to which data would be collected. To set up this frame, three markers were attached to the ARM so that their exact positions from the origin of the inertial reference frame (which is the ball joint) were known. These positions were fed to the computer and the internal program set up the desired reference frame. Each time a new set of data was taken, a calibration on the D-H frame was performed.

After the reference frame was set up, data could be collected. The data of interest was the three motor angles and the end-effector position. A marker was attached to the end of the ARM to acquire the position. To record the motor angles the data acquisition unit on the Optotrak had to be used. It had the capability of collecting information in the form of voltages, so the potentiometers were used. The potentiometers were connected to a power source of 10 volts so that a range of voltages from 0 to 10 was produced. These voltages then had to be converted to motor angles for analysis. Motor 3 used a ten turn pot. This meant that for every turn of the pot, one volt was produced. Simply multiplying the voltage to a conversion factor of 2π radians/volt yielded the desired motor angles. The conversion factor for the five turn potentiometers on motors 1 and 2 was π radians/volt, because the potentiometers produced two volts for every turn.

Data was collected in several different sets to insure accurate comparisons. Comparison of the data collected to the model was mainly a graphical trend analysis. Absolute position data was hard to obtain. The data from the Optotrak can only be as accurate as the measurements used to set up the reference frame. Other errors such as marker placement, lens placement, and obstructed views could cause data collection errors. The model it self is only as accurate as the geometric measurements presented in the previous chapter. Therefore relating absolute error of the measured data to the

model was of less importance than just trend analysis because of the unknown errors present.

A data collection profile was used that incorporated isolated movement of each motor and the actual motion of retrieving metal disks. Figure 31 shows the comparison of measured position to calculated position using the forward kinematic model for this profile. Each plot is a position coordinate (x, y, or z) versus the collection frame which was taken every 0.1 seconds. Presenting the graph in this fashion in essence allows the three coordinates to be plotted versus the three motor angles which dictated the position. To compare the model to the collected data, the motor angles recorded by the Optotrak were merely substituted into the forward kinematic equations. The overall results show that the model follows the trends of the collected data very well. Most impressive was the x coordinate. The two lines that were graphed are nearly identical. This seems reasonable because this was the direction least affected by the troubles with the cable system.

The graphs of the y components also matched up well, except for several spikes in the model. The spikes in the model graph can be explained rather easily. A close examination of the plot shows that when the spikes occur in the model, the measured data levels off. This suggests that the end of the ARM was touching the ground at these points. The data would thus show a flat line and the model would show that the end-effector continued to move because the potentiometers had continued to rotate with the motor as if the arm was still moving. The next chapter will give some details on how this problem might be addressed.

The graph of the z component comparison is the result of some adjustments to the data and to the model. When the comparison was first made, there was a 50 mm difference from frames 400 to 1200. This was the exact position in the profile that the arm was extended. In collecting the data, it was noticed that the springs created a spiraling effect in the tubes as the arm extended. Because the infrared marker was

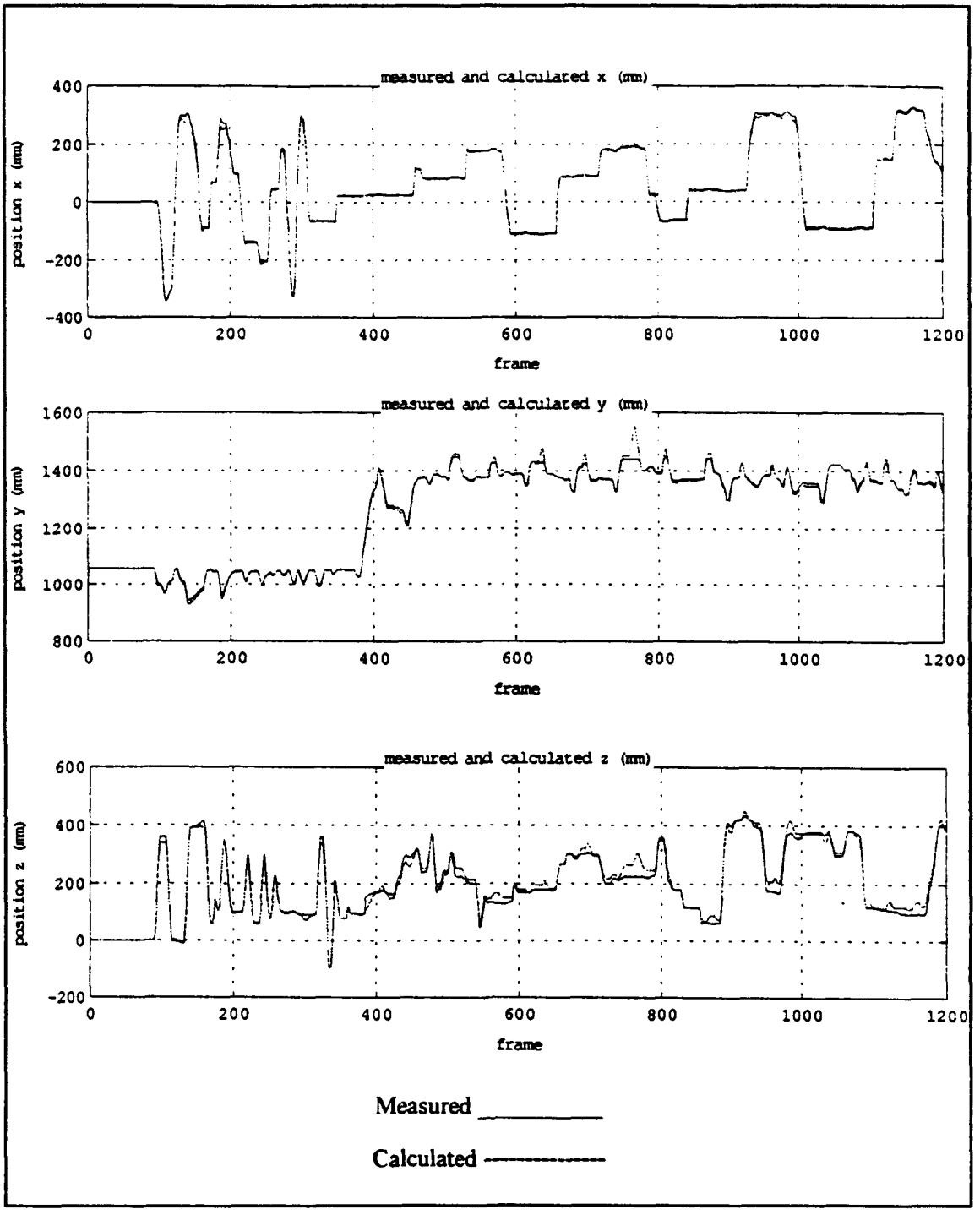

Figure 31. Measured and Calculated Position Comparison

placed on the side of the end tube (off the centerline of the tube), the marker turned with the tube as it extended, creating a 20 mm error in the z direction. This error was

corrected by adjusting the data accordingly. The remaining difference was due, most likely, to the wrong kinematic model being used. Going back to chapter IV, the transformation from motor angles to joint angles presented a right and left kinematics, which manifested itself as a plus or minus sign. For the initial model calculation the wrong kinematics was used. Changing the sign in the equation corrected the difference. Overall, the comparison in the z direction was the worst of the three. The trends of both plots matched fairly well with each other. Some of the magnitudes did not match, however. There was a maximum error of approximately 100 mm. This was probably due in part to the fact that there was some problems with cable tension in this direction.

Examination of the trends of the graphs shows that the forward kinematic model is valid. The next step is to use the same profile and graphical set up to equate each motor angle to its respective coordinates for the inverse kinematic validation. As before they are being plotted against the collection frames (or time, if you wish). To achieve motor angles from the model, the measured coordinates were substituted into the inverse kinematic equations. Trends in the plots were the main focal point as before. Because the inverse kinematic equations were derived from the forward kinematic model, the plots should have been very similar. As it turned out, they were similar. Figure 32 shows the measured and calculated motor angle comparison. The results are very much the same. The x coordinate graph was nearly identical. The y coordinate plot was fairly close except for the spikes that were explained above. And the z coordinate had the worst difference in magnitude, but the trends of the measured and calculated plot were virtually the same. Thus the inverse kinematic model must be valid also. Other profiles of data collection were run and their graphical representations resulted in similar trends.

Another area of interest in terms of performance is the question of coupled operation. To answer the question graphically, it is necessary to move only one motor

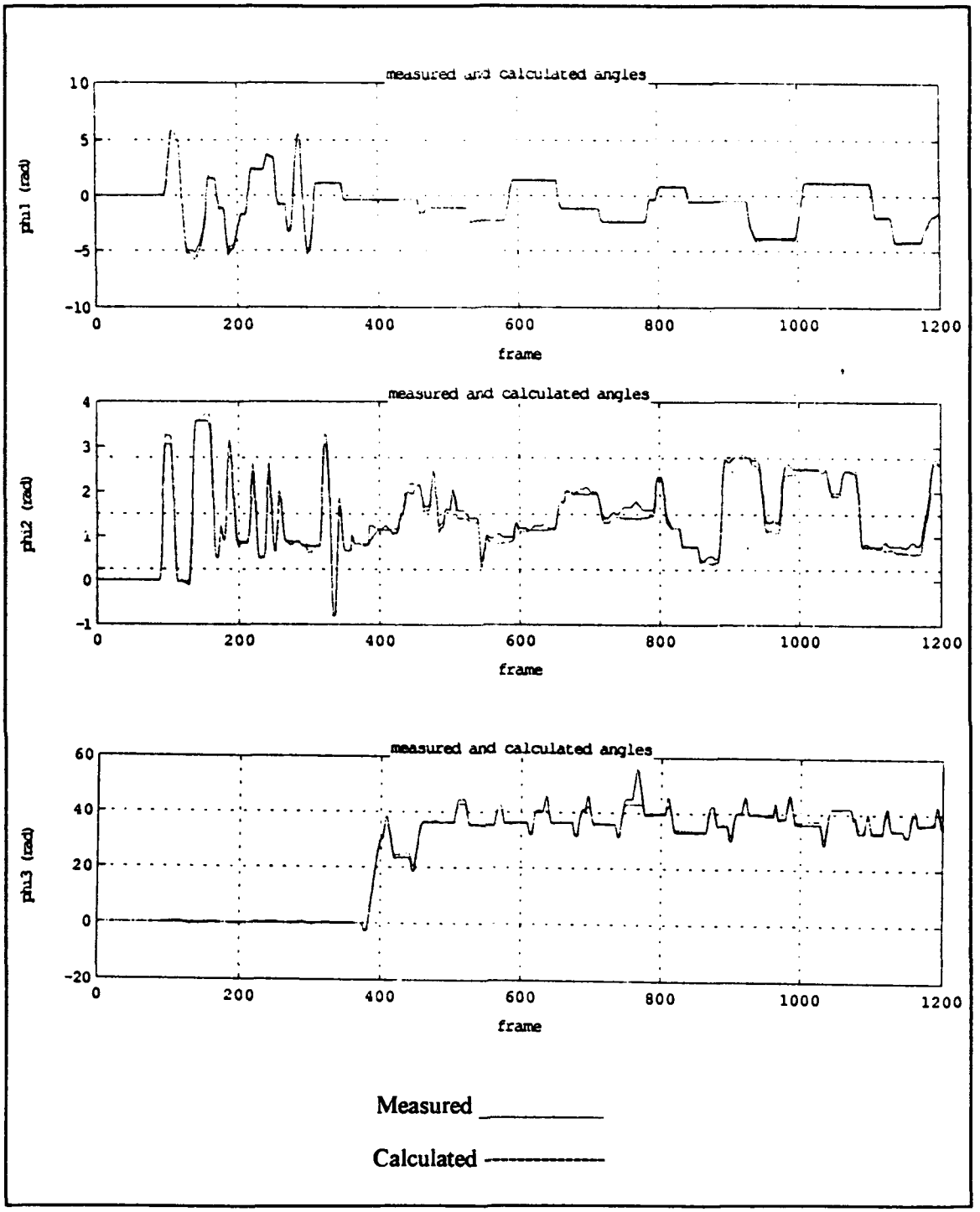

Figure 32. Measured and Calculated Motor Angle Comparison

at a time and evaluate how this motion changes all three coordinates of the end-effector. Because there may be different regions of operation the decision was to divide the x, z

plane into different quadrants. Operation of one motor at time was examined graphically in each quadrant and the assumption was that because of the symmetry there is no difference in the quadrants. Figures 33, 34, and 35 show the change in position for each isolated motor angle. Figure 33 are plots of the position change versus motor angle 1, while the other two motor angles are kept constant. The graphs shows that the greatest change is in the x direction. The other two components, y and z, hardly changed at all. There seems to be more change in y than in z, which is logical when the kinematic model is examined. According to the model the z component does not involve motor angle 1. The graphs should show that the change in is approximately zero, which it does. Because of the very small change in y and z, the operation of motor angle 1 can be approximated as being decoupled. Remember that the operation of the ARM is restricted to about 20° from vertical, therefore these observations are not valid outside this region.

A check of Figure 34 shows the same type of relationship as before. This time the greatest change is in the z component. Motor angle 2 influences the change in z more than in x or y. From the plots, the y component is influenced more than x. Looking at the model again shows that this is also logical. The y component changes more because the magnitude of y is larger than x for this particular plot. Thus operation of motor angle 2 can also be approximated as being decoupled.

Figure 35 shows that the greatest influence of motor angle 3 is on the y component. The other coordinates are only slightly affected by this change. The position of the arm (whether z or x is larger in magnitude) determines which of the other two coordinates will change the greatest. And as seen before this operation can also be considered decoupled. One curious observation can be seen in the plot for quadrant 4, the change in the z component suddenly switches from 0 to about -20. This peculiarity can be explained through the observation that the tubes turned when the arm was extended. The error in the z dimension that resulted because the turning was

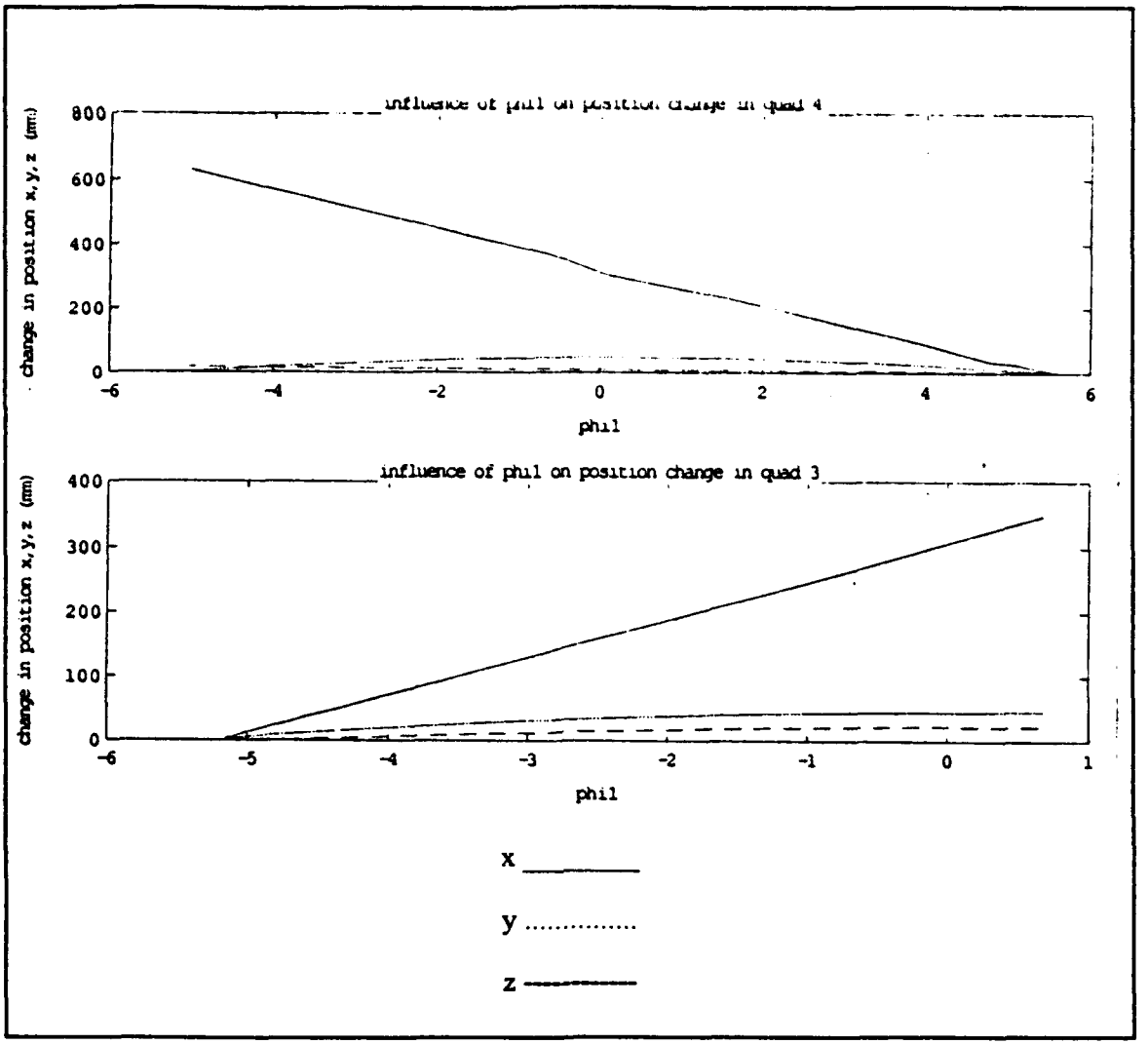

Figure 33. Position Change for Motor Angle 1

approximately 20 mm. Taking into account that the plot is displaced 20 mm, the effect of motor angle 3 is negligible on the z component.

One other analysis can be made using these three figures. In each plot, the coordinate that is affected the most produces a straight line. This suggests that there is a linear relationship between the motor angles and the position, at least in this small angle area. A quick check of the kinematic model shows that the actual equations are not linear. They include square roots and sinusoidal terms. Evidently , though the equations are not linear, their results are linear.

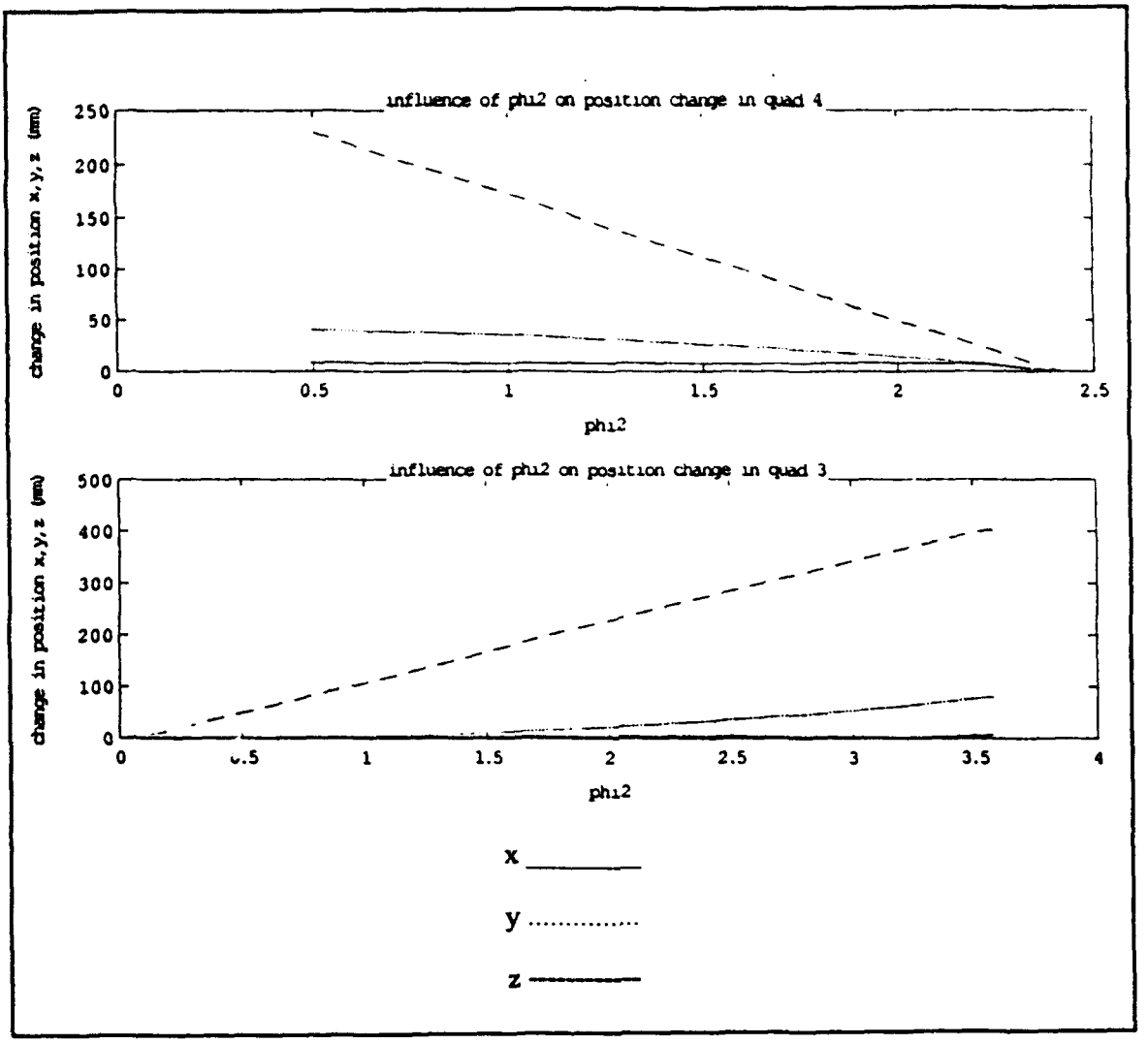

Figure 34. Position Change for Motor Angle 2

The main use of the fact that operation of the ARM is both linear and decoupled is in the area of automation. Computation time is greatly reduced because of these traits. Since the equations do not need linear approximations, the accuracy should also be better.

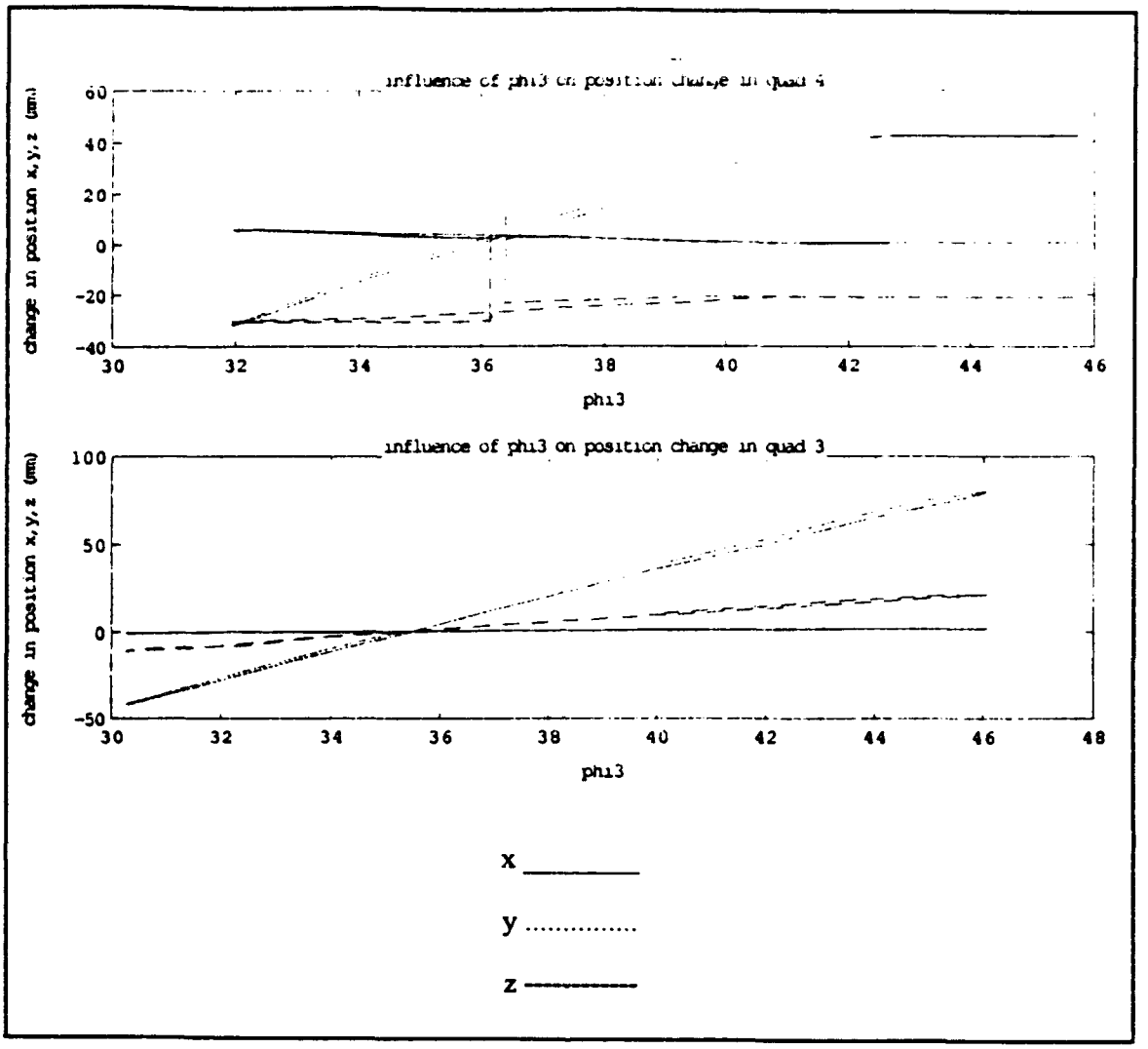

Figure 35. Position Change for Motor Angle 3

VI. Results, Conclusions, and Recommendations

To finalize this thesis, a brief summary is in order. The project started with the identification of the problem, namely, creating a robotic manipulator for the Aerobot to compete in the Aerial Robotics Competition. Parameters for the robot were established and conceptual designs were considered. Once the conceptual design was finalized, the design and construction of each component began. After the ARM was completely assembled, it was tested and evaluated under the specifications for which it was built. A mathematical model of the manipulator was derived for its future automation and the model was evaluated against test data.

A. Lessons Learned and Their Solutions

Several problems with the final design have been noted throughout the report. They are presented again along with possible solutions because of their importance. One of the very first problems noted was the ball joint. The ball joint was used because of the ease in construction. Choosing the ball joint created two problems. One problem was that an unwanted degree-of-freedom was added. With the ball joint the bottom plate and telescoping arm could rotate about the arm's centerline. Cable tension was the only thing restricting this motion. This motion did not hinder the operation of the ARM during testing, but it could be a problem when it is attached to the Aerobot. Any extra motion, like this one, that is unwanted and uncontrollable will cause vibrations and inaccurate operation.

Because the ball joint was used the pivot point of the telescoping arm had to be located on the top plate, and this caused another problem. This was the cable tension problem resulting from using two pivot points. When one axis was moved out of the nominal position, the cable tension loosened in the other axis. While gravity kept the arm from moving very much on the bench tests, operation inflight will not be so

forgiving.

The actual solution to both of these problems is to replace the ball joint with a universal joint. As part of this project, the universal joint was designed and built, but not installed. Figure 36 shows the completed universal joint. To solve the first problem the extra degree-of-freedom must be restricted. This type of joint restricts the rotational motion allowed by the ball joint. To solve the problem of two pivot points in the cable system, the universal joint must be mounted on the top of the bottom plate. The cable connection to the bottom plate will require swivel joints that operate through the centerline of the universal joint. This new arrangement allows the cables to remain perpendicular to the top plate no matter which axis is moved. Because the cable will be pivoting at the bottom plate attachment, the swivel pulleys will not rotate. Mounting the universal joint in this fashion will change the model. The D-H reference frame convention uses rotating reference frames which is what the old cable system emulated. The motion provided through the new cable system will stay within the planes set up by the inertial frames. Therefore, care must be taken when deriving the model because the D-H conventions must be modified somewhat to work in this set up.

A lesson to be learned here is that when designing something, no one criteria can dominate the decisions being made. In the example of the ball joint the one driving factor was the ease of construction. Had other criteria been considered at the same level, then the universal joint might have been the first choice instead of the ball joint.

One problem that the universal joint will not solve is the cable tension problem created by the double spool system. Because the geometry of the cables and lever arms is ruled by the Law of Cosines, which is a non-linear equation, there is a difference between the amount of cable needed to pull the lever arm and the amount needed to release the opposing lever arm. This problem is inherent to the design chosen. By concentrating on decoupled, simple operation, the criteria for rigidity was unknowingly neglected. Fixing the cable system as it stands can be accomplished in two ways. One

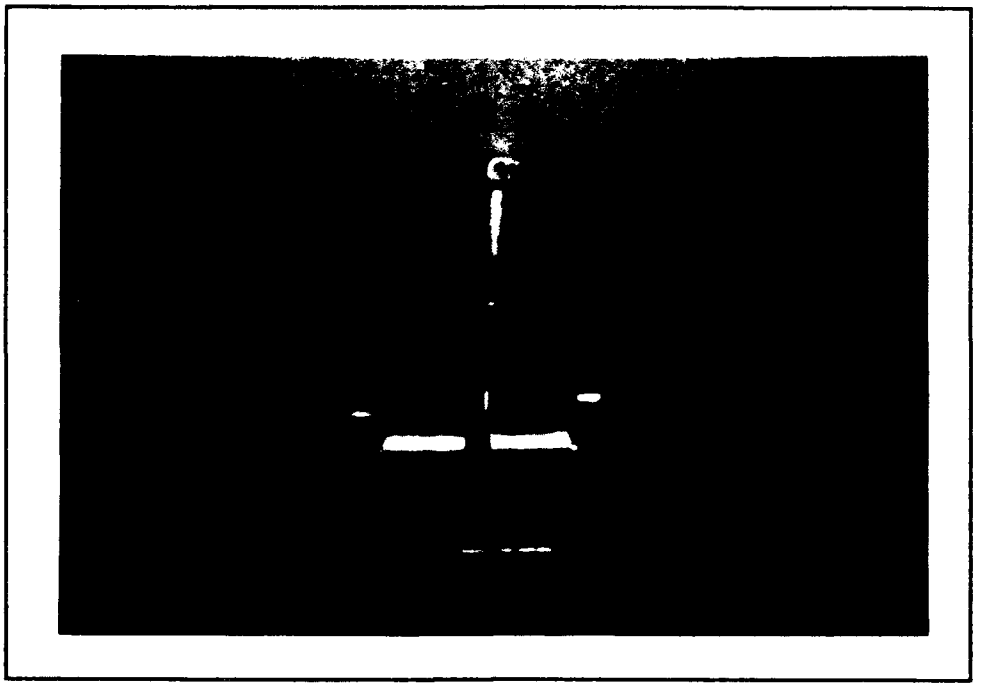

Figure 36. The Universal Joint

way is to use two motors instead of one motor with a double spool. One motor pulls while the other motor releases the exact amount of cable to keep the tension constant. This type of system is used successfully on the Utah-MIT hand which AFIT presently owns. By using the two motors and keeping the same cable geometry, decoupled operation is still available. The control of the twin motors would obviously be more complicated but not restrictive. The major problem of adding the second motor is the weight increase. Adding two more motors to the ARM would mean adding two more pounds which could be quite significant. An alternative to adding more motors is to create a variable radius double spool. The geometry of the spool would allow for the cable to remain taunt during operation. The principle behind the variable double spool lies in the radius of the spool. Varying the radii of the spool allows one side to create tension while the other side reels out cable.

One idea for solving the tension problem was to add spring loaded turnbuckles to the cable connections at the bottom plate. The springs would be fully compressed at

the nominal position and when the arm was moved out of that position the springs would take up any slack that was present. While this idea alleviates the problem without adding significant weight, it decreases the rigidity by adding an uncontrollable passive force to the cable system. The turnbuckles or some other type of tensioning device should be incorporated with this prototype. A set screw now provides this function.

As was just presented, passive control is not always appropriate in every situation. The system of telescoping the arm uses passive control for extension. The only real problem with that operation is when the end-effector touched the ground or an object. When this happens the motor continues to turn and coils continue to unravel. The problem of tangling was solved by making the spool larger. Figure 37 shows the new spool that was developed. The problem that remains is because the motor makes extra turns and the potentiometer(or optical encoder) sends out information that, when processed through the model, yields position error. The solution for this problem is to

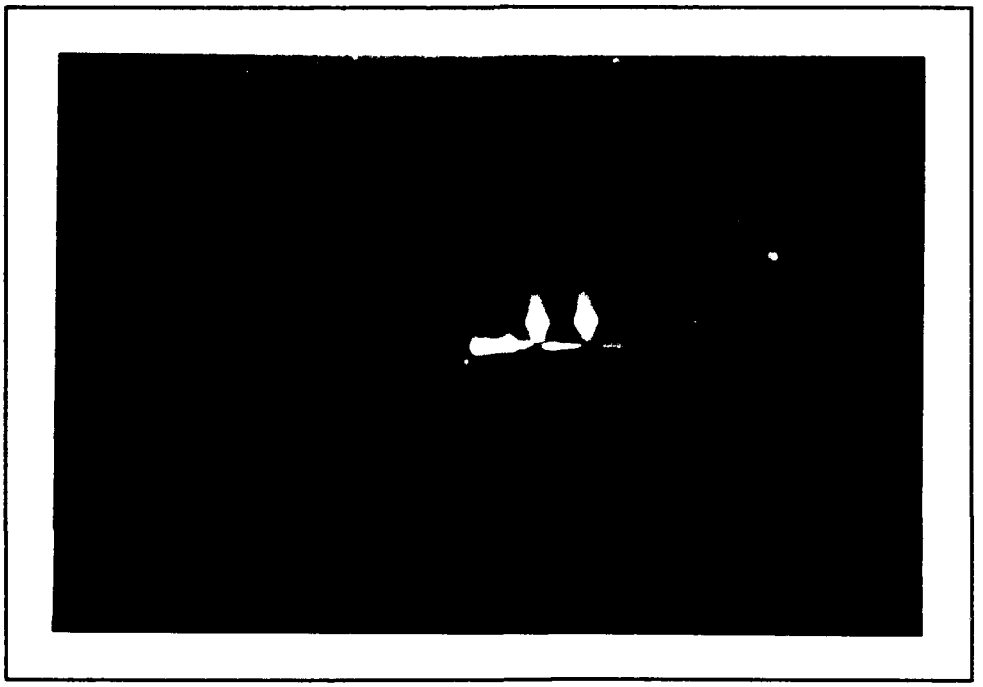

Figure 37. The New Single Spool

mount touch sensors to the end-effector that would relay whether or not something was touched, providing logic that could be used to stop at an obstacle. Another approach might be to use a visual acquisition unit to relay the same position information to the controller. This method might not be as accurate, depending on the resolution of the acquisition unit. The best approach might be to use both methods together. The visual system could provide the rough information of movement trends and the touch sensors could provide the accuracy needed to touch an object.

B. Conclusions

A large part of this report concentrated on the problems of the design as it stands now. Even though there were problems with the final product, the ultimate goal was achieved. A prototype robotic arm was constructed for the Aerobot and it performed the task it was designed for. The problems that were noted did not have a profound significance in the performance of the ARM. They were merely presented to allow the design to be improved upon.

To conclude the discussion of the ARM, its characteristics will be compared to the criteria from chapter two. First of all the target weight of 10 pounds can be achieved with reasonable modifications. With the compact design of the ARM, the center-of-gravity concerns are not as great as they might have been for another design. Exactly how much the added weight will effect the Aerobot controller is unknown and will not be known until the model of that controller is finalized. Using the design of the telescoping arm, the final product could retract out of the way for land or collapse down in the case of a crash landing. Also because of the telescoping ability, the manipulator was able to work outside of the blast area underneath the vehicle. It was also able to reach the target workspace set up to avoid lateral blast and to overcome navigation and disk location errors. Moderate rigidity was obtained with the small problems noted.

A strong point of the ARM is it simplicity. Because of decoupled operation

within its workspace, the computation time required to automate it will be minimal. Computation time will also be saved because the kinematic model yields linear results. Programming the automation of the ARM should be easier due to its simplistic design.

C. Recommendations

The first recommendation that should be made is to have all of the previously developed improvements installed. These include the universal joint, the larger single spool for the bottom motor, and motors with optical encoders. This will cure many of the small problems noted. Another recommendation would be to replace the electromagnet now installed on the prototype. It seemed a little underpowered and had some difficulties picking up painted metal disks. The overall problem of cable tension will need further study, particularly if the two motor approach is taken (or the variable radius spool for that matter). Other pieces of hardware that might benefit from further study include, a constant radius spool for the bottom motor (simplifies the equations when the radius is constant), touch sensors for the end-effector, and incorporation of video equipment for position information.

The next logical step for the ARM, after the specific modifications have been made, is to examine its dynamics. This study would then lead itself to controlling the ARM. Serious consideration should be made to adapting the device to operate by man-in -the-loop radio control as well as computer automation. As it stands now, the arm is a good example of telerobotic abilities; radio control would make an even better example. Also in the first stages of test flying with the arm, radio control might be helpful. Obviously the ultimate goal is to automate the ARM through the use of a computer. This could possibly be done at the same time for the vehicle also, because the process of transferring information to a computer will be similar.

A recommendation to AFIT is also in order. Because of the complexity of the Aerobot, students from other disciplines should be involved in thesis projects dealing

with the vehicle. Specific projects like automation are going to be very difficult for single disciplined personnel to accomplish. This is why all of the other universities competing in the Aerial Robotics Competition form teams that include electrical engineers, mechanical engineers, aerospace engineers and computer science. AFIT should likewise try to involve other disciplines in the Aerobot project.

Appendix A:

Competition Rules

This appendix contains a copy of the official rules of the Aerial Robotics Competition.

Official Competition Rules

for the 1994 International Aerial Robotics Competition

GENERAL RULES GOVERNING ENTRIES (please reference attached Competition Arena and disk drawings)

1. Vehicles must be unmanned and autonomous. They must compete based on their ability to sense the structured environment of the Competition Arena. They may be intelligent or preprogrammed, but they must *not* be flown by a remote human operator.

2. Computational power need not be carried by the air vehicle. Computers operating from standard commercial power may be set up outside the Competition Arena foul-line boundary and uni- or bidirectional data may be transmitted to/from the air vehicle.

3. Data links will be by radio, infrared, acoustic, or other means so long as *no* tethers are employed. The air vehicles must be free-flying with no entangling encumbrances, however, tethered subvehicles are allowed. Subvehicle(s) must be attached permanently to the autonomous air vehicle at all times. Subvehicles must themselves be autonomous. They may be deployed within the rings to search for, and/or acquire the disks. Subvehicles may not operate outside of the rings.

4. Any form of propulsion is acceptable if deemed safe in preliminary AUVS review.

5. Air vehicles may be no larger than a 10-foot (side) cube when operational.

6. **Intention to compete must be received no later than December 1 , 1993.** To avoid unnecessary delay due to the mail (particularly for international entries), intention to compete can be transmitted by FAX to Robert C. Michelson, AUVS Technical Chairman at (404) 528-3271. **The completed application form can follow by mail, but must be received no later than December 31, 1993.** A brief concept outline describing the air vehicle must be submitted at that time for safety review by AUVS (the application form provides space for this). AUVS will either confirm that the submitting team is a qualified competitor, or will suggest safety improvements that must be made in order to qualify.

   The competition will be held in Atlanta Georgia on the campus of the Georgia Institute of Technology on Thursday, May 19, 1994 (with Friday, May 20 as an alternate). Prize money will be distributed during the Awards Banquet at the AUVS national symposium being held May 23 through 25 in Detroit, Michigan.

7. Teams may be comprised of a combination of students, faculty, industrial partners, or government partners. Students may be undergraduate and/or graduate students. Inter-disciplinary teams are encouraged (EE, AE, ME, etc.). Members from industry, government agencies (or universities, in the case of faculty) may participate, however full-time students *must* be associated with each team. Participants must be enrolled at their schools for at least 12 credit hours or more per quarter/semester during winter and spring 1993 to be considered "students." The student members of a joint team must make significant contributions to the development of their entry. Only the student component of each team will be eligible for the *cash awards*.

COMPETITION RULES

1. Air vehicles must transfer six randomly placed disks from the pick-up ring to the drop-off ring on the other side of the three-foot high central barrier. The disks must be transported one at a time. Though randomly placed, the disks will initially be at least three inches from the edge of the pick-up ring.

2. All air vehicles must start from the designated starting area. Only two members from the team may be within the boundaries of the Competition Arena once attempts to start the vehicle begin. From lift-off until the end of the round, all team members must remain outside the Competition Arena.

3. Teams will be allotted 60 minutes to complete the task. Each team will be assigned a specific 60-minute time slot in which they must set up and perform as many attempts as they wish. Judges will score each valid attempt, with the highest score being used to determine the winner.

   To accommodate the number of competing teams within a reasonable time, three arenas will be constructed side-by side as shown at the top of the next page. A team will be assigned to one of the three arenas. Non-flight activities such as set-up, calibration, and take-down will be performed simultaneously by the three teams occupying the arenas.

   Upon notice that a team is ready to fly, the clocks will be stopped for the other two teams and the field will be cleared except for designated officials and two members of the currently flying team. Once that run is complete, the other teams may return to their on-field activities and the clocks will be allowed to continue. After 60 minutes of arena time, a new team will be allowed to take control of the arena and the clock for that arena will be reset.

4. Teams may have more than one entry. Each entry must be based on a different air vehicle technology or navigation scheme and must be documented by a separate application form, submitted in accordance with all deadlines. A round will be declared a valid try if the vehicle leaves the starting area.

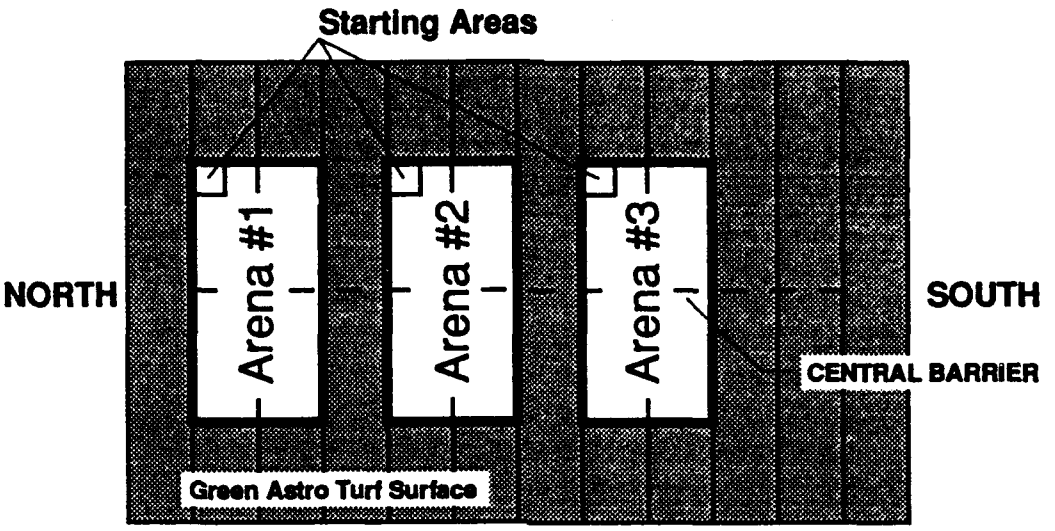

5. Subvehicle tethers may only touch the three-inch high edge of either ring, the six-foot diameter base of either ring, or the region designated as the starting area. A run will be terminated if any part of an air vehicle, subvehicle, or subvehicle tether touches the ground outside of the starting area or the pick-up and drop-off rings.

6. The score will be based on a number of factors as follows:

Effectiveness Measures:

1. The number of disks (c) successfully transferred from the pick-up ring to the drop-off ring (50 points per disk)
2. The elapsed time (d) between take-off (*leaving starting area*) and the first valid disk acquisition measured in seconds divided by 10, and subtracted from the total score during a given round.
3. Successfully leaving the starting area and "operating autonomously and intelligently" for *not less than* 30 seconds (e) is worth 99 points.†
4. The number of successful disk acquisitions from pick-up ring (200 points each). Disks dropped within 25 feet of the center of the pick-up ring do not count as successful acquisitions.
5. Successful autonomous landing at the end of a round (g) is worth 30 points.

† *Evidence of intelligent operation must include deliberate changes in platform speed and direction which result in the correct positioning of the air vehicle subsystems during the various phases of task execution.*

Subjective Measures:

6. Elegance of design and craftsmanship (h) on a scale of zero to 30 (highest).
   - 6.1 Component integration (0 - 10).
   - 6.2 Craftsmanship (0 - 10).
   - 6.3 Durability (0 - 10).
7. Innovation in air vehicle design (i) on a scale of zero to 50 (highest).
   - 7.1 Primary propulsion mechanism {lift} (0 - 10).
   - 7.2 Attitude adjustment scheme {yaw/pitch/roll/lateral} (0 - 10).
   - 7.3 Disk retrieval mechanism/scheme (0-30).
8. Safety of design to bystanders (j) on a scale of zero to 40 (highest).
   - 8.1 Isolation/shielding of propulsors (0 - 10).
   - 8.2 Containment of fuel and exhaust by-products (0 - 10).
   - 8.3 Crashworthiness (0 - 10).
   - 8.4 Emergency flight termination mechanisms (0 - 10).
9. Each team is required to submit a journal-quality paper (written in English) documenting their project. This paper (m) is worth 50 - 100 points depending on technical quality. Papers are limited to 10 pages (including figures and references, if any). The format shall be single-sided with text occupying a space no greater than 9 inches tall by 6.5 inches wide on each page. Font size shall be 12 point (serif font) with 14 point leading. The example format is provided on page 12 of these rules. Topics to be covered include: competitive strategy, how your vehicle design achieves your strategy, propulsion, stability augmentation schemes, navigation schemes, and disc retreival mechanism. Five copies of your paper are due to the application submission address by March 20, 1994.
10. Best team Tee Shirt (l) (one point to the best).

The points for a given round will be totalled according to the following formula:

$$\text{SCORE} = (c * 50) + e + (f * 200) + g + h + i + j + l - (d/10) + m$$

The highest score accumulated by any entry after all rounds have been completed will be declared the winner.

7. A minimum of $10,000 will be awarded to the team having the highest score achieved during any fully autonomous round in which a disk is successfully moved. In the event that *no* air vehicle is capable of successfully moving even a single disk during any round, the method of prize money distribution will be at the discretion of the judges— however any partial awards resulting shall not exceed $1,000 per award with the total allocated to such partial awards not to exceed $5,000.

8. Air vehicles may only land within one of the two rings or within the starting area. The air vehicle must be airborne at all other times. "Air vehicles" are considered to be those capable of sustained flight *out of ground effect* while requiring the earth's atmosphere as a medium of interaction to achieve lift (as such, pogo sticks and similar momentary

ground-contact vehicles are not considered to be *flying air vehicles*). The scoring formula and arena have been carefully designed to normalize advantages inherent to a given class of air vehicles such that all may compete fairly to perform the same task. Prospective teams must decide how best to allocate resources to maximize their potential score in light of the constraints imposed by the arena, the task, and the scoring algorithm.

9. Air vehicles may not latch onto, or use, the central barrier for locomotion or stability. Vehicles crossing over the foul line will be disqualified for that round and must be returned to the starting area.

10. Disks placed within the drop-off ring, but which are later knocked out by other disks or the air vehicle itself, still count toward the total. Disks which bounce or roll out of the drop-off ring during initial placement do not count.

11. Each air vehicle must be equipped with a non-pyrotechnic termination mechanism that can render the vehicle ballistic upon command of the judges. This termination mechanism must be demonstrated to the judges prior to the first round. Air vehicles may be landed under manual control if desired, but the points that could be awarded for an autonomous landing will be forfeited. Both autonomous and manually-assisted landings must occur within the foul lines of the Competition Arena. Fully autonomous flights which successfully move a disk but have manually-assisted landings are still considered "fully autonomous rounds" and are eligible to receive the $10,000 award.

HOW COMPETITORS WILL BE JUDGED

1. A team of three judges will determine compliance with all rules. Official times and measures will be determined by the judges. Subjective measures (6 - 10) will be judged the day prior to the competition at a location near the arenas and in accordance with a schedule to be announced a week prior to the competition. Team papers will be ranked and scores assigned to them at this time.

GROUNDS FOR DISQUALIFICATION

1. Vehicles crossing over the foul line will be disqualified for that round only.
2. Judges will disqualify any vehicle which appears to be a safety hazard.
3. Intentional interference with a competitor's run will result in disqualification of the offending contestant's entry.
4. Damaging the Competition Arena, disks, or navigation aids may result in disqualification.
5. Actions designed to damage or destroy an opponent's vehicle are not in the spirit of the competition and will result in disqualification of the offending contestant's entry.

AWARDS

1. $10,000 Cash tuition award to winning student team members.

2. National recognition for the winning student's university.

3. National recognition through AUVS for the winning industrial/government/faculty organization.

4. Free full-page advertisement for the winning company, governmental agency, or university faculty department in *Unmanned Systems* magazine. If more than one industrial/government/academic entity is supporting the team, then the student component shall designate which partner has supplied the greatest assistance (in whatever form), and *that* partner shall receive the free full-page advertisement.

5. Special recognition to the winning team at AUVS '94 to be held in Detroit, Michigan including free attendance to the symposium and awards banquet for up to 10 team members, an invitation to display the winning air vehicle in the exhibit hall, and the opportunity to present a paper to the unmanned vehicle community detailing winning design and construction strategies. Other competing teams will receive two complementary registrations to the symposium.

All teams are invited to submit their papers describing their designs and strategies at the symposium by submitting them for publication in the symposium proceedings by the regular submission deadline. Also, exhibit space can be made available to all teams wishing to showcase their technology at the symposium by contacting AUVS headquarters.

ATTACHMENTS TO OFFICIAL RULES PACKAGE

Incorporated into this rules package are the following figures and drawings:

1. *Competition Arena*
2. *One Possible Flight Path*
3. *Navigation Aid Locations*
4. *Disk Geometry*

Example Scorings for Various Levels of Competition Performance

CATEGORIES	*Case 1*	*Case 2*	*Case 3*	*Case 4*	*Case 5*	*Case 6*	*Case 7*	*Case 8*	*Case 9*
			none transferred: Partial award at Judge's discretion				*>1 disk transferred:* Eligible for $10,000		
c Number of disks transferred (0 - 6 at 50 points each)	0	0	0	0	0	0	1	1	2
d Elapsed time from take-off to first disk acquisition (seconds/10)	0	0	0	0	0	360	360	40	360
e 30 second intelligent autonomous operation (99)	0	0	0	0	99	99	99	99	99
f Number of successful disk acquisitions (200 each)	0	0	0	0	0	1	1	1	2
g Successful autonomous landing (30)	0	0	0	30	0	0	0	0	0
h Elegance of design and craftsmanship (0 - 30)	0	30	30	30	0	0	0	0	0
i Innovation in air vehicle design (0 - 50)	0	50	50	0	50	0	0	0	0
j Safety of design to bystanders (0 - 40)	0	40	40	40	0	0	0	0	0
l Best team tee shirt (0 or 1)	0	1	1	1	0	0	0	0	0
m Team paper (50 - 100)	0	75	75	75	75	75	75	75	75
SCORE =	0	196	196	176	224	338	388	420	638

Scoring Formula:

$$(c*50) + e + (f*200) + g + h + i + j + l - (d/10) + m$$

Maximum theoretical score = 1850

CONDITIONS								
no show	no fly	fly	fly	fly	fly	fly	fly	fly
No Prize Money Awarded	Recognition, but no prize money awarded	none xfer'd	none xfer'd	none xfer'd	none xfer'd	one xfer'd	one xfer'd	two xfer'd
		none acq'd	none acq'd	none acq'd	disk acq'd	disk acq'd	disk acq'd	disk acq'd
		crash landing	auton. landing	crash landing	manual landing	crash landing	manual landing	crash landing
	best design	best design	worst design	best design	worst design	worst design	worst design	worst design
		<30 sec flight	<30 sec flight	≥30 sec flight	≥30 sec flight	≥30 sec flight	≥30 sec flight	≥30 sec flight
					6 min flight	6 min flight	40 sec flight	6 min flight

COMPETITION ARENA

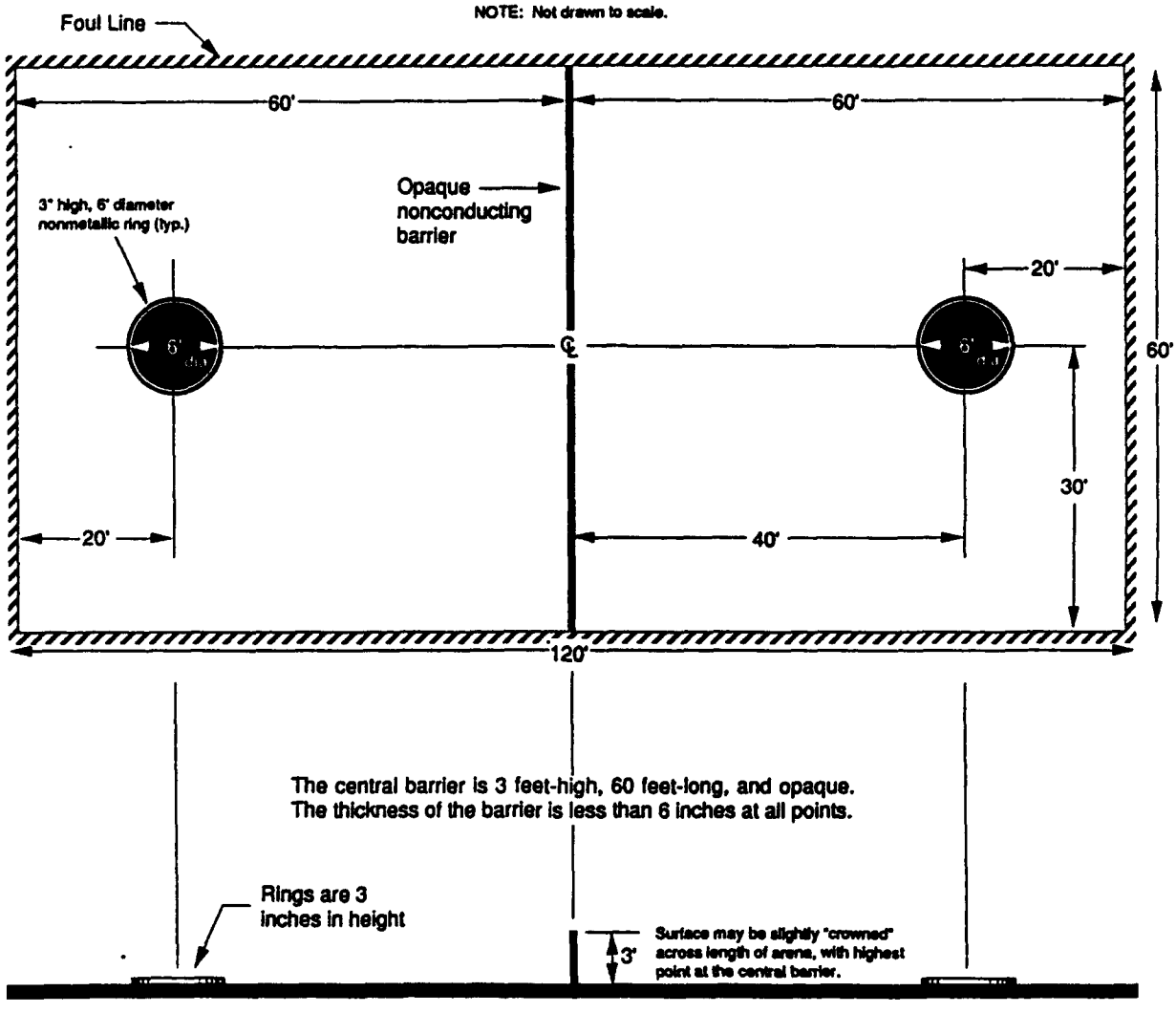

ONE POSSIBLE FLIGHT PATH

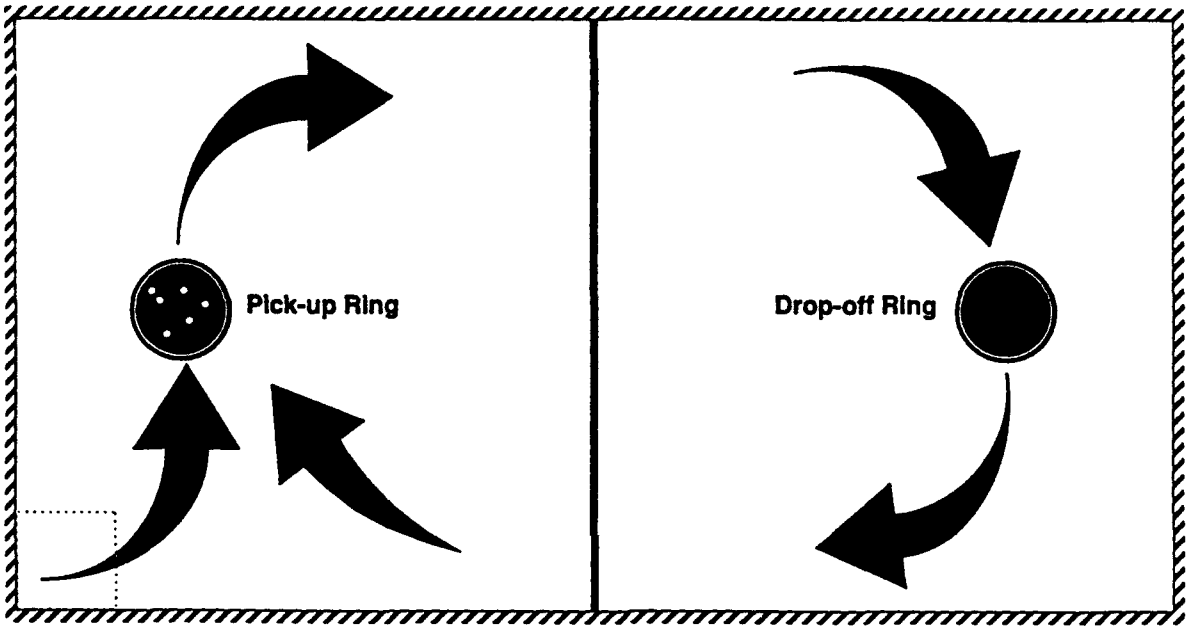

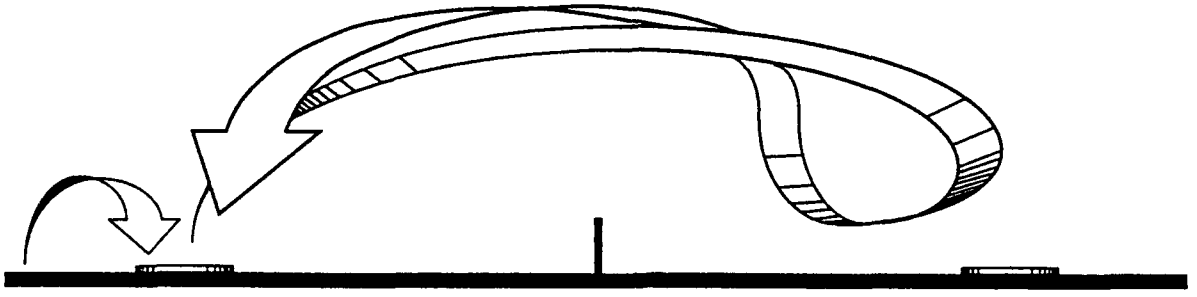

NAVIGATION AID LOCATIONS

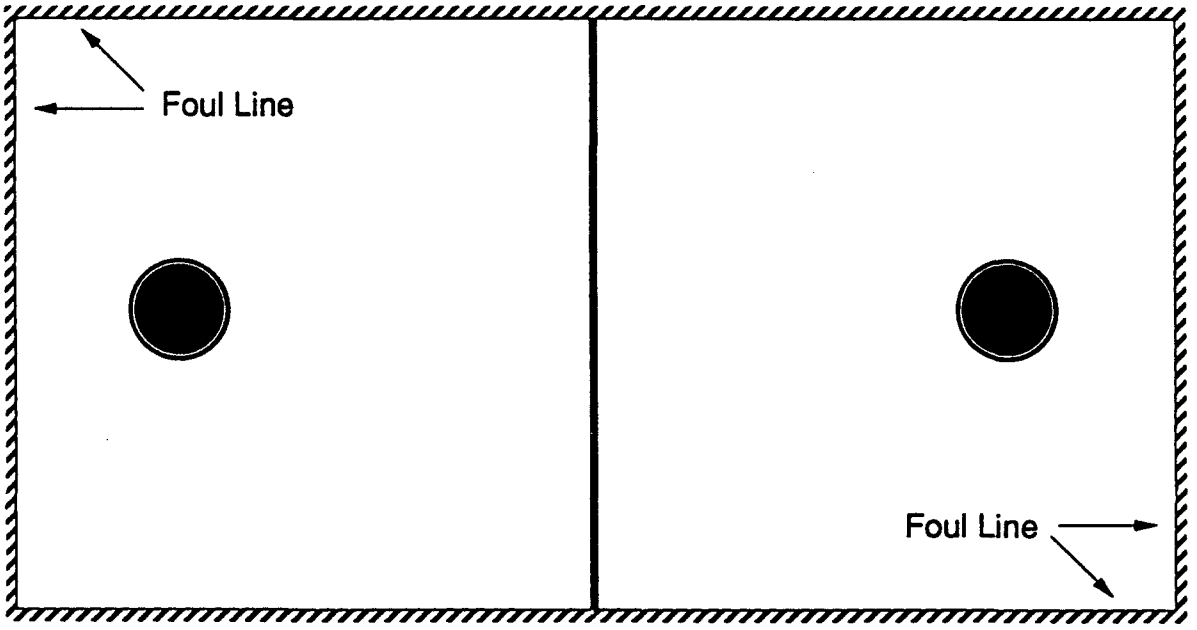

External navigation aids *are* permissible, however, they must be placed outside the foul line.

DISK GEOMETRY

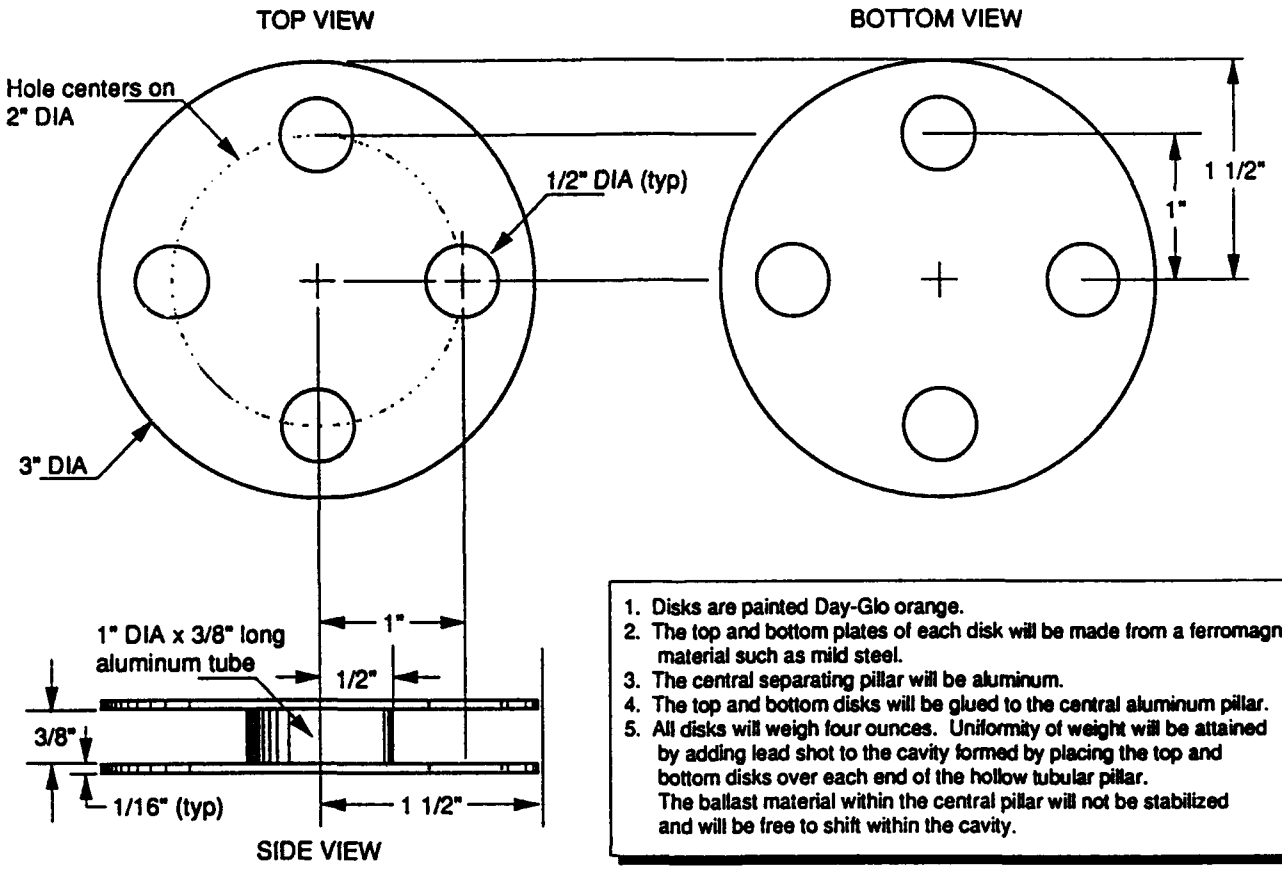

1. Disks are painted Day-Glo orange.
2. The top and bottom plates of each disk will be made from a ferromagnetic material such as mild steel.
3. The central separating pillar will be aluminum.
4. The top and bottom disks will be glued to the central aluminum pillar.
5. All disks will weigh four ounces. Uniformity of weight will be attained by adding lead shot to the cavity formed by placing the top and bottom disks over each end of the hollow tubular pillar. The ballast material within the central pillar will not be stabilized and will be free to shift within the cavity.

Appendix B.

Dimensioned Drawings

This appendix contains the dimensioned drawings and other specifications of selected parts of the ARM.

Telescoping Tube Dimensions

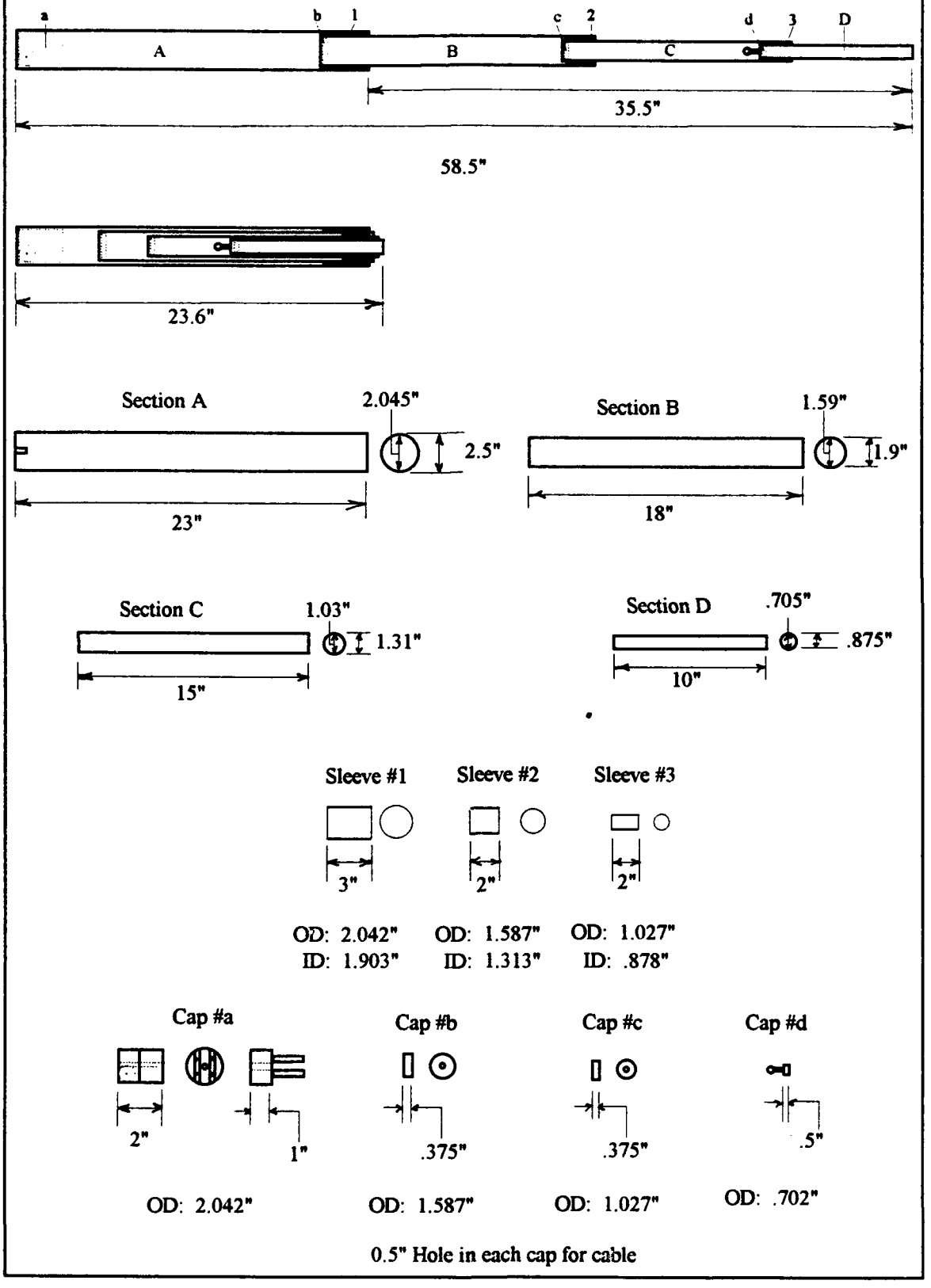

Movement Mechanisms

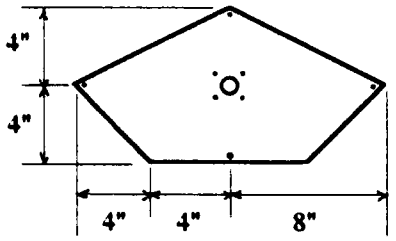

3/16" sheet aluminimum

Bottom Plate

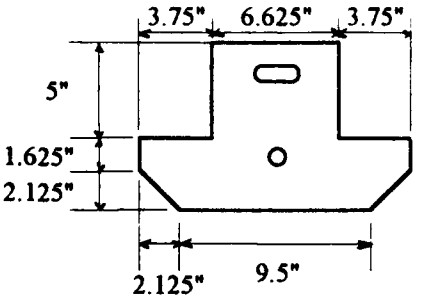

5/16" sheet aluminimum

Top Plate

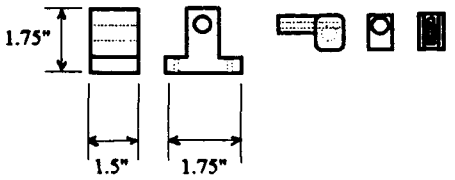

Swivel Pulley Assembly

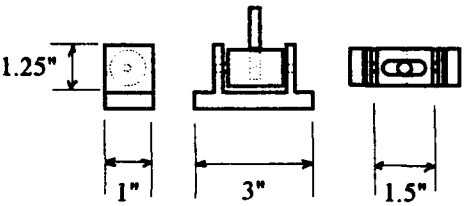

Universal Joint

Specifications for Spring #1

Material Type: 01 PM PHOS MUSIC ASTM-A228

Diameters

Outside:	1.8750				
Inside :	1.7410	*			

Average Diameter

Outside :	1.8750
Inside :	1.7410
Mean Diameter:	1.8080

Wire Size	:	0.0670	
Total Coils	:	29.000	
Active Coils	:	27.000	
Load Lbs.	:	1.9968	*
Load Height	:	19.0000	
Free Length	:	30.0000	
Percent Scrap	:	10.0000	
Load Tolerance:			*

ROUND

Solid Ground	:	1.9430
Solid Unground	:	2.0100
Rate Lbs/Inch	:	0.182
Weight/M pcs.	:	180.787
FL/Load Tol.	:	
Load Stress	:	32145.955
Solid Stress	:	81992.641
Dev. Length Inch:		164.7204
Spring Index	:	26.9851
OD at Solid Grd.:		1.9088

[Compression Design Calculation]

Material Type: 01 PM PHOS MUSIC ASTM-A228

Diameters

Outside:	1.8750	
Inside :	1.7410	*

Average Diameter

Outside :	1.8750
Inside :	1.7410
Mean Diameter:	1.8080

Wire Size	:	0.0670	
Total Coils	:	29.000	
Active Coils	:	27.000	
Load Lbs.	:	4.9013	*
Load Height	:	3.0000	
Free Length	:	30.0000	
Percent Scrap	:	10.0000	
Load Tolerance:		0.0000	*

ROUND

Solid Ground	:	1.9430
Solid Unground	:	2.0100
Rate Lbs/Inch	:	0.182
Weight/M pcs.	:	180.787
FL/Load Tol.	:	0.0000
Load Stress	:	78903.707
Solid Stress	:	81992.641
Dev. Length Inch:		164.7204
Spring Index	:	26.9851
OD at Solid Grd.:		1.9088

Specifications for Spring #2

[Compression Design Calculation]

Material Type: 01 PM PHOS MUSIC ASTM-A228

Diameters

Outside: 1.5000

Inside : 1.3760 *

Average Diameter
Outside : 1.5000
Inside : 1.3760
Mean
Diameter: 1.4380

Wire Size	:	0.0620	
Total Coils	:	31.000	
Active Coils	:	29.000	
Load Lbs.	:	1.4779	*
Load Height	:	16.0000	
Free Length	:	22.0000	
Percent Scrap	:	10.0000	
Load Tolerance:		0.0000	*

ROUND

Solid Ground	:	1.9220
Solid Unground	:	1.9840
Rate Lbs/Inch	:	0.246
Weight/M pcs.	:	131.621
FL/Load Tol.	:	0.0000
Load Stress	:	24077.246
Solid Stress	:	80570.492
Dev. Length Inch:		140.0462
Spring Index	:	23.1935
OD at Solid Grd.:		1.5198

[Compression Design Calculation]

Material Type: 01 PM PHOS MUSIC ASTM-A228

Diameters

Outside: 1.5000

Inside : 1.3760 *

Average Diameter
Outside : 1.5000
Inside : 1.3760
Mean
Diameter: 1.4380

Wire Size	:	0.0620	
Total Coils	:	31.000	
Active Coils	:	29.000	
Load Lbs.	:	4.6801	*
Load Height	:	3.0000	
Free Length	:	22.0000	
Percent Scrap	:	10.0000	
Load Tolerance:		0.0000	*

ROUND

Solid Ground	:	1.9220
Solid Unground	:	1.9840
Rate Lbs/Inch	:	0.246
Weight/M pcs.	:	131.621
FL/Load Tol.	:	0.0000
Load Stress	:	76244.613
Solid Stress	:	80570.492
Dev. Length Inch:		140.0462
Spring Index	:	23.1935
OD at Solid Grd.:		1.5198

Specifications for Spring #3

[Compression Design Calculation]

Material Type: 01 PM PHOS MUSIC ASTM-A228

Diameters

Outside:	0.9500	
Inside :	0.8540	*

Average Diameter

Outside :	0.9500
Inside :	0.8540
Mean Diameter:	0.9020

Wire Size	: 0.0480	
Total Coils	: 34.000	
Active Coils	: 32.000	
Load Lbs.	: 0.6499	*
Load Height	: 13.0000	
Free Length	: 15.0000	
Percent Scrap	: 10.0000	
Load Tolerance:		*

ROUND

Solid Ground :	1.6320
Solid Unground :	1.6800
Rate Lbs/Inch :	0.325
Weight/M pcs. :	54.274
FL/Load Tol. :	
Load Stress :	14508.278
Solid Stress :	96973.328
Dev. Length Inch:	96.3466
Spring Index :	18.7917
OD at Solid Grd.:	0.9620

[Compression Design Calculation]

Material Type: 01 PM PHOS MUSIC ASTM-A228

Diameters

Outside:	0.9500	
Inside :	0.8540	*

Average Diameter

Outside :	0.9500
Inside :	0.8540
Mean Diameter:	0.9020

Wire Size	: 0.0480	
Total Coils	: 34.000	
Active Coils	: 32.000	
Load Lbs.	: 3.8993	*
Load Height	: 3.0000	
Free Length	: 15.0000	
Percent Scrap	: 10.0000	
Load Tolerance:	0.0000	*

ROUND

Solid Ground :	1.6320
Solid Unground :	1.6800
Rate Lbs/Inch :	0.325
Weight/M pcs. :	54.274
FL/Load Tol. :	0.0000
Load Stress :	87049.666
Solid Stress :	96973.328
Dev. Length Inch:	96.3466
Spring Index :	18.7917
OD at Solid Grd.:	0.9620

Bibliography

1. Allison, Jack. *Friendly Airfield Threat Detection and Damage Assessment.* Technical Report WL-TR-92-3013. Wright Laboratory (AFSC), Wright-Patterson AFB OH, May 1992

2. Michelson, Robert C. Executive Vice President, Association for Unmanned Vehicle Systems, Washington D.C. Personal Correspondence. 1 October 1991.

3. Association for Unmanned Vehicle Systems. Official Competition Rules for the 1994 International Aerial Robotics Competition. Arlington, VA, 31 August 1993.

4. Cochran, William L. AFIT Student, Air Force Institute of Technology (AU), Wright-Patterson AFB OH. Video Documentation. June 1993

5. Llewelyn, Daniel D. *The Design of a Guidance and Stability System for the Moller Aerial Vehicle.* MS thesis, AFIT/GAE/ENY/92D-18. School of Engineering, Air Force Institute of Technology (AU), Wright-Patterson AFB OH, December 1992 (AD-B169849).

6. Stewart, D. "Platform with Six Degrees-of-Freedom," *Proceedings of the Institute of Mechanical Engineering, 180:* Part 1., No. 15., 371-386 (1965-1966).

7. Landsberger, S.E. *Design and Construction of a Cable-Controlled Parallel Link Manipulator.* MS thesis, Massachusetts Institute of Technology, Cambridge MA, September 1984.

8. Perry, David J. and J.J. Azar. *Aircraft Structures.* New York: McGraw-Hill Book Company, 1982.

9. Harker, Ralph J. *Elastic Energy Methods of Design Analysis.* New York: Elsevier, 1986.

10. Oberg, Erik. and others. *Machinery's Handbook.* New York: Industrial Press Inc., 1979.

11. Spong, Mark W. and M. Vidyasagar. *Robot Dynamics and Control.* New York: John Wiley & Sons, 1989.

Vita

Captain William L. Cochran was born on 4 December 1957 in Charlotte, North Carolina. He graduated from North Mecklenburg High School in Huntersville, NC in 1977. After three years of undergraduate study at the University of North Carolina at Charlotte, he graduated cum laude from North Carolina State University in May 1984 with a Bachelor of Science in Aerospace Engineering. Upon graduation he received a commission in the USAF through Officer Training School. After commissioning, he earned his wings at Undergraduate Pilot Training, Laughlin AFB, Texas in February 1986. His first tour of duty was at McClellan AFB, California where he was assigned to the 55th Weather Recon Squadron as a WC-135 pilot. During his stay at the 55th WRS, he upgraded from copilot to aircraft commander to instructor pilot to simulator instructor. His stay at the 55th WRS lasted until May 1992, when he entered the School of Engineering, Air Force Institute of Technology

Permanent Address: 98 Peach Orchard Ave.
Dayton, OH 45419

REPORT DOCUMENTATION PAGE

Form Approved
OMB No. 0704-0188

Public report ng burden for this collection of nformation is estimated to average 1 hour per response, including the time for reviewing instructions, searching existing data sources, gathering and maintaining the data needed, and completing and reviewing the collection of information. Send comments regarding this burden estimate or any other aspect of this collection of nformation, including suggestions for reducing this burden to Washington Headquarters Services, Directorate for information Operations and Reports, 1215 Jefferson Davis Highway, Suite 1204, Arlington, VA 22202-4302, and to the Office of Management and Budget, Paperwork Reduction Project (0704-0188), Washington, DC 20503

1. AGENCY USE ONLY (Leave blank)	2. REPORT DATE	3. REPORT TYPE AND DATES COVERED
	December 1993	Master's Thesis

4. TITLE AND SUBTITLE

Design and Construction of the Aerobot Robotic Manipulator (ARM)

5. FUNDING NUMBERS

6. AUTHOR(S)

William L. Cochran, Capt, USAF

7. PERFORMING ORGANIZATION NAME(S) AND ADDRESS(ES)

Air Force Institute of Technology, WPAFB OH 45433

8. PERFORMING ORGANIZATION REPORT NUMBER

AFIT/GA/ENY/93D-2

9. SPONSORING / MONITORING AGENCY NAME(S) AND ADDRESS(ES)

10. SPONSORING / MONITORING AGENCY REPORT NUMBER

11. SUPPLEMENTARY NOTES

12a. DISTRIBUTION / AVAILABILITY STATEMENT

Approved for public release; distribution unlimited

12b. DISTRIBUTION CODE

13. ABSTRACT *(Maximum 200 words)*

This thesis designed, constructed, and tested a robotic arm for the Aerobot (Aerial Robot). The main purpose of the ARM is to enable the Aerobot to retrieve objects for use in an annual robotics competition. Design of the ARM involved synthesizing the characteristics of simplicity, weight, strength, and size. The result was a three-degree-of-freedom manipulator that uses electric motors, cable linkages, and telescoping tubes to access a work space below the Aerobot. Forward and inverse kinematics were investigated to enable automation of the ARM. Data was collected from infrared sensors to validate the model. Manipulation of the ARM is presently under open loop control (joy stick) which demonstrates the use of tele-robotics and its capabilities.

14. SUBJECT TERMS

Vertical Takeoff Aircraft, Unmanned Aerial Vehicles, Aerial Robotics, Electronics, Controls, Robotics, Kinematics, Structures, Design.

15. NUMBER OF PAGES

108

16. PRICE CODE

17. SECURITY CLASSIFICATION OF REPORT	18. SECURITY CLASSIFICATION OF THIS PAGE	19. SECURITY CLASSIFICATION OF ABSTRACT	20. LIMITATION OF ABSTRACT
Unclassified	Unclassified	Unclassified	UL